UNIVERSIDADE DA BEIRA INTERIOR
Engenharia

Dynamics of a Gyrostat Satellite with the Vector of Gyrostatic Moment along the Principal Plane of Inertia

(versão corrigida após defesa)

Pedro Afonso Gomes Dias

Dissertação para obtenção do Grau de Mestre em
Engenharia Aeronáutica
(Ciclo de estudos integrado)

Orientador: Prof. Doutor Luís Filipe Ferreira Marques Santos
Orientador: Prof. Doutor André Resende Rodrigues da Silva

Covilhã, dezembro de 2018

Agradecimentos

Primeiro que tudo, quero agradecer à minha família, em especial aos meus pais e irmãos, que me deram a possibilidade de estudar nesta universidade e por todo o apoio e força, ao longo de todo este tempo.

Em seguido quero dar um agradecimento especial ao meu orientador, Professor Doutor Luís Filipe Ferreira Marques Santos, por me ter sempre ajudado com todos os tipos de problemas que ocorreram ao longo desta investigação, a qualquer hora do dia. Agradeço todas as sugestões, conhecimento, conselhos e disponibilidade que houve da sua parte.

Quero também agradecer ao Professor Doutor André Resende Rodrigues da Silva pela sugestão do tema desta dissertação e, por me ter ajudado em todas as questões colocadas no início deste trabalho.

À Universidade da Beira Interior, ao departamento de Ciências Aeroespaciais e à cidade da Covilhã, agradeço o facto de me terem acolhido e permitido estudar no curso de Engenharia Aeronáutica ao longo destes cinco anos.

Por fim, e não menos importante, quero agradecer a todos os meus amigos, o apoio, o companheirismo e a amizade ao longo de todo o meu percurso académico. Quero ainda deixar um agradecimento especial, a quem me deu dormida quando já não tinha quarto alugado na Covilhã.

Resumo

Satélites artificias são uns dos componentes cruciais da vida moderna. O estudo do controlo da atitude e estabilização de um satélite é necessário para assegurar uma missão bem-sucedida. Existem dois tipos de métodos de estabilização: os métodos passivos e os métodos ativos.

Nesta dissertação é investigado a dinâmica de um satélite tipo giróstato, sujeito a um método semi-passivo de estabilização, nomeadamente o momento gravítico e as propriedades giroscópicas de rotores, ao longo de uma órbita circular.

No caso particular, quando o vetor de momento girostático está ao longo de um dos principais planos de inércia do satélite. Para resolver este problema é proposto um modelo matemático numérico-analítico para determinar todos as posições de equilíbrio de um satélite giróstato, em um sistema coordenado orbital em função das componentes adimensionais do vetor de momento girostático ($H_i\ i = 1,2,3$) e do parâmetro inercial adimensional v. As condições de existência das soluções de equilíbrio são obtidas. As condições suficientes de estabilidade para cada grupo de soluções de equilíbrio são derivadas, a partir da análise do integral de energia generalizado como uma função de *Lyapunov*.

O estudo da evolução da bifurcação do equilíbrio foi realizado em detalhe em função do parâmetro v. Também, a evolução das soluções de equilíbrio em função dos ângulos do satélite é analisada e é verificado a existência de pequenas regiões de 12 e 16 posições de equilíbrio referidas em [14] e [20].

Este trabalho mostra que o número de posições de equilíbrio de um satélite tipo giróstato, neste caso particular, não ultrapassa 24 e não é inferior a 8. O estudo da bifurcação do equilíbrio revela a existência de regiões de 12 posições de equilíbrio que se aproximam, para valores infinitos de H_3 e que nunca desaparecem, estas regiões sugerem ter uma relação com as regiões referidas por Santos [14] e Santos et al.[20].

O estudo da evolução da estabilidade para cada solução de equilíbrio em função de v e H_3 revela que o número de posições de equilíbrio estáveis varia entre 2 e 6.

Palavras-chave

Satélite tipo giróstato, equilíbrio, estabilidade, girostático e inércia.

Abstract

Artificial satellites are one of the most crucial components of modern life. The study of attitude control and stabilization of satellite is necessary to ensure a successful operation. There are two types of stabilization schemes: the passive methods and active methods.

In this dissertation is investigated the dynamics of a gyrostat satellite, subjected to a semi-passive method of stabilization, namely the gravitational torque and the gyroscopic proprieties of rotating rotors, along a circular orbit.

In a particular case, when the gyrostatic moment vector is along one of satellite's principal central planes of inertia. To solve the problem is proposed a mathematical analytical-numerical method for determining all equilibrium positions of the gyrostat satellite in the orbital coordinate system in function of dimensionless gyrostatic moment vector components ($H_i \;\; i = 1,2,3$) and the dimensionless inertial parameter v. The conditions of existence of the equilibrium solutions are obtained. Sufficient conditions of stability for each group of equilibrium solutions are derived from the analysis of the generalized integral energy used as a Lyapunov's function.

The study of the evolution of equilibria bifurcation of the gyrostat is carried out in function of parameter v in detail. Also, the evolution of equilibrium solutions in function of spacecraft angles is analyzed and it is verified the existence of small regions of 12 and 16 equilibrium positions referred in [14] and [20].

This work shows that the number of equilibria of a gyrostat satellite, in this particular case, does not exceeds 24 and does not go below 8. The study of the equilibria bifurcation shows that there are small regions of 12 equilibrium positions that approach each other for infinite H_3 and never vanish, these regions seems to have a relation with the regions referred by Santos in [14] and Santos et. al. [20].

The study of the evolution of stability for every equilibrium solution in function v and H_3, shows that the number of stable equilibria varies between 2 and 6.

Keywords

Gyrostat-satellite, equilibria, stability, gyrostatic and inertia.

Table of Contents

List of Figures

List of Tables

Nomenclature

O: Gyrostat Center of Mass.

$OX_1X_2X_3$: Orbital Reference Frame.

OX_1: Axis aligned with the orbital plane, with positive direction in the direction of speed.

OX_2: Axis normal to the orbital plane.

OX_3: Axis that connects the center of mass of the planet with center of mass of the gyrostat.

$Ox_1x_2x_3$: Gyrostat's fixed reference frame.

Ox_i $(i = 1,2,3)$: Gyrostat's principal axes of inertia.

α, β and γ: the spacecraft angles between the gyrostat's fixed reference frame and orbital reference frame.

a_{ij}: direction cosines between the principal axis and gyrostat axis.

A, B and C: principal moments of inertia in relation to the gyrostat's center of inertia.

p, q and r: absolute angular velocity of the gyrostat.

$\overline{h_i}$ $(i = 1, 2, 3)$: projections of the gyrostatic moment vector onto axes Ox_i.

ω_0: angular velocity of motion of the gyrostat's center of mass along the circular orbit.

H: Hamiltonian.

v: inertia dimensionless parameter of the gyrostat satellite.

Chapter 1

Introduction

Artificial satellites are one of the most crucial components of modern life. Communications satellites lets billions of people connect with each other all over the world. The Global Positioning System (GPS) satellites constellation gives geolocation and time information to a GPS receiver leading to many civilian and military applications, such as accurate real-time navigation, clock synchronization, target tracking, among others. Meteorological satellites give us information about Earth's environment. Finally, there are the scientific satellites, they allow scientists to study Earth, the solar system and even our universe in great detail and accuracy. These types of satellites have two big advantages compared to Earth-based solutions, like radio and optical telescopes: (a) observing celestial objects without the interference of gases, lights and magnetic fields produced on earth and (b) orbiting around other celestial objects, like sun, moon and other planets.

The attitude control and stabilization of an artificial satellite needs to be studied to ensure a successful operation, for example, in the case of a GPS satellite, its antenna must be pointing towards Earth. There are many methodologies that can be used in this case and they can be separated in two categories: passive methods can employ properties of the gravitational and magnetic fields, atmospheric drag, solar radiation pressure and gyroscopic properties of rotating bodies; and active methods, more accurate than the passive ones, using reaction wheels, thrusters and/or magnetic torques. Passive orientation systems own an important advantage comparing with active ones, as they can operate for a long time without energy and(or) a working body, and the last ones have a limited quantity of fuel and(or) need to ensure the reliability of the flywheels.

The motivating problem considered in this dissertation is the dynamics of the rotational motion of an artificial satellite, namely the gyrostat satellite family, in a circular orbit. This satellite is subjected to a gravitational torque and is equipped with internal rotors, as a semi-passive attitude stabilization. The internal rotors rotate at constant angular velocity relative to the satellite body and the gyrostatic moment vector lies along the Principal Plane of Inertia ($H_1 = 0$) leading to new equilibrium positions that can be interesting in practical applications.

1.1 Important Concepts

In this section, it is introduced three important concepts related to the current work, which are: the gyrostat satellite, the relative equilibria of a gyrostat satellite and the Lyapunov's stability of a gyrostat satellite.

A gyrostat satellite is mechanical system composed of a rigid body with one or more symmetrical rotors, whose spin axes are fixed in the rigid body and which can rotate about their axes of symmetry; it is also a satellite that is in orbit about a massive body. The gyrostat does not model several effects including flexible structures, bearing friction and dynamic and static imbalance. An example of a gyrostat motion in a circular orbit is given in figure 1.1.

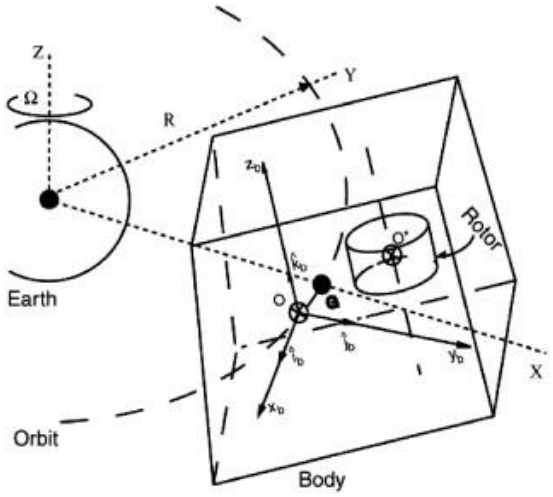

Figure 1.1 – Gyrostat's orbital scheme [1].

The relative equilibria of a gyrostat satellite is when the satellite rotates about the normal vector of the gyrostat's orbital plane at the orbital rate, in a motionless way with respect to an observer in an orbit-fixed reference frame.

The Lyapunov's stability of a gyrostat satellite is when the satellite motion remains always within a specific interval, i.e., an equilibrium position is stable when in reaction to small disturbances, there is small changes in its state of motion. The method used is the second method of Lyapunov, which makes use of a constant Lyapunov's function. In this case, the system is stable when the Lyapunov's matrix is positive definite and if a Lyapunov's function is not dependent from time, it can be said that it remains time-invariant.

1.2 Literature Review

Since the ending of the 20th century until now, a widespread of studies in Celestial Mechanics were conducted about the problems of gyrostat-satellites and its dynamics. The problem of controlling the motion of this type of rigid body with either internal or external torques was one of them. Among several studies, this dissertation has focused in gyrostat satellites with internal rotors attached to their principal axes of inertia. Exists two types of internal rotors applied to gyrostat satellites platforms, with freely spinning rotors and with constant-spin rotors.

The focus of this work is not on the case of freely spinning rotors but is important to have a wide view about the subject, so in 1998, El-Gohary [2], one relevant author, studied successfully how to reach asymptotic stability of relative programmed motion of a gyrostat-satellite using control moments applied on three internal rotors attached to its principal axes of inertia. In another study [3], the problem of exponential stability of the permanent rotational motion of a gyrostat satellite was investigated, but now stabilizing servo-control moments were applied to internal rotors. The equations of motion in this study are used without any approximations and the servo-control moments are obtained exactly. The same author in 2000 [4] proposed a control scheme that guarantee an optimal stabilization of a given rotational motion of a symmetric gyrostat on circular orbit. The control action is generated by rotating internal rotors. The asymptotic stability of this motion is proved using Barbachen and Krasovskii theorem and, as a particular case, for the equilibrium position of the gyrostat. In [5], a new control scheme is proposed for a gyrostat satellite, but in comparison with previous studies, this one has the advantage of choosing the time needed for stabilizing an arbitrary position to an equilibrium position.

For the next decade, the interest in dynamics of a gyrostat satellite moving along a circular orbit with constant speed rotors led to studies focused in different orientations of the vector of gyrostatic moment: in 2001, Sarychev and Mirer [6], show the special case when the vector of gyrostatic moment is collinear to the principal axis of inertia of the gyrostat and obtained a new analytical solution for equilibria. The authors concluded that the number of isolated equilibria is shown to be no less than 8 and no more than 24. Afterwards, in 2005, Sarychev et al. [7] investigated the same case but now shows the evolution of the regions of validity of the conditions of stability of the gyrostat and all bifurcation values of the parameters when these regions changes were obtained. In 2008, the same authors, focused their work in a different special case [8], when a gyrostatic moment vector lies on one of the satellite's principal central planes of inertia. For this case, the equilibria were determined, and conditions of their existence were analyzed. A numerical-analytical method was used to study the evolution of the regions where the number of equilibria positions changes and to study the regions of validity of the conditions of stability. Other authors studied the problem of equilibria and stability of a

gyrostat satellite in circular orbit around a spherical planet or with a symmetry axis [9], and the problem of stabilization of a rigid body motion with internal friction rotors, achieving new control laws.

In recent years, there was a change of focus and several authors start to discuss the general case of equilibria and stability of a gyrostat satellite subjected to gravitational torque, i.e. when all gyrostatic moment vector's parameters are non-zero. The knowledge about the special cases [6], [7] and [8] added to new improvements in numerical computation led to deeper analysis of this case. The most relevant authors were Sarychev et al. In 2012 [10], it was determined the equilibria of a gyrostat satellite and was shown the number of equilibria is not less than 8 and no more than 24, like in previous cases. A year after [11], the same authors confirmed that for the same case the number of stable equilibria changes from 4 to 2 with increasing of the gyrostatic torque. A new symbolic-numerical method of computer algebra was proposed, in 2014, to study equilibrium positions of a gyrostat satellite [12-13]. The method uses an algorithm of constructing the Groebner bases and it results in a conversion of the system of 9 equations of 9 variables into a single algebraic equation of the 12^{th} order with one variable. This study reconfirms the same conclusions of previous studies about the maximum and minimum number of equilibria positions of gyrostat satellite.

In 2015, Luís Santos conducted a deep analysis into the dynamics of a gyrostat satellite in a circular orbit [14-15], specifically the general case of equilibria and stability. The author used the concepts and knowledge from [10-13], like the symbolic-numerical method from [12], which led to a vastly number of equilibria and stability configuration analysis, also unveiling the complete bifurcation of equilibria. In addition, it led to a deep understanding of the equilibria's bifurcation curves, which corresponds to changes in number of equilibrium positions and to the study of its stability. This work unveiled small regions of 16 and 12 equilibrium positions near $H_1 = 0$, which up to date were unknown; these conclusions will be analyzed later in the present study. Henceforward, the conclusions of this study were reconfirmed in [16-17].

In [18], Gutnik and Sarychev investigated the proprieties of a non-linear algebraic system that determines equilibria of a gyrostat satellite. It is proposed a computer algebra method similar to last studies, which converts a very complex system into a simpler one. The focus of this work was when the gyrostatic moment vector lies in one of the satellite's principal central planes of inertia (Case $H_1 = 0$, H_2 and H_3 non-zero; Case $H_2 = 0$, H_1 and H_3 non-zero; Case $H_3 = 0$, H_1 and H_2 non-zero). Equilibria and the bifurcation curves were all obtained symbolically. It is again reconfirmed for this cases that the number of equilibria ranges from 24 to 8 with decrement of 4 upon successive increase of the vector of gyrostatic moment.

Lastly, in 2017, a particular case ($H_1 = 0$, H_2 and H_3 non-zero) [19] of equilibria of an asymmetrical inertial distribution gyrostat satellite was studied using the same symbolical-numerical method previously referred in [14]. The bifurcation curves in function of system

dimensionless parameters at which there was a change in number of equilibrium positions were determined. The study confirmed the existence of the small equilibria regions near $H_1 = 0$ shown on the general case of equilibria in [14] and [20]. In this dissertation, this special case will be analyzed furtherly.

1.3 Objectives

Many authors discussed the problem of attitude dynamics of a gyrostat satellite with constant spin-rate internal rotors, in different inertial distributions and different orientations of the gyrostatic moment vector. It was found in [14] and [20], small regions of 12 and 16 positions of equilibria which appear when one of component of gyrostatic moment vector is near zero ($H_1 \approx 0$). Similarly, there are many studies about equilibria and stability of a gyrostat satellite when the gyrostatic moment vector lies in one of the satellite's principal central planes of inertia ($H_1 \neq 0$, $H_2 = 0$, $H_3 \neq 0$) in [8] and [18]; or when it is parallel to one of the satellite's principal central axes of inertia ($H_1 = 0$, $H_2 \neq 0$, $H_3 = 0$) in [6], [7] and [18]; but there are no published results when $H_1 = 0$, $H_2 \neq 0$, $H_3 \neq 0$.

This dissertation has the objective of providing a detail equilibria and stability study of a gyrostat satellite when the gyrostatic moment vector is along the principal plane of inertia ($H_1 = 0$, $H_2 \neq 0$, $H_3 \neq 0$) using an analytical-numerical method. The study will be in function of a dimensionless inertia parameter and dimensionless gyrostatic moment vector components. To verify the appearance of the regions spoken above and for comparing purposes with [8], the complete bifurcation of equilibria with the bifurcation curves will be obtained and discussed. The evolution of the regions where sufficient conditions of stability is valid will be also investigated.

1.4 Dissertation overview

The present work is organized in five chapters: Introduction, Gyrostat's Dynamics, Results and Discussion, and Conclusions and Future Work.

Chapter 2 develops an analytical-numerical approach to the mathematical problem of determining the equilibria and stability of the gyrostat satellite. All the equilibrium positions and the conditions of their existence are determined. The bifurcation curves equations and the sufficient conditions of stability of equilibria are also derived. The chapter also sets the assumptions, nomenclature and conventions used throughout the dissertation.

Chapter 3 discusses the results of equilibria and stability, in function of system parameters v, H_2 and H_3, obtained using the mathematical model. The evolution of equilibria bifurcation is discussed, as the evolution of stability of each equilibrium positions.

For the final chapter – Chapter 4 – it is presented the main conclusions and results, but also discusses recommendations, in which the study can be continued.

Chapter 2

Gyrostat's Dynamics

In this chapter, a mathematical model based on a numerical-analytical approach for the calculation of the equilibrium positions and the sufficient conditions of stability of the gyrostat satellite is described. The equations of motion and conditions of existence of equilibrium for the gyrostat are obtained.

2.1 Equations of motion

This section describes the equations of motion that rules a solid body with rotors inside that are balanced both statically and dynamically. It is assumed the angular velocity of rotation of these rotors to be constant relative to the satellite's main body, while the center of mass of the satellite moves along a circular orbit in a central Newtonian field of force.

It is introduced two right-handed Cartesian reference frames with an origin at the satellite's center of mass O. $OX_1X_2X_3$ is the orbital reference frame whose axis OX_3 is directed along the radius vector connecting the center of mass of the satellite and the Earth; the OX_1 axis is directed along the linear velocity of the center of mass O.$Ox_1x_2x_3$ is the satellite-fixed reference frame; Ox_i ($i = 1, 2, 3$) are the satellite's principal axes of inertia.

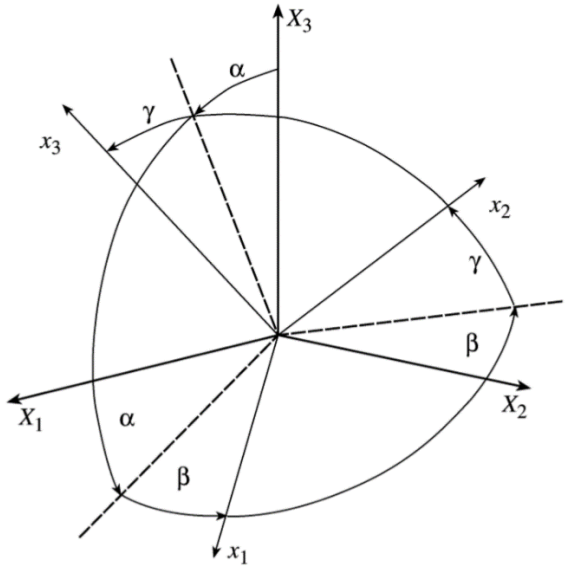

Figure 2.1. – Relation between Orbital and Gyrostat's reference frames [8].

Let's us define the orientation of the satellite-fixed reference frame relative to the orbital reference frame by the spacecraft angles α, β and γ represented in Figure 2.1, consequently, the direction cosines $a_{ij} = \cos(X_i, x_j)$ are specified by the following expressions [8]:

$$\begin{cases} a_{11} = cos\alpha \times cos\beta \\ a_{12} = sin\alpha \times sin\gamma - cos\alpha \times sin\beta \times cos\gamma \\ a_{13} = sin\alpha \times cos\gamma + cos\alpha \times sin\beta \times sin\gamma \\ a_{21} = sin\beta \\ a_{22} = cos\beta \times cos\gamma \\ a_{23} = -cos\beta \times sin\gamma \\ a_{31} = -sin\alpha \times cos\beta \\ a_{32} = cos\alpha \times sin\gamma + sin\alpha \times sin\beta \times cos\gamma \\ a_{33} = cos\alpha \times cos\gamma - sin\alpha \times sin\beta \times sin\gamma \end{cases} \tag{2.1}$$

The spacecraft angles α, β and γ can be written in function of the above direction cosines as:

$$\begin{cases} \alpha = \cos^{-1}(a_{11}/cos\beta) \\ \beta = \sin^{-1}(a_{21}) \\ \gamma = \cos^{-1}(a_{22}/cos\beta) \end{cases} \tag{2.2}$$

The equations of motion of a gyrostat satellite with respect to its center of mass are written in the form [6,8-19]:

$$\begin{cases} A\dot{p} + (C-B)qr - 3\omega_0^2(C-B)a_{32}a_{33} - \overline{h_2}r + \overline{h_3}q = 0 \\ B\dot{q} + (A-C)rp - 3\omega_0^2(A-C)a_{33}a_{31} - \overline{h_3}p + \overline{h_1}r = 0 \\ C\dot{r} + (B-A)pq - 3\omega_0^2(B-A)a_{31}a_{32} - \overline{h_1}q + \overline{h_2}p = 0 \end{cases} \tag{2.3}$$

$$\begin{cases} p = (\dot{\alpha} + \omega_0)a_{21} + \dot{\gamma} = \bar{p} + \omega_0 a_{21} \\ q = (\dot{\alpha} + \omega_0)a_{22} + \dot{\beta}sin\gamma = \bar{q} + \omega_0 a_{22} \\ r = (\dot{\alpha} + \omega_0)a_{23} + \dot{\beta}cos\gamma = \bar{r} + \omega_0 a_{23} \end{cases} \tag{2.4}$$

Here, A, B, C are the principal central moments of inertia of the gyrostat; p, q, r are the absolute angular velocity of the gyrostat and $\overline{h_i}$ $(i = 1,2,3)$ the projections of the gyrostatic moment vector onto axes Ox_i; and ω_0 is the angular velocity of motion of the gyrostat center of mass along the circular orbit. The dots designate differentiation with respect to time.

2.2 Gyrostat's equilibria

Following [8] and others, for comparing reasons, it is used the same designations and parameters. First, it is introduced the designation $\bar{h_i}/\omega_0 = h_i$ and the following system of equations is obtained:

$$\begin{cases} 4(Aa_{21}a_{31} + Ba_{22}a_{32} + Ca_{23}a_{33}) + h_1a_{31} + h_2a_{32} + h_3a_{33} = 0 \\ Aa_{11}a_{31} + Ba_{12}a_{32} + Ca_{13}a_{33} = 0 \\ Aa_{11}a_{21} + Ba_{12}a_{22} + Ca_{13}a_{23} + h_1a_{11} + h_2a_{12} + h_3a_{13} = 0 \end{cases} \tag{2.5}$$

This system allows one to determine all equilibrium positions of the gyrostat in the orbital reference frame.

In this case, a_{ij}, as elements of an orthogonal matrix, satisfy the following conditions:

$$\begin{cases} a_{11}^2 + a_{12}^2 + a_{13}^2 = 1 \\ a_{21}^2 + a_{22}^2 + a_{23}^2 = 1 \\ a_{31}^2 + a_{32}^2 + a_{33}^2 = 1 \\ a_{11}a_{21} + a_{12}a_{22} + a_{13}a_{23} = 0 \\ a_{11}a_{31} + a_{12}a_{32} + a_{13}a_{33} = 0 \\ a_{21}a_{31} + a_{22}a_{32} + a_{23}a_{33} = 0 \end{cases} \tag{2.6}$$

At $A \neq B \neq C$ one can solve system (2.5) and (2.6) for $a_{11}, a_{12}, a_{13}, a_{21}, a_{22}, a_{23}$ and a_{23}. As a result, we get [8]:

$$\begin{cases} a_{11} = \dfrac{4(C-B)a_{32}a_{33}}{F} \\ a_{12} = \dfrac{4(A-C)a_{33}a_{31}}{F} \\ a_{13} = \dfrac{4(B-A)a_{31}a_{32}}{F} \\ a_{21} = \dfrac{4(I_3-A)a_{31}}{F} \\ a_{22} = \dfrac{4(I_3-B)a_{32}}{F} \\ a_{23} = \dfrac{4(I_3-C)a_{33}}{F} \end{cases} \tag{2.7}$$

Here, $F = h_1a_{31} + h_2a_{32} + h_3a_{33}$, $I_3 = Aa_{31}^2 + Ba_{32}^2 + Ca_{33}^2$ and direction cosines a_{31}, a_{32} and a_{33} are determined from the following three equations:

$$16[(B-C)^2a_{32}^2a_{33}^2+(C-A)^2a_{33}^2a_{31}^2+(A-B)^2a_{31}^2a_{32}^2]=(h_1a_{31}+h_2a_{32}+h_3a_{33})^2$$

$$4(B-C)(C-A)(A-B)a_{31}a_{32}a_{33}+[h_1(B-C)a_{32}a_{33}+h_2(C-A)a_{33}a_{31}+h_3(A-B)\times a_{31}a_{32}]\times(h_1a_{31}+h_2a_{32}+h_3a_{33})=0 \quad (2.8)$$

$$a_{31}^2+a_{32}^2+a_{33}^2=1$$

After solving system (2.8) formulas (2.7) allow one to determine the remaining six direction cosines. Notice that solutions (2.7) exist only when out of three direction cosines a_{31}, a_{32} and a_{33}, none two vanish simultaneously. The cases $a_{31}=a_{32}=0$, $a_{32}=a_{33}=0$ and $a_{33}=a_{31}=0$ are special and they should be considered immediately addressing to system (2.5) and (2.6). The case $a_{32}=a_{33}=0$ will be discussed later.

2.2.1 Case $H_1=0, H_2\neq 0$ and $H_3\neq 0$

In previous studies, it is analyzed the general case of the gyrostat ($H_1\neq 0, H_2\neq 0$ and $H_3\neq 0$) [14] and many particular cases, the case when the gyrostatic moment vector is collinear to one of the satellite's principal central axes of inertia ($H_1=0, H_2\neq 0$ and $H_3=0$) [6] and the case when the gyrostatic moment vector is parallel to the satellite's principal central planes of inertia ($H_1\neq 0, H_2=0$ and $H_3\neq 0$) [8]. In this study, we deepen the knowledge about the case when the gyrostatic moment vector is along the satellite's principal central plane of inertia, which parameter H_1 is zero ($H_1=0, H_2\neq 0$ and $H_3\neq 0$).

The system (2.8) after introducing the dimensionless parameters:

$$H_2=\frac{h_2}{C-A} \quad H_3=\frac{h_3}{C-A} \quad v=\frac{A-B}{C-A} \quad (2.9)$$

Takes on form:

$$\begin{cases}16[a_{32}^2a_{33}^2(v+1)^2+a_{31}^2a_{33}^2+a_{31}^2a_{32}^2v^2]=(H_2a_{32}+H_3a_{33})^2\\ a_{31}\{-4v(1+v)a_{32}a_{33}+[H_2a_{33}+H_3a_{32}v]\times(H_2a_{32}+H_3a_{33})\}=0\\ a_{31}^2+a_{32}^2+a_{33}^2=1\end{cases} \quad (2.10)$$

Notice that the dimensionless parameters v, being an inertial parameter of the satellite, does not in itself determine the shape of its ellipsoid of inertia.

When investigating system (2.10) it is necessary to consider three cases: ($a_{31}=0$, $a_{32}\neq 0$ and $a_{33}\neq 0$), ($a_{31}\neq 0$ and $a_{32}=a_{33}=0$) and ($a_{31}\neq 0$, $a_{32}\neq 0$ and $a_{33}\neq 0$).

2.2.1.1 Case $a_{31} \neq 0$ and $a_{32} = a_{33} = 0$

The following system takes on the form:

$$\begin{cases} 16[a_{32}^2 a_{33}^2 (v+1)^2 + a_{31}^2 a_{33}^2 + a_{31}^2 a_{32}^2 v^2] = (H_2 a_{32} + H_3 a_{33})^2 \\ -4v(1+v)a_{32}a_{33} + [H_2 a_{33} + H_3 a_{32} v] \times (H_2 a_{32} + H_3 a_{33}) = 0 \\ a_{31}^2 + a_{32}^2 + a_{33}^2 = 1 \end{cases} \quad (2.11)$$

From the second equation of system (2.11) it follows that, if $a_{32} = 0$, then also $a_{33} = 0$. The existence of a solution for which:

$$a_{32} = a_{33} = 0 \quad (2.12)$$

It is investigated by analyzing original equations (2.5) and (2.6):

$$\begin{cases} 4Aa_{21}a_{31} = 0 \\ Aa_{11}a_{31} = 0 \\ Aa_{11}a_{21} + Ba_{12}a_{22} + Ca_{13}a_{23} + h_2 a_{12} + h_3 a_{13} = 0 \end{cases} \Leftrightarrow$$

$$\Leftrightarrow \begin{cases} a_{21} = 0 \\ a_{11} = 0 \\ Ba_{12}a_{22} + Ca_{13}a_{23} + h_2 a_{12} + h_3 a_{13} = 0 \end{cases} \quad (2.13)$$

$$\begin{cases} a_{12}^2 + a_{13}^2 = 1 \\ a_{22}^2 + a_{23}^2 = 1 \\ a_{31}^2 = 1 \end{cases} \quad (2.14)$$

$$\begin{cases} a_{12}a_{22} + a_{13}a_{23} = 0 \\ 0 = 0 \\ 0 = 0 \end{cases} \quad (2.15)$$

In this case, equations (2.5) after conversion to dimensionless parameters (2.9) and orthogonality (2.6) leads to the system:

$$\begin{cases} (B-C)a_{12}a_{22} + h_2 a_{12} + h_3 a_{13} = 0 \\ a_{12}a_{22} = -a_{12}a_{22} \end{cases} \Leftrightarrow$$

$$\Leftrightarrow \begin{cases} -(1+v)a_{12}a_{22} + H_2 a_{12} + H_3 a_{13} = 0 \\ - \end{cases} \quad (2.16)$$

In summary, the system becomes:

$$\begin{cases} -(1+v)a_{12}a_{22} + H_2a_{12} + H_3a_{13} = 0 \\ a_{31}^2 = 1 \\ a_{11} = 0 \\ a_{21} = 0 \\ a_{12}^2 + a_{13}^2 = 1 \\ a_{22}^2 + a_{23}^2 = 1 \\ a_{12}a_{22} + a_{13}a_{23} = 0 \end{cases} \tag{2.17}$$

Analyzing the first equation of this system, we obtain:

$$-(1+v)a_{12}a_{22} + H_2a_{12} + H_3a_{13} = 0 \Leftrightarrow$$

$$\Leftrightarrow a_{12}\big(H_2 - a_{22}(v+1)\big) + H_3a_{13} = 0 \Leftrightarrow$$

$$\Leftrightarrow a_{12} = -\frac{H_3a_{13}}{H_2 - a_{22}(v+1)} \tag{2.18}$$

From the last equation of system (2.17) and the expression for a_{12} obtained above (2.18), it can be achieved the following relationship:

$$a_{12}a_{22} + a_{13}a_{23} = 0 \Leftrightarrow$$

$$\Leftrightarrow a_{12} = -\frac{a_{13}a_{23}}{a_{22}} \Leftrightarrow$$

$$\Leftrightarrow -\frac{H_3a_{13}}{H_2 - a_{22}(1+v)} = -\frac{a_{13}a_{23}}{a_{22}} \Leftrightarrow$$

$$\Leftrightarrow \frac{a_{23}}{a_{22}} = \frac{H_3}{H_2 - a_{22}(v+1)} \tag{2.19}$$

Introducing $a_{23}^2 = 1 - a_{22}^2$ and raising the previous relationship to the power 2, it is obtained an equation of fourth order in $x_1 = a_{22}$:

$$\left(\frac{a_{23}}{x_1}\right)^2 = \left(\frac{H_3}{H_2 - x_1(v+1)}\right)^2 \Leftrightarrow$$

$$\Leftrightarrow \frac{1 - x_1^2}{x_1^2} = \frac{H_3^2}{\big(H_2 - x_1(v+1)\big)^2} \Leftrightarrow$$

$$\Leftrightarrow -(v+1)^2x_1^4 + 2H_2(v+1)x_1^3 + ((v+1)^2 - H_3^2 - H_2^2)x_1^2 - 2H_2(v+1)x_1 + H_2^2 = 0 \tag{2.20}$$

Two equilibrium positions of the gyrostat correspond to each real root of this equation. The direction cosines are defined in function of x_1:

$$a_{12} = -\frac{a_{13}a_{23}}{a_{22}} \tag{2.21}$$

$$a_{12}a_{22} + a_{13}a_{23} = 0 \Leftrightarrow$$

$$\Leftrightarrow \frac{-H_3 a_{13}x_1}{H_2 - x_1(v+1)} + a_{13}a_{23} = 0 \Leftrightarrow$$

$$\Leftrightarrow a_{23} = \frac{H_3 x_1}{H_2 - x_1(v+1)} \tag{2.22}$$

Using the 5th equation of (2.17) and equation (2.21), it is achieved:

$$\frac{a_{23}^2 a_{13}^2}{x_1^2} + a_{13}^2 = 1 \Leftrightarrow$$

$$\Leftrightarrow a_{23}^2 a_{13}^2 + a_{13}^2 x_1^2 = x_1^2 \Leftrightarrow$$

$$\Leftrightarrow a_{13}^2(x_1^2 + a_{23}^2) = x_1^2 \Leftrightarrow$$

$$\Leftrightarrow a_{13}^2 = x_1^2 \Leftrightarrow$$

$$\Leftrightarrow a_{13} = a_{31}x_1 \tag{2.23}$$

$$a_{12} = -\frac{a_{23}}{x_1}a_{13} \Leftrightarrow$$

$$\Leftrightarrow a_{12} = -\frac{a_{23}}{x_1}a_{31}x_1 \Leftrightarrow$$

$$\Leftrightarrow a_{12} = -a_{23}a_{31} \tag{2.24}$$

Together, they form the group of solutions I:

$$\begin{cases} a_{11} = 0 \\ a_{12} = -a_{23}a_{31} \\ a_{13} = a_{31}x_1 \\ a_{21} = 0 \\ a_{22} = x_1 \\ a_{23} = \dfrac{H_3 x_1}{H_2 - x_1(v+1)} \\ a_{31} = \pm 1 \\ a_{32} = 0 \\ a_{33} = 0 \end{cases} \tag{2.25}$$

Let us determine boundaries in the plane of the parameters H_2 and H_3 that separate domains with different numbers of solutions of system (2.17). Bifurcation points are points in the plane (H_2,H_3) that simultaneously belong to the hyperbola branch that does not pass through the origin and to the circle; the tangent lines to the hyperbola and the circle coincide at the bifurcation points. The condition that the tangent lines coincide has the form [18]:

$$\frac{d(a_{23})}{d(a_{22})} = \frac{H_3(v+1)a_{22}}{\left(H_2 - a_{22}(v+1)\right)^2} + \frac{H_3}{H_2 - a_{22}(v+1)} = \frac{(v+1)a_{23} + H_3}{H_2 - a_{22}(v+1)} = -\frac{a_{22}}{a_{23}} \Leftrightarrow$$

$$\Leftrightarrow (v+1)(a_{23}^2 - a_{22}^2) + a_{22}H_2 + a_{23}H_3 = 0 \tag{2.26}$$

Substituting the expression for a_{23} from (2.25) into the sixth equation of (2.17) and equation (2.26), it is obtained the following system:

$$\begin{cases} a_{22}^2 + a_{23}^2 = 1 \\ a_{23} = \dfrac{H_3 a_{22}}{H_2 - a_{22}(v+1)} \end{cases} \Leftrightarrow$$

$$\Leftrightarrow \begin{cases} \dfrac{H_3^2 a_{22}^2}{\left(H_2 - a_{22}(v+1)\right)^2} = 1 - a_{22}^2 \\ \_ \end{cases} \tag{2.27}$$

$$\begin{cases} (v+1)(a_{23}^2 - a_{22}^2) + a_{22}H_2 + a_{23}H_3 = 0 \\ a_{23} = \dfrac{H_3 a_{22}}{H_2 - a_{22}(v+1)} \end{cases} \Leftrightarrow$$

$$\Leftrightarrow \begin{cases} -a_{22}^2(v+1) + \dfrac{a_{22}^2 H_3^2 (v+1)}{\left(H_2 - a_{22}(v+1)\right)^2} + a_{22}H_2 + \dfrac{a_{22}H_3^2}{H_2 - a_{22}(1+v)} = 0 \Leftrightarrow \\ \_ \end{cases}$$

$$\Leftrightarrow a_{22}^2H_3^2(v+1)-a_{22}^2(v+1)\big(H_2-a_{22}(1+v)\big)^2+a_{22}H_2\big(H_2-a_{22}(1+v)\big)^2$$
$$+a_{22}H_3^2\big(H_2-a_{22}(v+1)\big)=0\Leftrightarrow$$

$$\Leftrightarrow a_{22}\big(H_2-a_{22}(v+1)\big)^2\big(H_2-a_{22}(v+1)\big)+a_{22}H_3^2(a_{22}(v+1)+\big(H_2-a_{22}(1+v)\big)=0\Leftrightarrow$$

$$\Leftrightarrow \frac{H_3^2H_2}{\big(H_2-a_{22}(v+1)\big)^2}=-\big(H_2-a_{22}(1+v)\big) \tag{2.28}$$

$$\begin{cases}\dfrac{H_3^2a_{22}^2}{\big(H_2-a_{22}(v+1)\big)^2}=1-a_{22}^2\\ \dfrac{H_3^2H_2}{\big(H_2-a_{22}(v+1)\big)^2}=-\big(H_2-a_{22}(1+v)\big)\end{cases} \tag{2.29}$$

Dividing the first equation by the second equation from system (2.29), it is obtained:

$$\frac{\dfrac{H_3^2a_{22}^2}{\big(H_2-a_{22}(v+1)\big)^2}}{\dfrac{H_3^2H_2}{\big(H_2-a_{22}(v+1)\big)^2}}=\frac{1-a_{22}^2}{-\big(H_2-a_{22}(1+v)\big)}\Leftrightarrow$$

$$\Leftrightarrow \frac{a_{22}^2}{H_2}=\frac{1-a_{22}^2}{-\big(H_2-a_{22}(v+1)\big)}\Leftrightarrow$$

$$\Leftrightarrow -a_{22}^2H_2+a_{22}^3(v+1)=H_2-H_2a_{22}^2\Leftrightarrow$$

$$\Leftrightarrow a_{22}=\left(\frac{H_2}{v+1}\right)^{1/3} \tag{2.30}$$

Ultimately, substituting the expression for a_{22} into the second equation (2.29), it is obtained the following astroid equation:

$$-\frac{H_3^2H_2}{\big(H_2-a_{22}(v+1)\big)^2}=-\big(H_2-a_{22}(v+1)\big)\Leftrightarrow$$

$$\Leftrightarrow H_3^2H_2=\big(H_2-a_{22}(v+1)\big)^3\Leftrightarrow$$

$$\Leftrightarrow -H_3^{2/3}H_2^{1/3}=H_2-a_{22}(v+1)\Leftrightarrow$$

$$\Leftrightarrow -H_3^{2/3}H_2^{1/3}=H_2^{1/3}H_2^{2/3}-H_2^{1/3}(v+1)^{2/3}\Leftrightarrow$$

$$\Leftrightarrow H_2^{2/3}+H_3^{2/3}=(v+1)^{2/3} \tag{2.31}$$

Therefore, equation (2.20) has four roots at $H_2^{2/3} + H_3^{2/3} < (v+1)^{2/3}$ and two roots at $H_2^{2/3} + H_3^{2/3} > (v+1)^{2/3}$. Consequently, the total number of equilibrium positions for case (2.12), i.e., the number of solutions of group I, can be either 8 or 4, depending on the relation between dimensionless parameters H_2 and H_3.

2.2.1.2 Case $a_{31} \neq 0, a_{32} \neq 0$ and $a_{33} \neq 0$

Let us consider system (2.11) at $a_{32} \neq 0$ and $a_{33} \neq 0$. Dividing the second equation of this system by a_{33}^2 and designating $x_2 = a_{32}/a_{33}$, it can be rewritten in the form:

$$-4v(v+1)a_{32}a_{33} + H_2^2 a_{32}a_{33} + H_2H_3a_{33}^2 + H_2H_3va_{32}^2 + H_3^2va_{32}a_{33} = 0 \Leftrightarrow$$

$$\Leftrightarrow -4v(v+1)a_{32}/a_{33} + H_2^2 a_{32}/a_{33} + H_2H_3 + H_2H_3va_{32}^2/a_{33}^2 + H_3^2va_{32}/a_{33} = 0 \Leftrightarrow$$

$$\Leftrightarrow H_2H_3vx_2^2 + \left(H_2^2 + H_3^2v - 4v(v+1)\right)x_2 + H_2H_3 = 0 \tag{2.32}$$

The solution to this equation has the form:

$$x_2 = \frac{-\left(H_2^2 + H_3^2v - 4v(v+1)\right) \pm \sqrt{\Delta}}{2H_3H_2v} \tag{2.33}$$

Where:

$$\Delta = \left(H_2^2 + H_3^2v - 4v(1+v)\right)^2 - 4H_2^2H_3^2v \tag{2.34}$$

The first and third equations of system (2.11) after substitution in them $a_{32} = x_2a_{33}$ leads to the following system:

$$\begin{cases} 16[x_2^2a_{33}^4(v+1)^2 + a_{31}^2a_{33}^2 + v^2x_2^2a_{31}^2a_{33}^2] = (H_2a_{33}x_2 + H_3a_{33})^2 \\ a_{31}^2 + a_{32}^2 + a_{33}^2 = 1 \end{cases} \Leftrightarrow$$

$$\Leftrightarrow \begin{cases} 16[x_2^2a_{33}^4(v+1)^2 + a_{31}^2a_{33}^2 + v^2x_2^2a_{31}^2a_{33}^2] = a_{33}^2(H_2x_2 + H_3)^2 \\ \_ \end{cases} \Leftrightarrow$$

$$\Leftrightarrow \begin{cases} a_{33}^2x_2^2(v+1)^2 + a_{31}^2(1 + v^2x_2^2) = \dfrac{(H_2x_2 + H_3)^2}{16} \\ \_ \end{cases} \Leftrightarrow$$

$$\Leftrightarrow \begin{cases} \_ \\ a_{31}^2 + x_2^2a_{33}^2 + a_{33}^2 = 1 \end{cases} \Leftrightarrow$$

$$\Leftrightarrow \begin{cases} a_{33}^2x_2^2(v+1)^2 + a_{31}^2(1 + v^2x_2^2) = \dfrac{(H_2x_2 + H_3)^2}{16} \\ a_{33}^2(1 + x_2^2) + a_{31}^2 = 1 \end{cases} \tag{2.35}$$

Resolving this system for a_{31}^2 and a_{33}^2, it gets:

$$\begin{cases} a_{31}^2 = \dfrac{(H_3 + H_2 x_2)^2 (x_2^2 + 1) - 16 x_2^2 (v+1)^2}{16(v x_2^2 - 1)^2} \\ a_{33}^2 = \dfrac{16(v^2 x_2^2 + 1) - (H_3 + H_2 x_2)^2}{16(v x_2^2 - 1)^2} \end{cases} \tag{2.36}$$

In order for the found solution would correspond to an equilibrium solution of the gyrostat, the conditions $\Delta \geq 0$, $a_{31}^2 \geq 0$ and $a_{33}^2 \geq 0$ must be met.

Let us consider the discriminant sign. It is clear that $\Delta \geq 0$ if $v \leq 0$. In order to determine the sign of Δ on the interval $v > 0$, the discriminant can be written as:

$$\Delta = \left[\left(H_3 + 2\sqrt{v+1} \right)^2 v - H_2^2 \right] \times \left[\left(H_3 - 2\sqrt{v+1} \right)^2 v - H_2^2 \right] \tag{2.37}$$

Analyzing this expression, it can be concluded that $\Delta \geq 0$ at:

$$\begin{cases} \left(H_2 + 2\sqrt{v+1} \right)^2 v \geq H_2^2 \\ \left(H_2 - 2\sqrt{v+1} \right)^2 v \geq H_2^2 \end{cases} \vee \begin{cases} \left(H_2 + 2\sqrt{v+1} \right)^2 v \leq H_2^2 \\ \left(H_2 - 2\sqrt{v+1} \right)^2 v \leq H_2^2 \end{cases} \tag{2.38}$$

Now, the conditions $a_{31}^2 \geq 0$ and $a_{33}^2 \geq 0$ will be analyzed. Considering the following relationship obtained from the second equation of system (2.11)):

$$x_2 + H_3 = \frac{4v(v+1)x_2}{H_2 + H_3 v x_2} \tag{2.39}$$

And introducing that on (2.36), these conditions became:

$$a_{31}^2 \geq 0 \Leftrightarrow$$

$$\Leftrightarrow \frac{(H_3 + H_2 x_2)^2 (x_2^2 + 1) - 16 x_2^2 (v+1)^2}{16(v x_2^2 - 1)^2} \geq 0 \Leftrightarrow$$

$$\Leftrightarrow (H_3 + H_2 x_2)^2 (x_2^2 + 1) - 16 x_2^2 (v+1)^2 \geq 0 \Leftrightarrow$$

$$\Leftrightarrow \frac{16 v^2 (v+1)^2 x_2^2 (x_2^2 + 1)}{(H_2 + H_3 v x_2)^2} - 16 x_2^2 (v+1)^2 \geq 0 \Leftrightarrow$$

$$\Leftrightarrow \frac{16 v^2 x_2^2 (v+1)^2 (x_2^2 + 1) - 16 x_2^2 (v+1)^2 (H_2 + H_3 v x_2)^2}{(H_2 + H_3 v x_2)^2} \geq 0 \Leftrightarrow$$

$$\Leftrightarrow v^2 (x_2^2 + 1) - (H_2 + H_3 v x_2)^2 \geq 0 \tag{2.40}$$

$$a_{33}^2 \geq 0 \Leftrightarrow$$

$$\Leftrightarrow \frac{16(v^2x_2^2+1)-(H_3+H_2x_2)^2}{16(vx_2^2-1)^2} \geq 0 \Leftrightarrow$$

$$\Leftrightarrow 16(v^2x_2^2+1)-(H_3+H_2x_2)^2 \geq 0 \tag{2.41}$$

In other way, the inequalities (2.40) and (2.41) can be grouped with the equation (2.32) forming the following system, similar to the one found in [8]:

$$\begin{cases} a_0x_2+a_1x_2+a_2 \geq 0 \\ b_0x_2+b_1x_2+b_2 \geq 0 \\ c_0x_2^2+c_1x_2+c_2=0 \end{cases} \Leftrightarrow$$

$$\Leftrightarrow \begin{cases} a_0x_2+a_1x_2+a_2 \geq 0 \\ b_0x_2+b_1x_2+b_2 \geq 0 \\ x_2=\dfrac{-c_1 \pm \sqrt{c_1^2-4c_0c_2}}{2c_0} \end{cases} \Leftrightarrow$$

$$\Leftrightarrow \begin{cases} \left(-c_1 \pm \sqrt{c_1^2-4c_0c_2}\right)(a_1c_0-a_0c_1)+2c_0(a_2c_0-a_0c_2) \geq 0 \\ \left(-c_1 \pm \sqrt{c_1^2-4c_0c_2}\right)(b_1c_0-b_0c_1)+2c_0(b_2c_0-b_0c_2) \geq 0 \\ - \end{cases} \tag{2.42}$$

Where:

$$\begin{cases} a_0=v^2(1-H_3^2) \\ a_1=-2H_2H_3v \\ a_2=-H_2^2+v^2 \end{cases}$$

$$\begin{cases} b_0=16v^2-H_2^2 \\ b_1=-2H_2H_3 \\ b_2=16-H_3^2 \end{cases}$$

$$\begin{cases} c_0=H_2H_3v \\ c_1=H_2^2+H_3^2v-4v(v+1) \\ c_2=H_2H_3 \end{cases}$$

A solution of system (2.11) only correspond to an equilibrium positions of a gyrostat when inequalities (2.42) and $\Delta = c_1^2-4c_0c_2 \geq 0$ are valid. In this case, $a_{32}=x_2a_{33}$, direction cosines a_{31} and a_{33} are determined from (2.36), and the remaining direction cosines, taking (2.7) and (2.9) into account, take on the form:

$$\begin{cases} a_{11} = \dfrac{4va_{32}a_{33}}{H_2a_{32} + H_3a_{33}} \\ a_{12} = -\dfrac{4a_{31}a_{33}}{H_2a_{32} + H_3a_{33}} \\ a_{13} = -\dfrac{4va_{31}a_{32}}{H_2a_{32} + H_3a_{33}} \\ a_{21} = 4a_{31}\dfrac{a_{33}^2 - va_{32}^2}{H_2a_{32} + H_3a_{33}} \\ a_{22} = 4a_{32}\dfrac{(v+1)a_{33}^2 + va_{31}^2}{H_2a_{32} + H_3a_{33}} \\ a_{23} = -4a_{33}\dfrac{(v+1)a_{32}^2 + a_{31}^2}{H_2a_{32} + H_3a_{33}} \end{cases} \tag{2.43}$$

It can be concluded that in this case, the number of possible equilibrium positions, forming the group of solutions II, does not exceed 8.

2.2.1.3 Case $a_{31} = 0$, $a_{32} \neq 0$ and $a_{33} \neq 0$

At last, let us consider systems (2.5) and (2.6) which leads to:

$$\begin{cases} 4(Ba_{22}a_{32} + Ca_{23}a_{33}) + h_2a_{32} + h_3a_{33} = 0 \\ 0 = 0 \\ 0 = 0 \end{cases} \tag{2.44}$$

$$\begin{cases} a_{11}^2 = 1 \\ a_{22}^2 + a_{23}^2 = 1 \\ a_{32}^2 + a_{33}^2 = 1 \end{cases} \tag{2.45}$$

$$\begin{cases} a_{21} = 0 \\ 0 = 0 \\ a_{22}a_{32} + a_{23}a_{33} = 0 \end{cases} \tag{2.46}$$

Utilizing the first equation from (2.44) and the last equation from (2.46), we can obtain a 4th order equation in function of $x_3 = a_{22}$:

$$a_{22}a_{32} + a_{23}a_{33} = 0 \Leftrightarrow$$

$$\Leftrightarrow a_{32} = -\frac{a_{23}a_{33}}{a_{22}} \tag{2.47}$$

$$4(B - C)a_{22}a_{32} + h_2a_{32} + h_3a_{33} = 0 \Leftrightarrow$$

$$\Leftrightarrow -4(v+1)a_{22}a_{32} + H_2a_{32} + H_3a_{33} = 0 \Leftrightarrow$$

$$\Leftrightarrow a_{32}(H_2 - 4(v+1)a_{22}) + H_3 a_{33} = 0 \Leftrightarrow$$

$$\Leftrightarrow a_{32} = -\frac{H_3 a_{33}}{H_2 - 4(v+1)a_{22}} \Leftrightarrow$$

$$\Leftrightarrow -\frac{a_{23}a_{33}}{a_{22}} = -\frac{H_3 a_{33}}{H_2 - 4(v+1)a_{22}} \Leftrightarrow$$

$$\Leftrightarrow \left(\frac{a_{23}}{a_{22}}\right)^2 = \left(\frac{H_3}{H_2 - 4(v+1)a_{22}}\right)^2 \Leftrightarrow$$

Introducing $a_{23}^2 = 1 - a_{22}^2$ and raising the previous relationship to the power 2:

$$\Leftrightarrow \frac{1 - x_3^2}{x_3^2} = \frac{H_3^2}{(H_2 - 4(v+1)x_3)^2} \Leftrightarrow$$

$$\Leftrightarrow -16(v+1)^2 x_3^4 + 8H_2(v+1)x_3^3 + (-H_2^2 - H_3^2 + 16(v+1)^2)x_3^2 - 8H_2(v+1)x_3 + H_2^2 = 0 \quad (2.48)$$

Similar to first case (2.2.1.1), two equilibrium positions of the gyrostat correspond to each real root of this equation. The direction cosines are defined in function of x_3:

$$a_{22}a_{32} + a_{23}a_{33} = 0 \Leftrightarrow$$

$$\Leftrightarrow -\frac{-x_3 H_3 a_{33}}{H_2 - 4(v+1)x_3} + a_{23}a_{33} = 0 \Leftrightarrow$$

$$\Leftrightarrow a_{23} = \frac{H_3 x_3}{H_2 - 4(v+1)x_3} \quad (2.49)$$

$$\frac{a_{23}^2 a_{33}^2}{x_3^2} + a_{33}^2 = 1 \Leftrightarrow$$

$$\Leftrightarrow a_{23}^2 a_{33}^2 + a_{33}^2 x_3^2 = x_3^2 \Leftrightarrow$$

$$\Leftrightarrow a_{33}^2(a_{23}^2 + x_3^2) = x_3^2 \Leftrightarrow$$

$$\Leftrightarrow a_{33} = x_3 a_{11} \quad (2.50)$$

$$a_{32} = -\frac{a_{23}a_{11}x_3}{x_3} \Leftrightarrow$$

$$\Leftrightarrow a_{32} = -a_{23}a_{11} \quad (2.51)$$

Together, they form the group of solutions III:

$$\begin{cases} a_{11} = \pm 1 \\ a_{12} = 0 \\ a_{13} = 0 \\ a_{21} = 0 \\ a_{22} = x_3 \\ a_{23} = \dfrac{H_3 x_3}{H_2 - 4(v+1)x_3} \\ a_{31} = 0 \\ a_{32} = -a_{23} a_{11} \\ a_{33} = x_3 a_{11} \end{cases} \tag{2.52}$$

Similarly to (2.20), the equation is of fourth order and can have either 4 or 2 real roots. The number of roots changes on the surface are determined, using the same method as in the case (2.2.1.1), by the equation:

$$H_2^{2/3} + H_3^{2/3} = \left(4(v+1)\right)^{2/3} \tag{2.53}$$

Four roots exist at $H_2^{2/3} + H_3^{2/3} < \left(4(v+1)\right)^{2/3}$ and two roots at $H_2^{2/3} + H_3^{2/3} > \left(4(v+1)\right)^{2/3}$. Thus, the number of solutions of group III can be either 4 or 8.

2.3 Gyrostat's stability

In this section, the *Lyapunov*'s stability theory is reviewed and the sufficient conditions of stability for the equilibrium positions of a gyrostat satellite are obtained.

Consider in this study a dynamical system which satisfies:

$$\dot{x} = f(x) \quad x(t_o) = x_0 \quad x \in \mathbb{R}^n \tag{2.54}$$

According to [21], it is assumed that $f(x)$ is *Lipschitz* continuous with respect to x and uniformly in t. A point $x^* \in \mathbb{R}^n$ is an equilibrium position of (2.54) if $f(x^*) = 0$.

The equilibrium position x^* is stable in the sense of *Lyapunov*, if for any $\epsilon > 0$ there exists a $\delta(\epsilon) > 0$ such that

$$\|x(t_0)\| < \delta \implies \|x(t)\| < \epsilon, \quad \forall t \geq 0 \tag{2.55}$$

This definition of stability does not require that trajectories starting close to the origin tend to the origin asymptotically, in other words, the solutions which start in a neighborhood of x^* remain near x^* for all time.

The case of asymptotic stability is different, as solutions that are near an equilibrium position tend to the equilibrium position itself. In a mathematical way, the equilibrium position x^* is asymptotically stable if x^* is stable in the sense of *Lyapunov* and x^* is attractive, i.e, there exists δ such that:

$$\|x(t_0)\| < 0 \implies \lim_{t\to\infty} x(t) = 0 \tag{2.56}$$

Figure 2.2 shows a comparison between stable and unstable equilibrium positions.

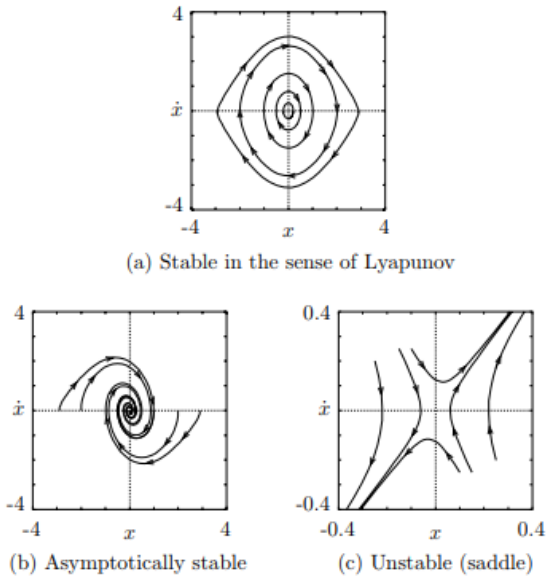

(a) Stable in the sense of Lyapunov

(b) Asymptotically stable

(c) Unstable (saddle)

Figure 2.2 – Phase portraits for stable and unstable equilibrium positions [21]

There is another method developed by *Lyapunov* called *Lyapunov*'s direct method (or second method of *Lyapunov*). In the literature in general, the method is seen as the most reliable in the study of stability of aerospace guidance systems, which typically contain strong nonlinearities. The method assumes that the energy of a system can be measured, therefore can be defined as a *Lyapunov*'s function. The study of the rate of change of the energy of the system can ascertain the stability of an equilibrium position.

As in previous studies [8] and [14], the generalized energy integral is continuous, therefore it can be used as Lyapunov's function:

$$\frac{1}{2}(A\bar{p}^2 + Bq^2 + C\bar{r}^2) + \frac{3}{2}\omega_0^2[(A-C)a_{31}^2 + (B-C)a_{32}^2] + \frac{1}{2}\omega_0^2[(B-A)a_{21}^2 + (B-C)a_{23}^2] - \omega_0\left[\overline{h_1}a_{21} + \overline{h_2}a_{22} + \overline{h_3}a_{23}\right] = H \tag{2.57}$$

Remembering the dimensionless parameters:

$$v = \frac{A-B}{C-A} \quad H_i = \frac{h_i}{C-A} \quad h_i = \frac{\overline{h_\iota}}{\omega_o} \tag{2.58}$$

It can be deducted that:

$$\begin{cases} h_i = \dfrac{\bar{h_\iota}}{\omega_0} \\ H_i = \dfrac{h_i}{C-A} \end{cases} \Leftrightarrow$$

$$\Leftrightarrow \begin{cases} \bar{h_i} = H_i(C-A) \end{cases} \Leftrightarrow$$

$$\Leftrightarrow \begin{cases} H_i(C-A) = \dfrac{\bar{h_\iota}}{\omega_0} \end{cases} \Leftrightarrow$$

$$\Leftrightarrow \begin{cases} \bar{h_\iota} = \omega_0 H_i(C-A) \end{cases} \tag{2.59}$$

Handily manipulating (2.57), the integral of energy can be presented as:

$$\frac{1}{2}(A\bar{p}^2 + Bq^2 + C\bar{r}^2) + \frac{3}{2}\omega_0^2[(A-C)a_{31}^2 + (B-C)a_{32}^2] + \frac{1}{2}\omega_0^2[(B-A)a_{21}^2 + (B-C)a_{23}^2] - \omega_0^2(C-A)(H_2a_{22} + H_3a_{23}) = H \Leftrightarrow$$

$$\Leftrightarrow \frac{1}{2}(A\bar{p}^2 + Bq^2 + C\bar{r}^2) + \frac{1}{2}\omega_0^2[3[(A-C)a_{31}^2 + (B-C)a_{32}^2] + [(B-A)a_{21}^2 + (B-C)a_{23}^2] - 2(C-A)(H_2a_{22} + H_3a_{23})] = H \tag{2.60}$$

Now, it will be introduced in this equation small variations in the direction angles, these variations might be interpreted as orbital disturbances, since the main purpose is to check how the system will respond to such disturbances near $\bar{\alpha}$, $\bar{\beta}$ and $\bar{\gamma}$. Thus, let us represent α, β and γ in the form:

$$\begin{cases} \alpha = \alpha_0 + \bar{\alpha} \\ \beta = \beta_0 + \bar{\beta} \\ \gamma = \gamma_0 + \bar{\gamma} \end{cases} \tag{2.61}$$

Where $\bar{\alpha}$, $\bar{\beta}$ and $\bar{\gamma}$ are small deviations from the satellite's equilibrium position with $\alpha = \alpha_0 = const$, $\beta = \beta_0 = const$ and $\gamma = \gamma_0 = const$. Then the energy integral can be written in the following form:

$$\frac{1}{2}(A\bar{p}^2 + Bq^2 + C\bar{r}^2) + \frac{1}{2}\omega_0^2\left(A_{\alpha\alpha}\bar{\alpha}^2 + A_{\beta\beta}\bar{\beta}^2 + A_{\gamma\gamma}\bar{\gamma}^2 + 2A_{\alpha\beta}\bar{\alpha}\bar{\beta} + 2A_{\beta\gamma}\bar{\beta}\bar{\gamma} + 2A_{\alpha\gamma}\bar{\gamma}\bar{\alpha}\right) + \sum = const \tag{2.62}$$

Where $\sum$ designates the terms of higher than second order of smallness with respect to $\bar{\alpha}$, $\bar{\beta}$, $\bar{\gamma}$.

Expanding the direction cosines according to a Taylor series [14]:

$$a_{ij}(\alpha,\beta,\gamma) = a_{ij}\left(\alpha_0+\bar{\alpha},\beta_0+\bar{\beta},\gamma_0+\bar{\gamma}\right) = a_{ij}(\alpha_o,\beta_0,\gamma_0) + \left(\frac{\partial \overline{a_{ij}}}{\partial\alpha}\bar{\alpha} + \frac{\partial \overline{a_{ij}}}{\partial\beta}\bar{\beta} + \frac{\partial \overline{a_{ij}}}{\partial\gamma}\bar{\gamma}\right) + \frac{1}{2}\left(\frac{\partial^2 \overline{a_{ij}}}{\partial\alpha^2}\bar{\alpha}^2 + \frac{\partial^2 \overline{a_{ij}}}{\partial\beta^2}\beta^2 + \frac{\partial^2 \overline{a_{ij}}}{\partial\gamma^2}\bar{\gamma}^2 + 2\frac{\partial^2 \overline{a_{ij}}}{\partial\alpha\partial\beta}\bar{\alpha}\bar{\beta} + 2\frac{\partial^2 \overline{a_{ij}}}{\partial\alpha\partial\gamma}\bar{\alpha}\bar{\gamma} + 2\frac{\partial^2 \overline{a_{ij}}}{\partial\beta\partial\gamma}\bar{\beta}\bar{\gamma}\right) \quad (2.63)$$

In order to study the stability of small displacements, it must be applied the expanded Taylor series above to the system of direction cosines (2.1), then when applied the small displacements described in (2.61), the system (2.1) is transformed into:

$$\begin{cases} \overline{a_{11}} = cos\alpha_0 \times cos\beta_0 \\ \overline{a_{12}} = sin\alpha_0 \times sin\gamma_0 - cos\alpha_0 \times sin\beta_0 \times cos\gamma_0 \\ \overline{a_{13}} = sin\alpha_0 \times cos\gamma_0 + cos\alpha_0 \times sin\beta_0 \times sin\gamma_0 \\ \overline{a_{21}} = sin\beta_0 \\ \overline{a_{22}} = cos\beta_0 \times cos\gamma_0 \\ \overline{a_{23}} = -cos\beta_0 \times sin\gamma_0 \\ \overline{a_{31}} = -sin\alpha_0 \times cos\beta_0 \\ \overline{a_{32}} = cos\alpha_0 \times sin\gamma_0 + sin\alpha_0 \times sin\beta_0 \times cos\gamma_0 \\ \overline{a_{33}} = cos\alpha_0 \times cos\gamma_0 - sin\alpha_0 \times sin\beta_0 \times sin\gamma_0 \end{cases} \quad (2.64)$$

After applying the Taylor series described in (2.63) to the system of direction cosines only for the relevant direction cosines a_{21}, a_{22}, a_{23}, $a_{31}$and a_{32}, it is obtained the following expressions:

$$a_{21} = \overline{a_{21}} + cos\beta_0\bar{\beta} + \frac{1}{2}\left(-\overline{a_{21}}\bar{\beta}^2\right)$$

$$a_{22} = \overline{a_{22}} + \left(-\overline{a_{21}}cos\gamma_0\bar{\beta} + \overline{a_{23}}\bar{\gamma}\right) + \frac{1}{2}\left(-\overline{a_{22}}\bar{\beta}^2 - \overline{a_{22}}\bar{\gamma}^2 + 2\overline{a_{21}}sin\gamma_0\bar{\beta}\bar{\gamma}\right)$$

$$a_{23} = \overline{a_{23}} + \left(-\overline{a_{22}}\bar{\gamma} + \overline{a_{21}}sin\gamma_0\bar{\beta}\right) + \frac{1}{2}\left(2\overline{a_{21}}cos\gamma_0\bar{\beta}\bar{\gamma} - \overline{a_{23}}\bar{\beta}^2 - \overline{a_{23}}\bar{\gamma}^2\right)$$

$$a_{31} = \overline{a_{31}} + \left(-\overline{a_{11}}\bar{\alpha} + \overline{a_{21}}sin\alpha_0\bar{\beta}\right) + \frac{1}{2}\left(-\overline{a_{31}}\bar{\alpha}^2 - \overline{a_{31}}\bar{\beta}^2 + 2\overline{a_{21}}cos\alpha_0\bar{\alpha}\bar{\beta}\right) \quad (2.65)$$

$$a_{32} = \overline{a_{32}} + \left(\overline{a_{22}}\sin\alpha_0\bar{\beta} - \overline{a_{12}}\bar{\alpha} + \overline{a_{33}}\bar{\gamma}\right) + \frac{1}{2}\left(2\overline{a_{11}}cos\gamma_0\bar{\alpha}\bar{\beta} - \overline{a_{21}}sin\alpha_0cos\gamma_0\bar{\beta}^2 + 2\overline{a_{23}}sin\alpha_o\bar{\beta}\bar{\gamma} - \overline{a_{32}}\bar{\alpha}^2 - \overline{a_{32}}\bar{\gamma}^2 - 2\overline{a_{13}}\bar{\alpha}\bar{\gamma}\right)$$

Adding the above calculated expanded Taylor's coefficients into the integral of energy (2.60), it is obtained the following coefficients:

$$
\begin{aligned}
A_{\alpha\alpha} &= 3\left[(A-C)\left(\overline{a_{11}}^2-\overline{a_{31}}^2\right)+(B-C)\left(\overline{a_{12}}^2-\overline{a_{32}}^2\right)\right]\\
A_{\beta\beta} &= (B-C)\left[3\left(\overline{a_{22}}^2\sin^2\alpha_0-\overline{a_{32}a_{21}}cos\gamma_0 sin\alpha_o\right)+\overline{a_{21}}^2\sin^2\gamma_0-\overline{a_{23}}^2\right]\\
&+(B-A)\left(\cos^2\beta_0-\overline{a_{21}}^2\right)+(A-C)\left[3\left(\overline{a_{21}}^2\sin^2\alpha_0-\overline{a_{31}}^2\right)-H_2\overline{a_{22}}-H_3\overline{a_{23}}\right]\\
A_{\gamma\gamma} &= (B-C)\left[\left(\overline{a_{22}}^2-\overline{a_{23}}^2\right)-3\left(\overline{a_{32}}^2-\overline{a_{33}}^2\right)\right]-(A-C)(H_2\overline{a_{22}}+H_3\overline{a_{23}})\\
A_{\alpha\beta} &= 3(A-C)(\overline{a_{21}a_{31}}cos\alpha_0-\overline{a_{11}a_{21}}sin\alpha_0)+3(B-C)(\overline{a_{11}a_{32}}cos\gamma_0-\overline{a_{12}a_{22}}sin\alpha_0)\\
A_{\beta\gamma} &= (B-C)[\overline{a_{21}}(\overline{a_{23}}cos\gamma_0-\overline{a_{22}}sin\gamma_0)+3sin\alpha_0(\overline{a_{22}a_{33}}+\overline{a_{23}a_{32}})]\\
&+(A-C)\overline{a_{21}}(H_2sin\gamma_0+H_3cos\gamma_0)\\
A_{\alpha\gamma} &= -3(B-C)(\overline{a_{12}a_{33}}+\overline{a_{13}a_{32}})
\end{aligned}
\tag{2.66}
$$

Where

$$\overline{a_{ij}}=a_{ij}(\alpha_o,\beta_o,\gamma_0)$$

Sarychev et.al [8] [14] referred that from the Lyapunov's theorem, it follows that the equilibrium solution $\alpha=\alpha_0$, $\beta=\beta_0$ and $\gamma=\gamma_0$ is asymptotically stable, if the quadratic form:

$$A_{\alpha\alpha}\bar{\alpha}^2+A_{\beta\beta}\bar{\beta}^2+A_{\gamma\gamma}\bar{\gamma}^2+2A_{\alpha\beta}\bar{\alpha}\bar{\beta}+2A_{\beta\gamma}\bar{\beta}\bar{\gamma}+2A_{\alpha\gamma}\bar{\gamma}\bar{\alpha} \tag{2.67}$$

is positive definite, i.e., at:

$$
\begin{cases}
A_{\alpha\alpha}>0\\
A_{\alpha\alpha}A_{\beta\beta}-A_{\alpha\beta}^2>0\\
A_{\alpha\alpha}A_{\beta\beta}A_{\gamma\gamma}+2A_{\alpha\beta}A_{\beta\gamma}A_{\alpha\gamma}-A_{\alpha\alpha}A_{\beta\gamma}^2-A_{\beta\beta}A_{\alpha\gamma}^2-A_{\gamma\gamma}A_{\alpha\beta}^2>0
\end{cases}
\tag{2.68}
$$

2.3.1 Solutions of Group I

First, taking (2.25) into account, it can be achieved that:

$$
\begin{cases}
a_{11}=0\\
a_{21}=0\\
a_{32}=0\\
a_{33}=0
\end{cases}
\Leftrightarrow
$$

$$\Leftrightarrow \begin{cases} cos\alpha_0 cos\beta_0 = 0 \\ sin\beta_0 = 0 \\ cos\alpha_0 sin\gamma_0 + sin\alpha_0 sin\beta_0 cos\gamma_0 = 0 \\ cos\alpha_0 cos\gamma_0 - sin\alpha_0 sin\beta_0 sin\gamma_0 = 0 \end{cases} \Leftrightarrow$$

$$\Leftrightarrow \begin{cases} sin\beta_0 = 0 \\ cos\alpha_0 = 0 \ \vee cos\beta_0 = 0 \\ cos\alpha_0 = 0 \ \vee cos\gamma_0 = 0 \\ cos\alpha_0 = 0 \ \vee sin\gamma_0 = 0 \end{cases} \Leftrightarrow$$

$$\Leftrightarrow \begin{cases} sin\beta_0 = 0 \\ cos\alpha_0 = 0 \end{cases} \tag{2.69}$$

Therefore, the coefficients of the quadratic form (2.67) take on the form:

$$A_{\alpha\alpha} = 3\left[(A-C)\left(-\overline{a_{31}}^2\right) + (B-C)\left(\overline{a_{12}}^2\right)\right]$$

$$A_{\beta\beta} = (B-C)\left[3\left(\overline{a_{22}}^2 \sin^2\alpha_0\right) - \overline{a_{23}}^2\right] + (B-A)(\cos^2\beta_0)$$
$$-(A-C)\left[3\left(\overline{a_{31}}^2\right) + H_2\overline{a_{22}} + H_3\overline{a_{23}}\right]$$

$$A_{\gamma\gamma} = (B-C)\left[\left(\overline{a_{22}}^2 - \overline{a_{23}}^2\right)\right] - (A-C)(H_2\overline{a_{22}} + H_3\overline{a_{23}}) \tag{2.70}$$

$$A_{\alpha\beta} = -3(B-C)(\overline{a_{12}a_{22}}sin\alpha_0)$$

$$A_{\beta\gamma} = 0$$

$$A_{\alpha\gamma} = 0$$

Thus, the sufficient conditions of stability are simplified to:

$$\begin{cases} A_{\alpha\alpha} > 0 \\ A_{\alpha\alpha}A_{\beta\beta} - A_{\alpha\beta}^2 > 0 \end{cases} \tag{2.71}$$

Introducing the expressions (2.25) and transforming the sufficient conditions of stability into dimensionless, they take on the form:

$$A_{\alpha\alpha} > 0 \Leftrightarrow$$

$$\Leftrightarrow \frac{3\left[(A-C)\left(-\overline{a_{31}}^2\right) + (B-C)\left(\overline{a_{12}}^2\right)\right]}{C-A} > 0 \Leftrightarrow$$

$$\Leftrightarrow \overline{a_{31}}^2 - (v+1)\overline{a_{12}}^2 > 0 \Leftrightarrow$$

$$\Leftrightarrow 1 - (v+1)\left(\frac{H_3^2 x_1^2}{\left(H_2 - x_1(v+1)\right)^2}\right) > 0 \tag{2.72}$$

$A_{\alpha\alpha}A_{\beta\beta} - A_{\alpha\beta}^2 > 0 \Leftrightarrow$

$$\Leftrightarrow 3\left[(A-C)\left(-\overline{a_{31}}^2\right) + (B-C)\left(\overline{a_{12}}^2\right)\right]$$
$$\times\left[(B-C)\left[3\left(\overline{a_{22}}^2\sin^2\alpha_0\right) - \overline{a_{23}}^2\right] + (B-A)(\cos^2\beta_0)\right.$$
$$\left. - (A-C)\left[3\left(\overline{a_{31}}^2\right) + H_2\overline{a_{22}} + H_3\overline{a_{23}}\right]\right] - [-3(B-C)(\overline{a_{12}a_{22}}sin\alpha_0)]^2 > 0 \Leftrightarrow$$

$$\Leftrightarrow 3\left[1-(v+1)\left(\frac{H_3^2x_1^2}{\left(H_2-x_1(v+1)\right)^2}\right)\right]\times\left[-(v+1)\left[3(x_1^2\sin^2\alpha_0) - \frac{H_3^2x_1^2}{\left(H_2-x_1(v+1)\right)^2}\right] - v(\cos^2\beta_0) + \right.$$
$$\left.\left[3 + H_2x_1 + \frac{H_3^2x_1}{H_2-x_1(v+1)}\right]\right] - \left[9(v+1)^2\left(\frac{H_3^2x_1^4}{\left(H_2-x_1(v+1)\right)^2}sin\alpha_0\right)\right] > 0 \quad (2.73)$$

2.3.2 Solutions of Group II

The study of the stability of the solutions of group II leads to a harder problem. In this case, the relations (2.33, 2.34 and 2.43) should be used to determine a_{31},a_{32} and a_{33} and (2.43) for the rest of elements of the matrix of direction cosines. Then, the angles α_0, β_0 and γ_0 are determined explicitly and the coefficients of quadratic form (2.66) are calculated, as well as the conditions of its positive definiteness.

2.3.3 Solutions of Group III

Let us take (2.52) into account, so it can be achieved these:

$$\begin{cases} a_{12} = 0 \\ a_{13} = 0 \\ a_{21} = 0 \\ a_{31} = 0 \end{cases} \Leftrightarrow$$

$$\Leftrightarrow \begin{cases} sin\alpha_0 sin\gamma_0 - cos\alpha_0 sin\beta_0 cos\gamma_0 = 0 \\ sin\alpha_0 cos\gamma_0 + cos\alpha_0 sin\beta_0 sin\gamma_0 = 0 \\ sin\beta_0 = 0 \\ -sin\alpha_0 cos\beta_0 = 0 \end{cases} \Leftrightarrow$$

$$\Leftrightarrow \begin{cases} sin\beta_0 = 0 \\ sin\alpha_0 = 0 \ \vee sin\gamma_0 = 0 \\ sin\alpha_0 = 0 \ \vee cos\gamma_0 = 0 \\ sin\alpha_0 = 0 \ \vee cos\beta_0 = 0 \end{cases} \Leftrightarrow$$

$$\Leftrightarrow \begin{cases} sin\beta_0 = 0 \\ sin\alpha_0 = 0 \end{cases} \quad (2.74)$$

Therefore, the coefficients of the quadratic form (2.67) take on the form:

$$
\begin{aligned}
A_{\alpha\alpha} &= 3\left[(A-C)\left(\overline{a_{11}}^2\right)+(B-C)\left(-\overline{a_{32}}^2\right)\right] \\
A_{\beta\beta} &= (B-C)\left[-\overline{a_{23}}^2\right]+(B-A)(\cos^2\beta_0)-(A-C)[H_2\overline{a_{22}}+H_3\overline{a_{23}}] \\
A_{\gamma\gamma} &= (B-C)\left[\left(\overline{a_{22}}^2-\overline{a_{23}}^2\right)-3\left(\overline{a_{32}}^2-\overline{a_{33}}^2\right)\right]-(A-C)(H_2\overline{a_{22}}+H_3\overline{a_{23}}) \\
A_{\alpha\beta} &= 3(B-C)(\overline{a_{11}a_{32}}cos\gamma_0) \\
A_{\beta\gamma} &= 0 \\
A_{\alpha\gamma} &= 0
\end{aligned}
\tag{2.75}
$$

Thus, the sufficient conditions of stability are simplified to:

$$
\begin{cases}
A_{\alpha\alpha} > 0 \\
A_{\alpha\alpha}A_{\beta\beta}-A_{\alpha\beta}^2 > 0
\end{cases}
\tag{2.76}
$$

Introducing the expressions (2.52) and transforming the sufficient conditions of stability into dimensionless, they take on the form:

$$
\begin{gathered}
A_{\alpha\alpha} > 0 \Leftrightarrow \\
\Leftrightarrow -\left(\overline{a_{11}}^2\right)+(v+1)\left(\overline{a_{32}}^2\right) > 0 \Leftrightarrow \\
\Leftrightarrow -1+(v+1)\left(\frac{H_3^2x_3^2}{(H_2-4(v+1)x_3)^2}\right) > 0
\end{gathered}
\tag{2.77}
$$

$$
\begin{aligned}
&A_{\alpha\alpha}A_{\beta\beta}-A_{\alpha\beta}^2 > 0 \Leftrightarrow \\
&\Leftrightarrow \left[3\left[(A-C)\left(\overline{a_{11}}^2\right)+(B-C)\left(-\overline{a_{32}}^2\right)\right]\right] \\
&\times\left[(B-C)\left[-\overline{a_{23}}^2\right]+(B-A)(\cos^2\beta_0)-(A-C)[H_2\overline{a_{22}}+H_3\overline{a_{23}}]\right] \\
&-[3(B-C)(\overline{a_{11}a_{32}}cos\gamma_0)]^2 > 0 \Leftrightarrow \\
&\Leftrightarrow \left[3\left[-1+(v+1)\left(\frac{H_3^2x_3^2}{(H_2-4(v+1)x_3)^2}\right)\right]\right] \\
&\times\left[(v+1)\left(\frac{H_3^2x_3^2}{(H_2-4(v+1)x_3)^2}\right)-v(\cos^2\beta_0)+\left[H_2x_3+\frac{H_3^2x_3}{H_2-4(v+1)x_3}\right]\right] \\
&-9(v+1)^2\left(\frac{H_3^2x_3^2}{(H_2-4(v+1)x_3)^2}\right)cos\gamma_0 > 0
\end{aligned}
\tag{2.78}
$$

Chapter 3

Results and Discussion

In this chapter, the mathematical model discussed in Chapter 3 is implemented to study the equilibria and stability of a gyrostat satellite. Several numeric computations are carried in function of different system parameters v, H_3 and H_2. First, in section 3.1 is shown the general behavior of equilibria for each group of solutions I, II and III. It is displayed the evolution of equilibrium positions in function of spacecraft angles α, β and γ and the evolution of equilibria bifurcation, in subsection 3.1.1 and 3.1.2. Without forgetting that is also verified the existence of the small regions found by Santos in [14] and Santos et al. [20], in subsection 3.1.3. Finally, in section 3.2 is discussed the stability of the gyrostat satellite in function of system parameters.

3.1 Gyrostat's equilibria

In this section, a study of the gyrostat's equilibria bifurcation is conducted in function of dimensionless parameters v, H_2 and H_3. In general, a bifurcation curve is a boundary at which the number of equilibrium positions changes from a fixed value to another. A comparison between the results obtained by *Sarychev et. al.* in [8] and the results obtained in the present work is shown, in order to verify if there is any correlation when a different component of the gyrostatic moment vector is zero ($H_1 = 0$) and when a similar mathematical model is used. Also, the existence of small regions of 12 and 16 equilibrium positions near $H_1 = 0$ revealed by Santos ([14] and [20]) in his study of the general case is verified and compared to this study.

The interval of values of inertial dimensionless parameter v depends on the inertial configuration used. In the specific case of this study and for comparing purposes, the inertial configuration used is $B > A > C$, which means that $v > 0$. The values analyzed are between $v = 0.1$ (near $v = 0$) and $v = 10$, giving an overview of the influence of parameter v on the results. For $v > 10$, although, all equilibria regions increase in size, they remain in equal number and shape. There is also no appearance or disappearance of new regions.

Solving the equations (2.20) and (2.48) in the plane (H_3, H_2) represents the equilibria bifurcation for cases ($a_{31} = 0$, $a_{32} \neq 0$ and , $a_{33} \neq 0$) and ($a_{31} \neq 0$ and $a_{32} = a_{33} = 0$), an example for $v = 1.5$ is shown in Figure 3.1. For case ($a_{31} \neq 0$, $a_{32} \neq 0$ and $a_{33} \neq 0$) is a more difficult problem because solutions of system (2.11) only correspond to an equilibrium position of the gyrostat when inequalities (2.42) and $\Delta = c_1^2 - 4c_0c_2 \geq 0$ are valid. The regions in the plane (H_3, H_2) in which $\Delta = c_1^2 - 4c_0c_2 \geq 0$ for $v = 1.5$ are presented in Figure 3.2 by a light gray coloring.

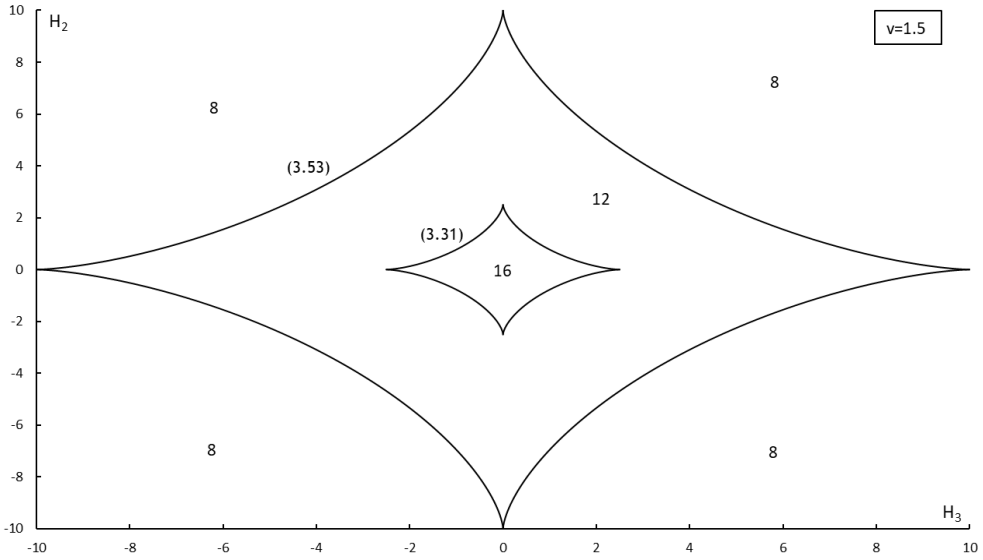

Figure 3.1 – Bifurcation curves for group of solutions I and III for $v = 1.5$.

Analyzing the Figure 3.1, the curves (2.31) and (2.53) divide the plane (H_3, H_2) in three sub-regions. If $H_2^{2/3} + H_3^{2/3} < (v+1)^{2/3}$, exits 16 solutions (i.e. equilibrium positions), 8 solutions for each group of solutions I and III; if $(v+1)^{2/3} < H_2^{2/3} + H_3^{2/3} < \left(4(v+1)\right)^{2/3}$, there are 12 solutions, 8 solutions from group of solutions III and 4 solutions of group I; and if $H_2^{2/3} + H_3^{2/3} > \left(4(v+1)\right)^{2/3}$, there are 8 solutions, 4 solutions from each group of solutions I and III. This result is like the ones found in [8].

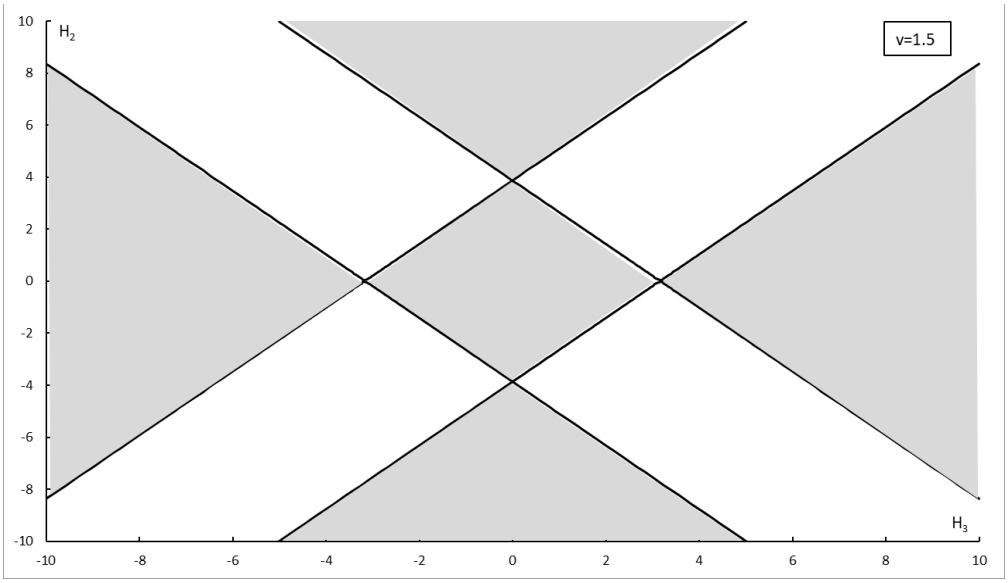

Figure 3.2 – The regions of validity of conditions (2.38) for $v = 1.5$.

As mentioned in [8], inequalities (2.42) needs a closer look since they can be valid either for both signs before the square root or only for one sign, which means the existence of equilibrium positions corresponding to both roots of (2.32) or only one root ($x_{2,1}$ or $x_{2,2}$). The analysis of the regions of validity of inequalities (2.42) for each root of (2.32) at $v = 1.5$, considering that $v > 0$, are presented in Figures 3.3 and Figure 3.4. The dashed lines represent when the discriminant (Δ) (2.34) is equal to zero, which is reflected in more detail in Figure 3.2.

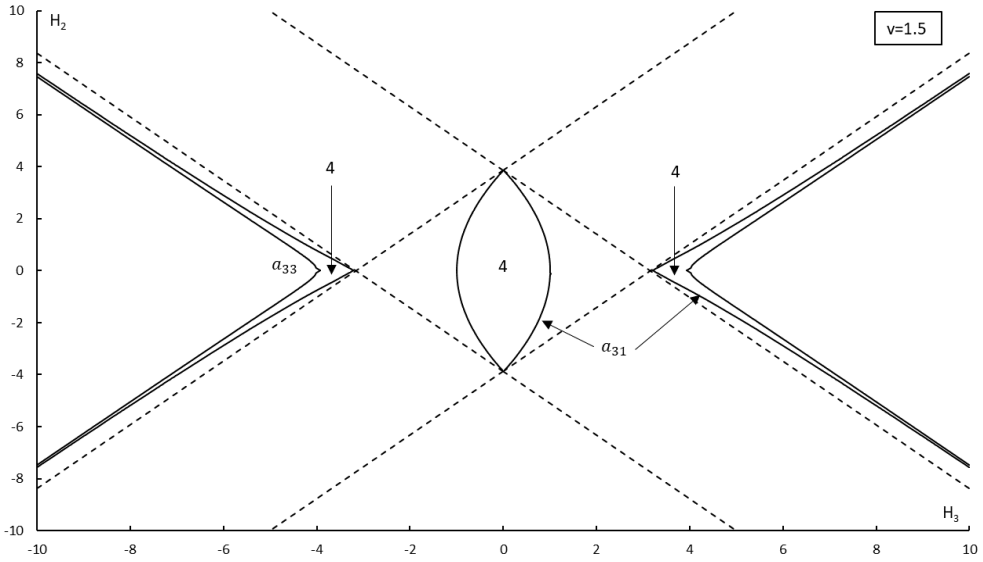

Figure 3.3 – Regions of validity of the conditions $a_{31}^2 \geq 0$ and $a_{33}^2 \geq 0$ for the positive root of (2.32) at $v = 1.5$.

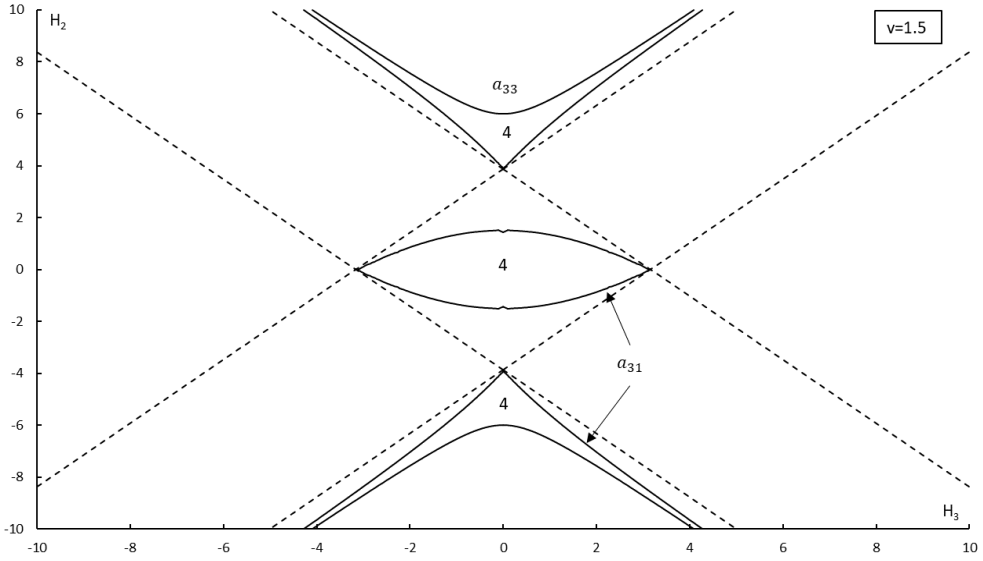

Figure 3.4 – Regions of validity of the conditions $a_{31}^2 \geq 0$ and $a_{33}^2 \geq 0$ for the negative root of (2.32) at $v = 1.5$.

For each case presented in Figures 3.3 and 3.4, the full lines represent when expressions (2.42) are equal to zero. The areas delimited by full lines are regions where the conditions (2.42) are valid for each root of equation (2.32). In each of these regions, there are four solutions of Group II; and beyond their boundaries, there are no solutions, since one or both conditions (2.42) are invalid. Combining results in Figure 3.3 and 3.4, the study of equilibria bifurcation of Group II is achieved in Figure 3.5.

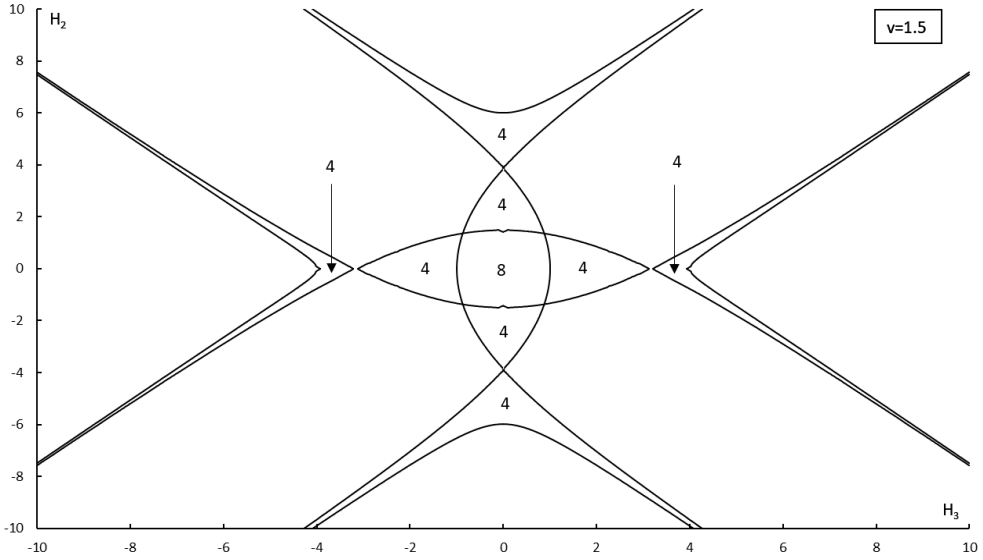

Figure 3.5 – Bifurcation curves for solutions of Group II at $v = 1.5$.

The complete equilibria bifurcation study of the gyrostat at $v = 1.5$, combining the study of bifurcation of solutions of Group I, II and III are presented in Figure 3.6. Notice that the plane (H_3, H_2) are portioned into sub-regions, in each of them there are a certain fixed number of equilibrium positions and the curves are symmetric in relation to the origin of the coordinated axes, as mentioned in [14] and [20] by Santos. To help visualize the different conditions of each group I, II and III presented in Figure 3.6, a color notation is used (see table 3.1).

Table 3.1 – Color notation of Figure 3.6.

Curve (2.31)	Curve $a_{31}^2 = 0$ (2.36)	Curve $a_{33}^2 = 0$ (2.37)	Curve (2.53)
Blue	Orange	Yellow	Green

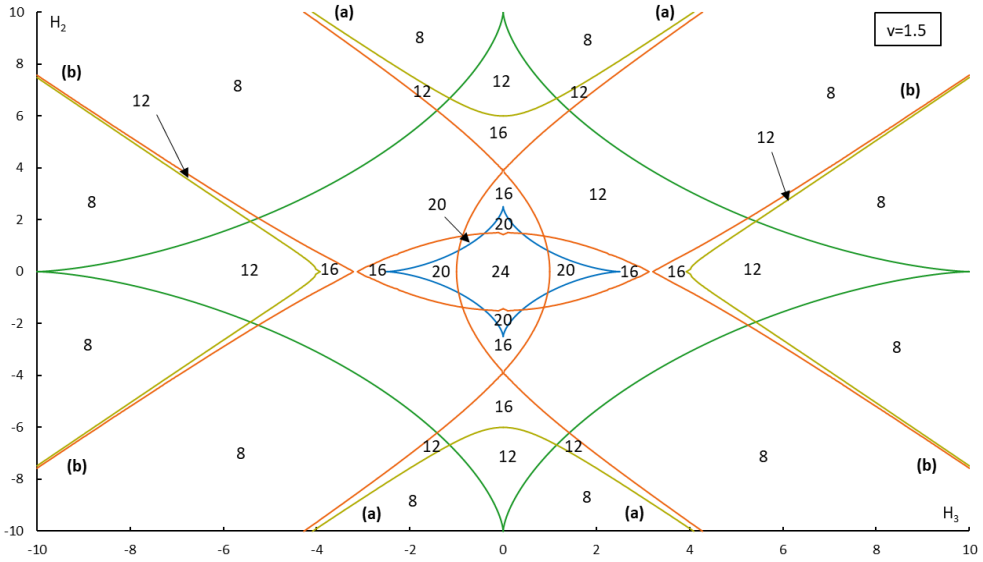

Figure 3.6 – Gyrostat's equilibria bifurcation at $v = 1.5$.

One can see from Figure 3.6 that there are no more than 24 equilibrium positions and no less than 8 equilibrium positions, the same conclusions were obtained in [6], [8], [14] and [20] for other configurations of the gyrostatic moment vector. It is important to mention the two regions of 12 equilibrium positions: (a) and (b). These regions are completely new in the study of this type of gyrostats, they head towards infinity by an oblique asymptote inside a region of eight equilibrium positions, the distance between the boundaries that define them decreases in direction to infinity and they seem to share a relation of parallelism between them.

3.1.1 Evolution of equilibrium positions of the gyrostat at specific $v = 1.5$

The evolution of equilibrium positions of the gyrostat along the plane (H_3, H_2) described by the spacecraft angles α, β and γ at a specific v is relevant to show the relation between gyrostat's equilibria bifurcation curves, shown in Figure 3.6, and the behavior of the spacecraft angles from these equilibrium solutions. Considering the straight line $R(H_2 = H_3)$ at fixed $v = 1.5$, from the origin of coordinates axes along the 1st quadrant of plane (H_3, H_2), for comparison with [8] and because it go through each type of region (24, 20, 16, 12 and 8), is represented in Figure 3.7.

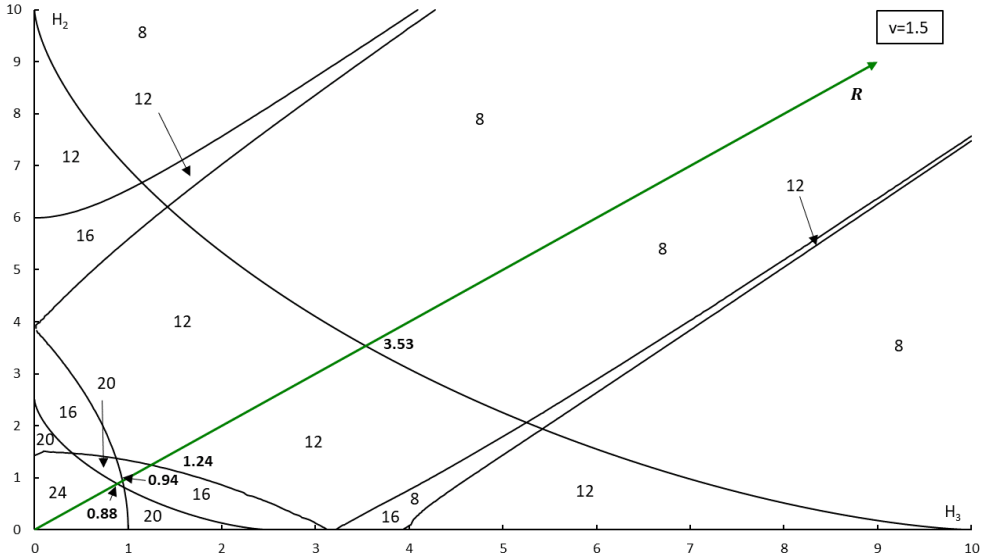

Figure 3.7 – Gyrostat's equilibria bifurcation at $v = 1.5$ and straight line $R(H_2 = H_3)$ with bifurcation values.

Each equilibrium positions of group I (group III) is determined by choosing one of roots of equation (2.20) (equation (2.48)), selecting the sign of direction cosine a_{31} (a_{11}) and using the expressions (2.25) (expressions (2.52)). The roots can have 4 real roots or 2 real roots depending if the ordered pair (H_3, H_2) is before or after the curve (2.31) (curve (2.53)). The equilibrium positions for group II are calculated in a more complex way: (a) choose one of roots of equation (2.32); (b) check the validity of conditions: $a_{31}^2 \geq 0$ and $a_{33}^2 \geq 0$; (c) select the signs of direction cosines a_{31} and a_{33}; and in last, (d) use expressions (2.43) to calculate the other direction cosines. The spacecraft angles α, β and γ are determined using expressions (2.2).

Table 3.2 – Equilibrium positions indexes for solutions of Group I, II and III.

Group I			Group II				Group III		
Root (2.20)	Sign a_{31}	Index	Root (2.32)	Sign a_{32}	Sign a_{33}	Index	Root (2.48)	Sign a_{11}	Index
1	-	1.1	1	-	-	2.1	1	-	3.1
	+	1.2		-	+	2.2		+	3.2
2	-	1.3		+	-	2.3	2	-	3.3
	+	1.4		+	+	2.4		+	3.4
3	-	1.5	2	-	-	2.5	3	-	3.5
	+	1.6		-	+	2.6		+	3.6
4	-	1.7		+	-	2.7	4	-	3.7
	+	1.8		+	+	2.8		+	3.8

Following this logic, it is built a chart describing the evolution of the spacecraft angles corresponding to $R(H_2 = H_3)$ shown in Figure 3.8, and it was introduced the equilibrium positions index (see Table 3.1). The notation used for the equilibrium indexes are adapted from [8], for the sake of comparison. The lines have three different colors: blue, orange and yellow and three chart markers: circle, square and triangle, corresponding to the solutions of group I, II and III, respectively. The horizontal dashed lines represent: $H_2 = \pi/4$, $H_2 = \pi/2$, $H_2 = \pi$, $H_2 = 3\pi/2$ and $H_2 = 2\pi$, when they are relevant in the chart.

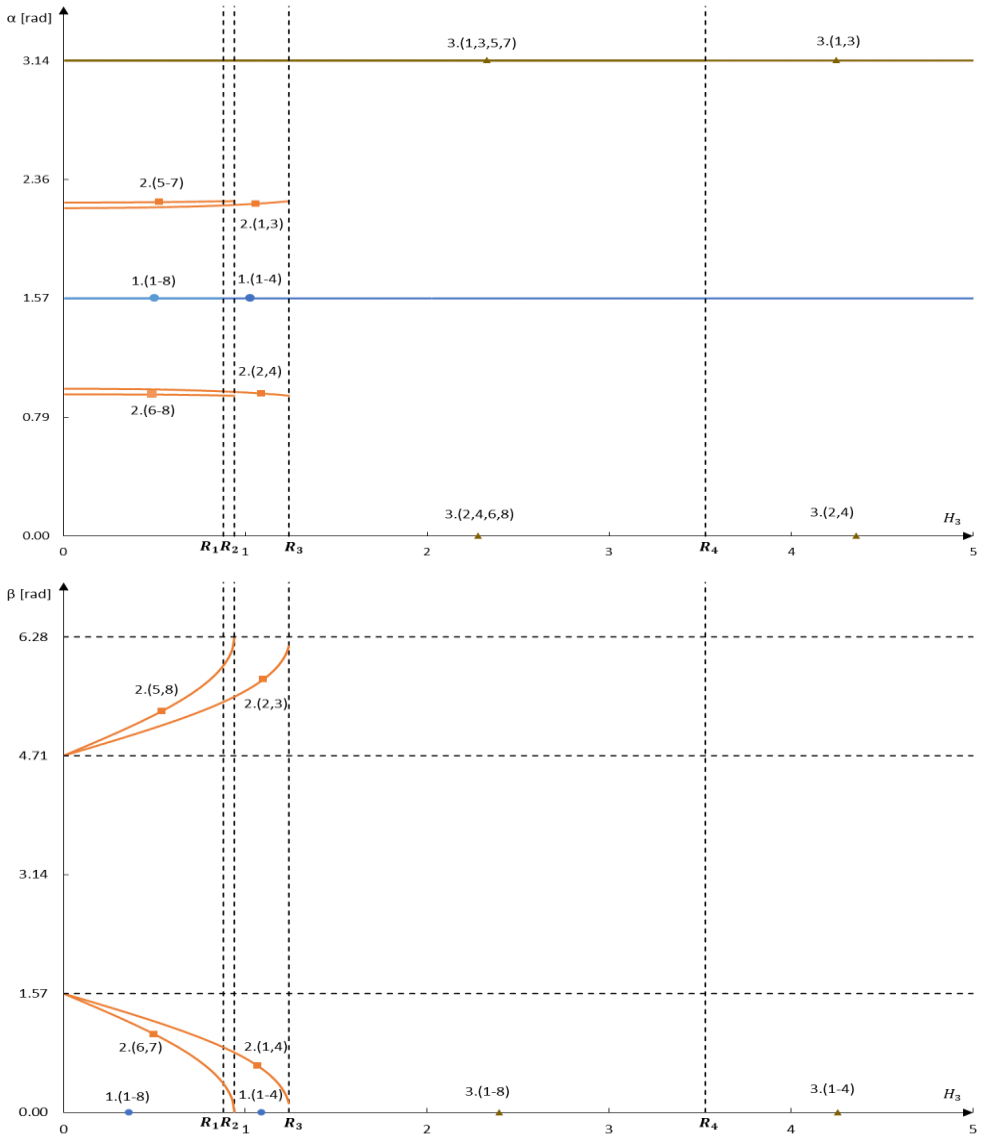

Figure 3.8 – Equilibrium positions of a gyrostat at $v = 1.5$ and for $R(H_2 = H_3)$ described by angles α, β and γ.

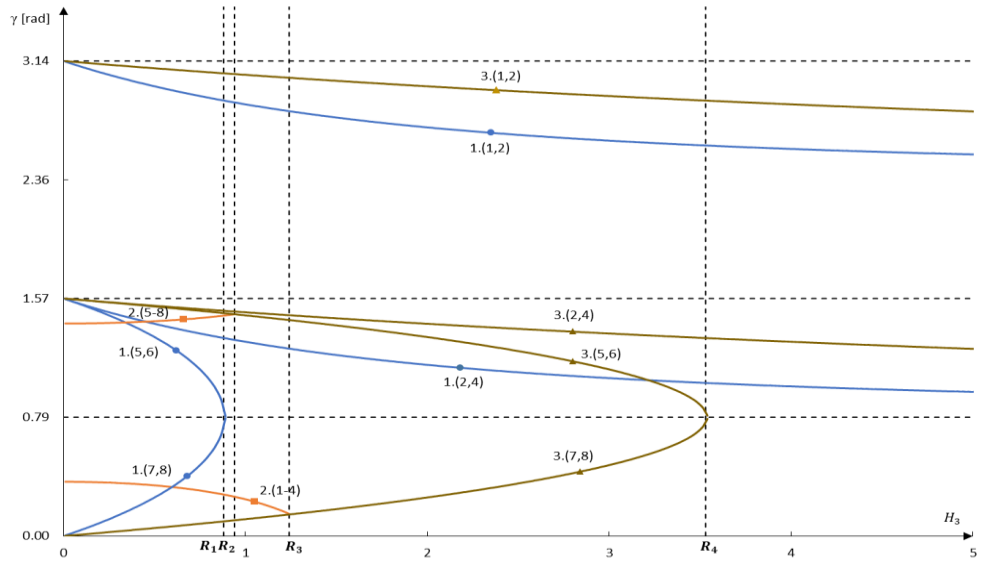

Figure 3.8 - Equilibrium positions of a gyrostat at $v = 1.5$ and for $R(H_2 = H_3)$ described by angles α, β and γ (cont.).

From analysis of Figure 3.8, there are four values ($R_1 = 0.88$, $R_2 = 0.94$, $R_3 = 1.24$ and $R_4 = 3.53$), at which the fixed number of equilibrium positions changes.

For $H_3 \in [0; 0.88]$, there are 24 solutions represented by the following indexes (1.(1-8); 2.(1-8) and 3.(1-8)), see Figure 3.8 for angle α; at the intersection of straight line $R_1 = 0.88$ and curve (2.31), four solutions of group I (1.(5-8)) disappear when the angle γ corresponding to these solutions is $\pi/4$.

For $H_3 \in [0.88; 0.94]$, there are 20 solutions (1.(1-4); 2.(1-8) and 3.(1-8)); at the intersection between straight line $R_2 = 0.94$ and curve a_{31} (2.36), four solutions of group II disappear when the angle β corresponding to these solutions is 0 (2.(6,7)) or 2π (2(5,8)).

For $H_3 \in [0.94; 1.24]$, there are 16 solutions (1.(1-4); 2.(1-4) and 3.(1-8)); at the intersection between $R_3 = 1.24$ and curve a_{31} (2.36), the last four solutions of group II disappear when the angle β corresponding to these solutions is 0 (2.(1,4)) or 2π (2.(2,3)).

For $H_3 \in [1.24; 3.53]$, there are 12 solutions (1.(1-4) and 3.(1-8)), at the intersection between $R_4 = 3.53$ and curve (2.53), four solutions of group III (3.(5-8)) disappear when the angle γ corresponding to these solutions is $\pi/4$.

At $R > 3.53$ until the end of the window of Figure 3.7, there are only 8 solutions (1.(1-4) and 3.(1-4)), the values of angles α and β remains constant and the angle γ tends to a constant value with increase R, for each solution.

A summary of the above analysis is shown in table 3.3.

Table 3.3 – Summary of equilibrium solutions and spacecraft angles β and γ from Figure 3.8.

	0	$\leftrightarrow$	R_1 ∩ Curve (2.31)	$\leftrightarrow$	R_2 ∩ curve a_{31} (2.36)	$\leftrightarrow$	R_3 ∩ curve a_{31} (2.36)	$\leftrightarrow$	R_4 ∩ Curve (2.31)	$\rightarrow$
Equilibrium solutions	24 (1.(1-8), 2.(1-8) and 3.(1-8))		–	20 (1.(1-4), 2.(1-8) and 3.(1-8))	–	16 (1.(1-4), 2.(1-4) and 3.(1-8))	–	12 (1.(1-4) and 3.(1-8))	–	8 (1.(1-4) and 3.(1-4))
Angle β	0 (1.(1-8) and (3.(1-8))		–	0 (1.(1-4)) and (3.(1-8))	0 (2.(6,7)) or 2π (2.(5,8))	0 (1.(1-4) and (3.(1-8))	0 (2.(1,4)) or 2π (2.(2,3))	0 (1.(1-4) and (3.(1-8	–	0 (1.(1-4) and (3.(1-4))
Angle γ	–		$\pi/4$ (1.(5-8))	–	–	–	–	–	$\pi/4$ (3.(5-8))	Tends to be constant

Now, let us analyze some peculiarities of the study of angles α, β and γ. One can see in Figure 3.8 for angle α, the solutions of group I overlap for the angle $\alpha = \pi/2$ and solutions of group III overlap for the angle $\alpha = 0$ and $\alpha = 2\pi$, remembering expressions (2.2), (2.25) and (2.52), this can be easily demonstrated:

Group I:

$$a_{21} = 0 \Leftrightarrow$$

$$\Leftrightarrow \beta = 0 \tag{3.1}$$

$$a_{11} = 0$$

$$\alpha = \cos^{-1}(a_{11}/cos\beta) \Leftrightarrow$$

$$\Leftrightarrow \alpha = \frac{\pi}{2} \tag{3.2}$$

Group III:

$$a_{21} = 0 \Leftrightarrow$$

$$\Leftrightarrow \beta = 0 \tag{3.3}$$

$$a_{11} = \pm 1$$

$$\alpha = \cos^{-1}(a_{11}/cos\beta) \Leftrightarrow$$

$$\Leftrightarrow \alpha = 0 \vee \alpha = 2\pi \tag{3.4}$$

For Figure 3.8 of angle β, solutions of group I and III overlap for $\beta = 0$, this can be easily explained by looking to the above demonstrations (3.1-3.4). In the case of angle γ, the solutions of group II overlap too but in a different way, 4 solutions (2.(1-4)) overlap in the form of a curve with the same equation and the other 4 solutions (2.(5-8)) overlap in the same manner but into different curve. This case can be demonstrated by remembering expressions (2.43) from group II:

$$\alpha = \sin^{-1}(a_{21})$$

$$\gamma = \cos^{-1}(a_{22}/\cos\beta)$$

$$a_{32} = x_2 a_{33}$$

$$a_{21} = 4a_{31}\frac{a_{33}^2 - va_{32}^2}{H_2a_{32} + H_3a_{33}} \Leftrightarrow$$

$$\Leftrightarrow a_{21} = \frac{4a_{31}}{a_{33}} \times \frac{(v+1)a_{33}^2 + a_{31}^2 v}{H_2x_2 + H_3} \tag{3.5}$$

$$a_{22} = 4a_{32}\frac{(v+1)a_{33}^2 + va_{31}^2}{H_2a_{32} + H_3a_{33}} \Leftrightarrow$$

$$\Leftrightarrow a_{22} = 4x_2\frac{(v+1)a_{32}^2 + a_{31}^2 v}{H_2x_2 + H_3} \tag{3.6}$$

For the same H_3, H_2 and v, the group II can have two roots x_2. For the first root, taking the case (2.(1-4)), the value of a_{31}^2, a_{33}^2 and a_{32}^2(see expression (2.36) and $a_{32} = x_2a_{33}$) is always the same for the 4 solutions, therefore the direction cosine a_{22} is also the same for the 4 solutions. In the case of direction cosine a_{21}, it depends only on quotient a_{31}/a_{33}; this remains the same in absolute value, but it alternates between positive sign and negative sign depending of the sign of a_{31} and a_{33}. Remembering the unit circle, a positive or negative sine of arbitrary angle always corresponds to a positive cosine. As direction cosine a_{22} and $cos\beta$ remains always constant for the 4 solutions, it can be concluded that the angle γ remains always constant for the 4 solutions. This demonstration can be extended for the case of solutions (2.(5-8)).

3.1.2 Evolution of equilibria bifurcation for different values of v

In this section, a study of the evolution of the regions with a fixed number of equilibrium positions of a gyrostat along the plane (H_3, H_2) is conducted for different values of parameter v. The inertia parameters v selected were: $v = 0.1$ (near limit value $v = 0$), $v = 0.2$, $v = 0.3$, $v = 0.5$, $v = 0.7$, $v = 0.9$, $v = 1.0$, $v = 1.5$, $v = 2.0$, $v = 4.0$, $v = 5.0$ and $v = 10.0$. The results are shown along the Figures 3.9 to 3.20.

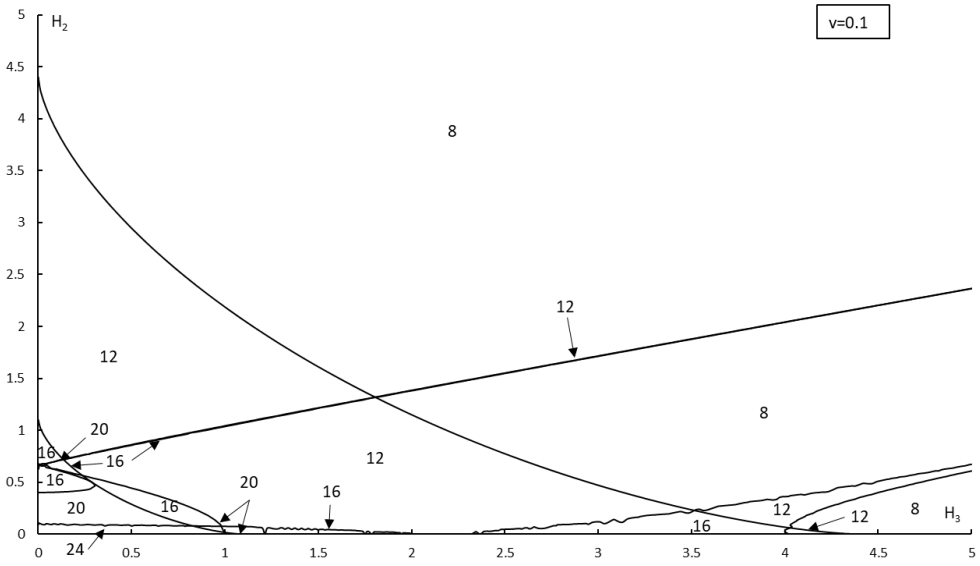

Figure 3.9 - Gyrostat's equilibria bifurcation at $v = 0.1$.

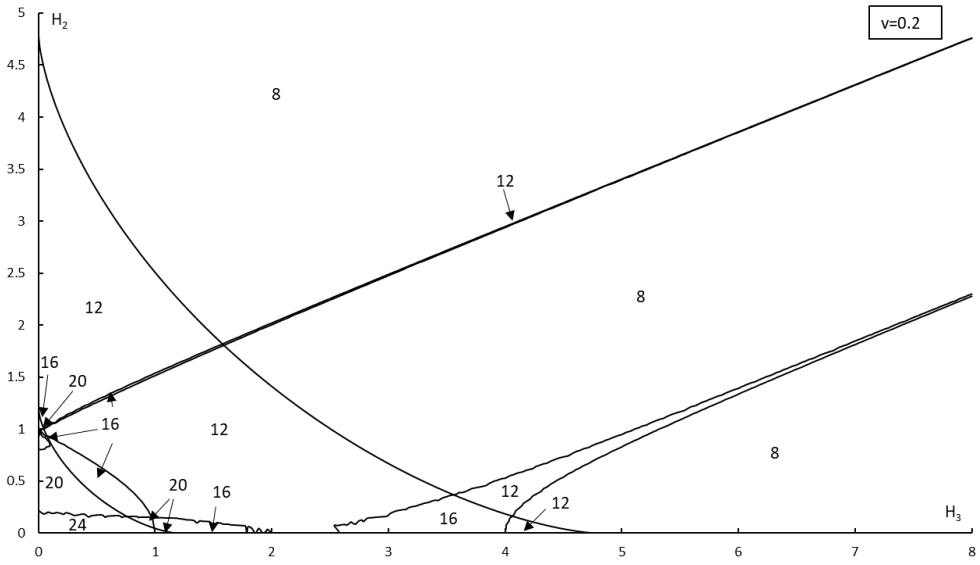

Figure 3.10 - Gyrostat's equilibria bifurcation at $v = 0.2$.

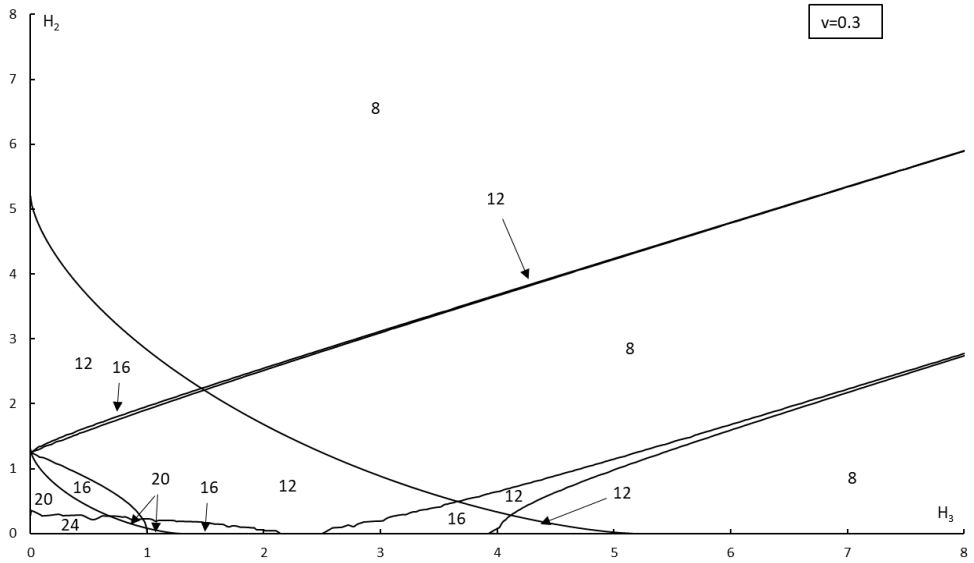

Figure 3.11 - Gyrostat's equilibria bifurcation at $v = 0.3$.

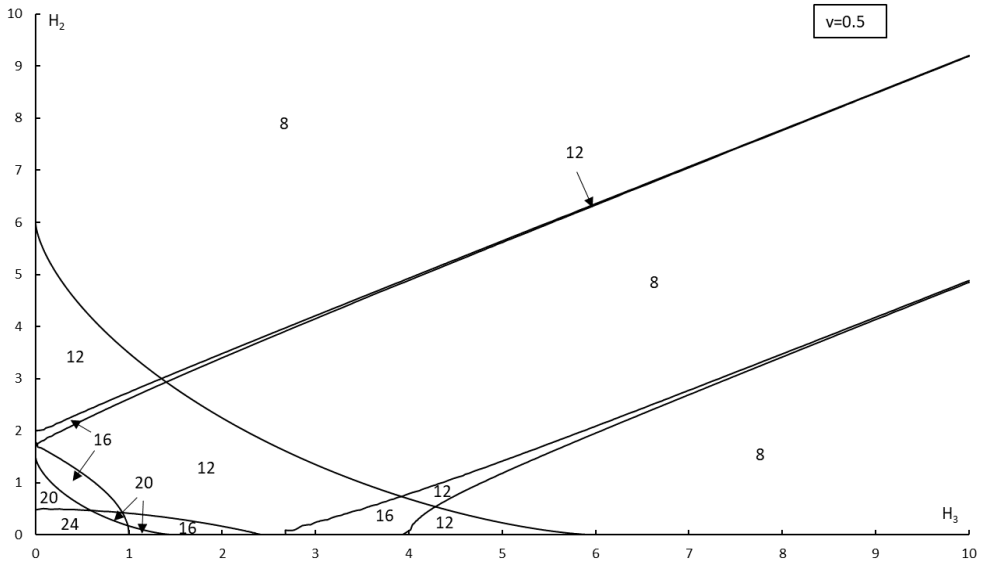

Figure 3.12 - Gyrostat's equilibria bifurcation at $v = 0.5$.

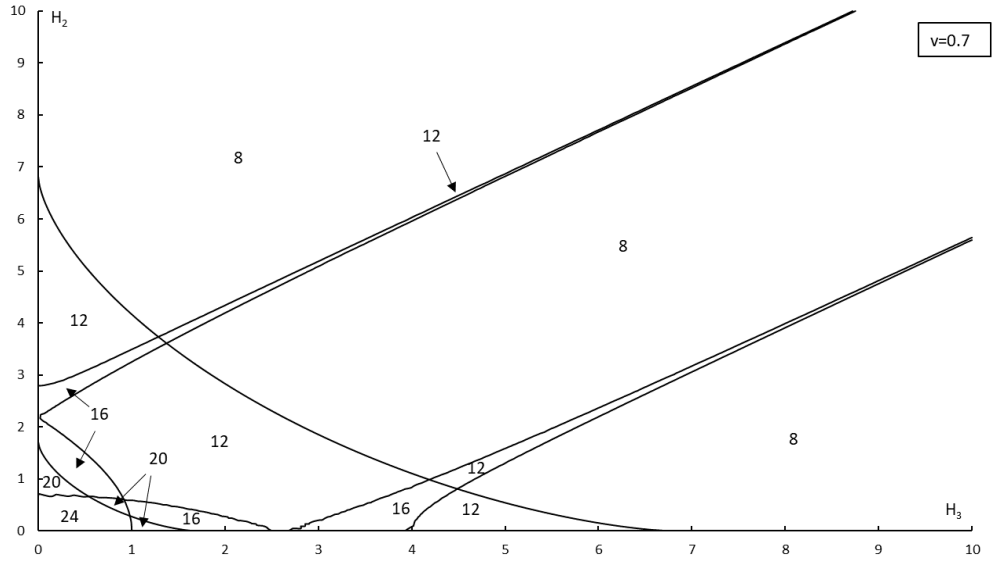

Figure 3.13 - Gyrostat's equilibria bifurcation at $v = 0.7$.

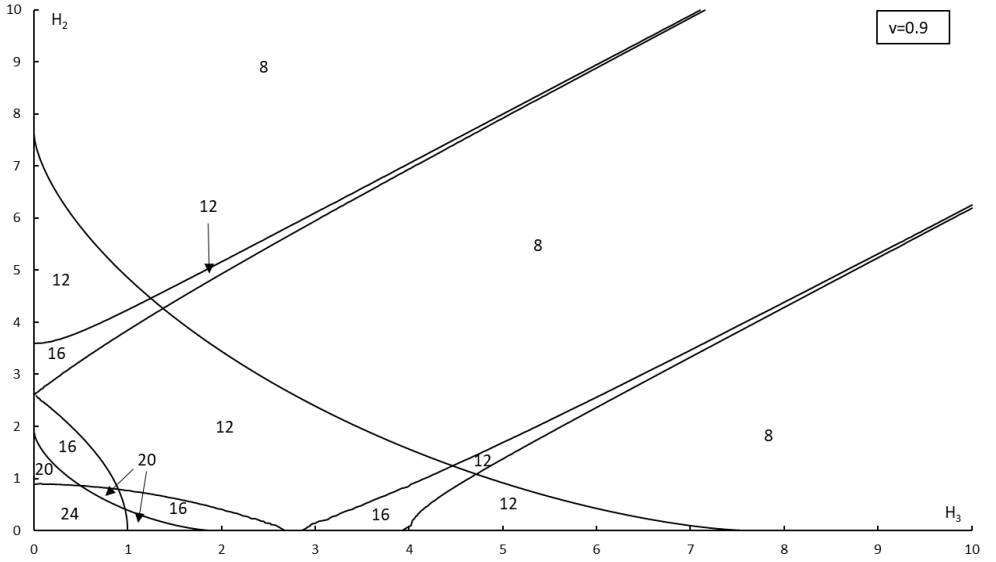

Figure 3.14 - Gyrostat's equilibria bifurcation at $v = 0.9$.

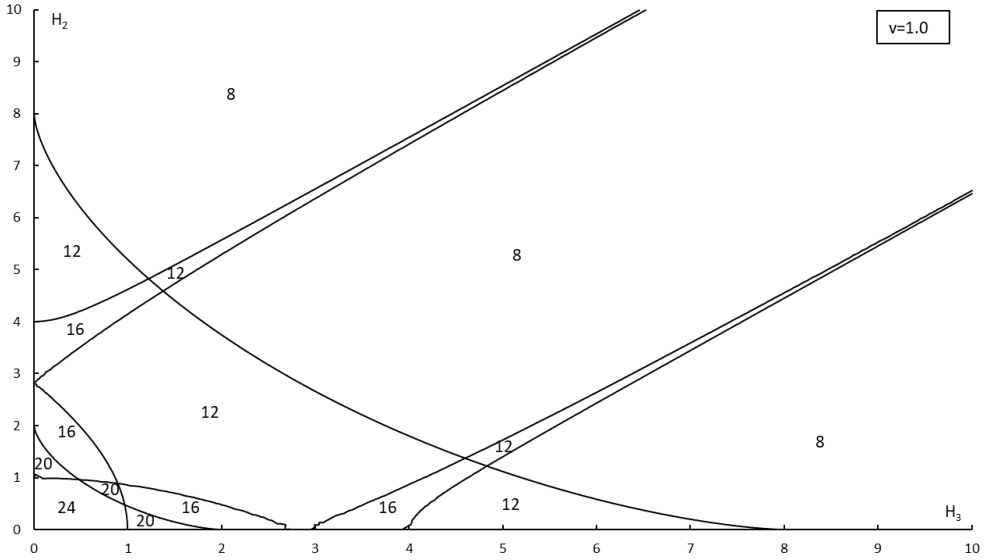

Figure 3.15 - Gyrostat's equilibria bifurcation at $v = 1.0$.

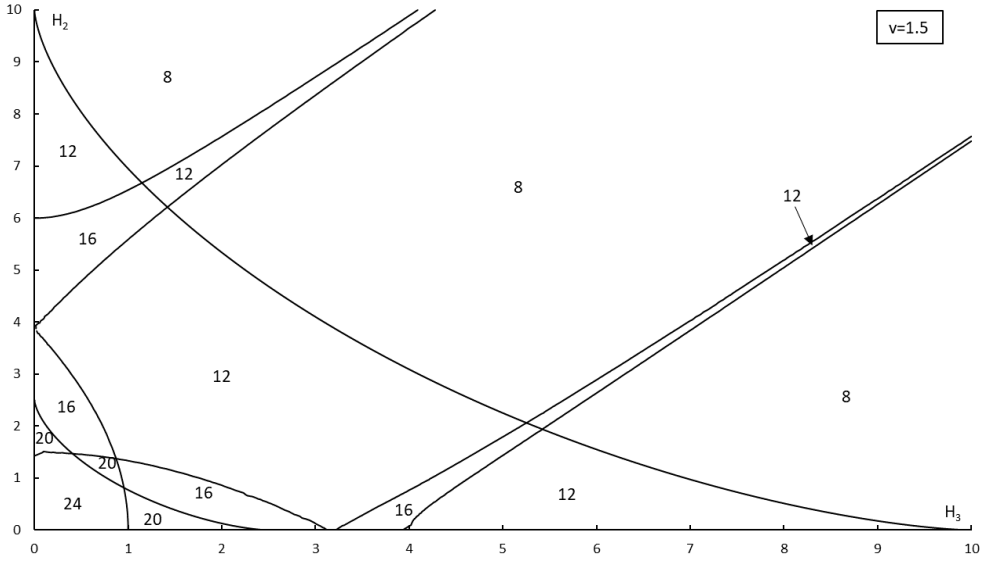

Figure 3.16 - Gyrostat's equilibria bifurcation at $v = 1.5$.

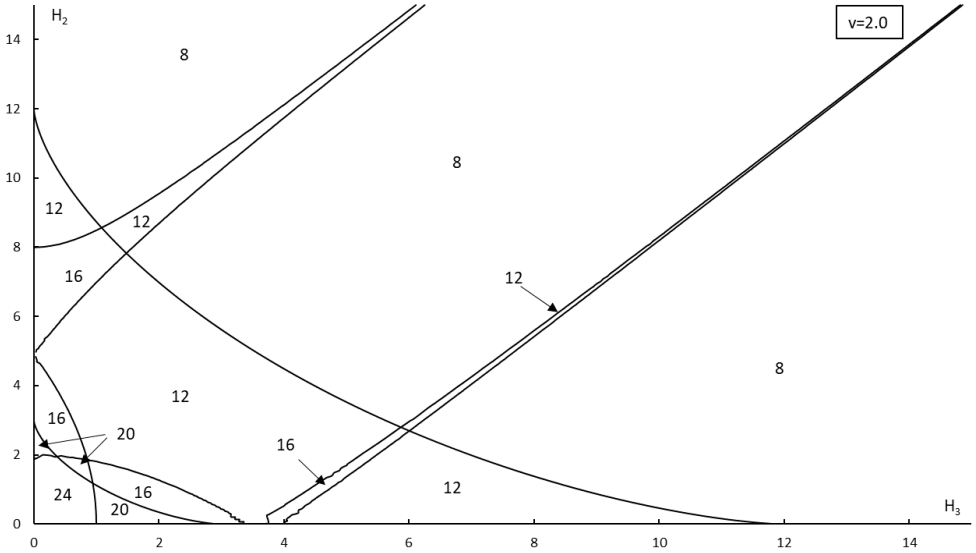

Figure 3.17 - Gyrostat's equilibria bifurcation at $v = 2.0$.

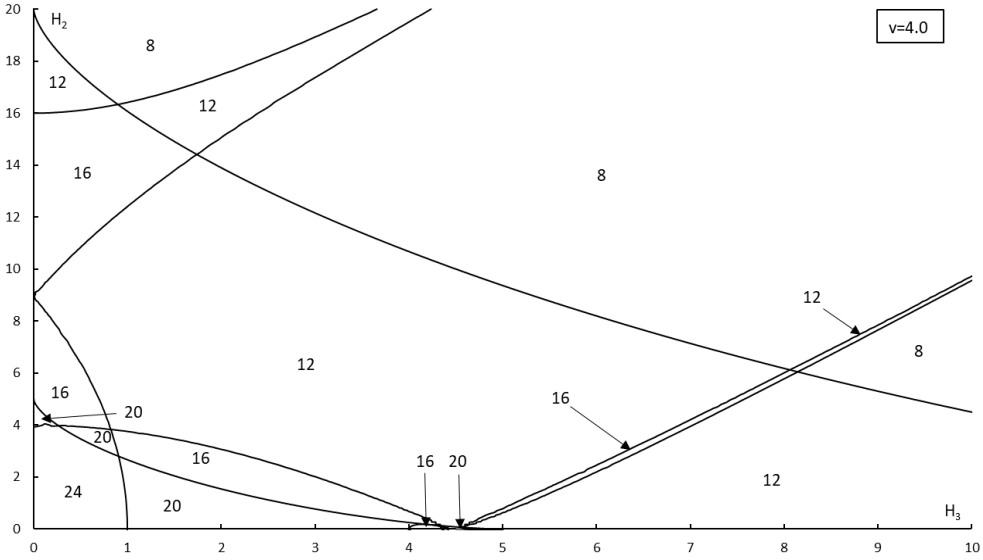

Figure 3.18 - Gyrostat's equilibria bifurcation at $v = 4.0$.

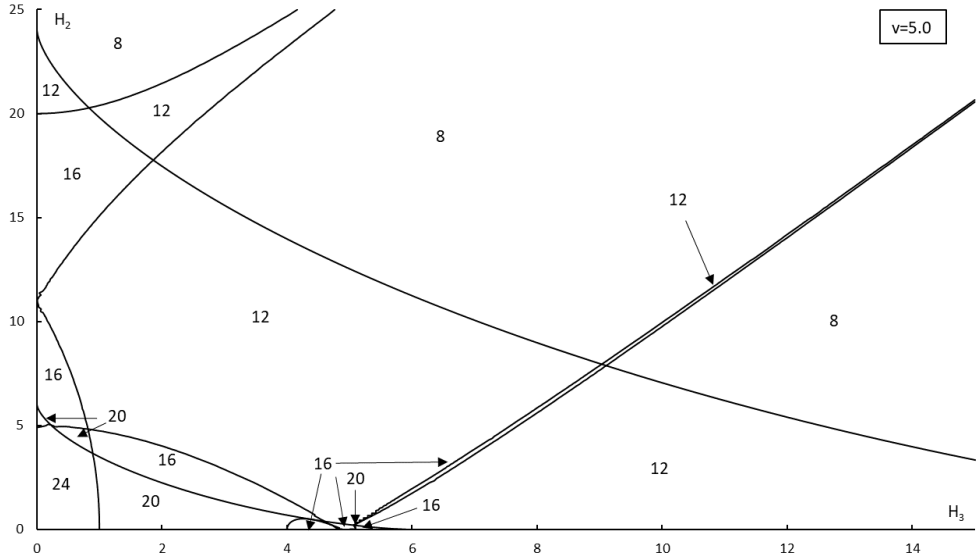

Figure 3.19 - Gyrostat's equilibria bifurcation at $v = 5.0$.

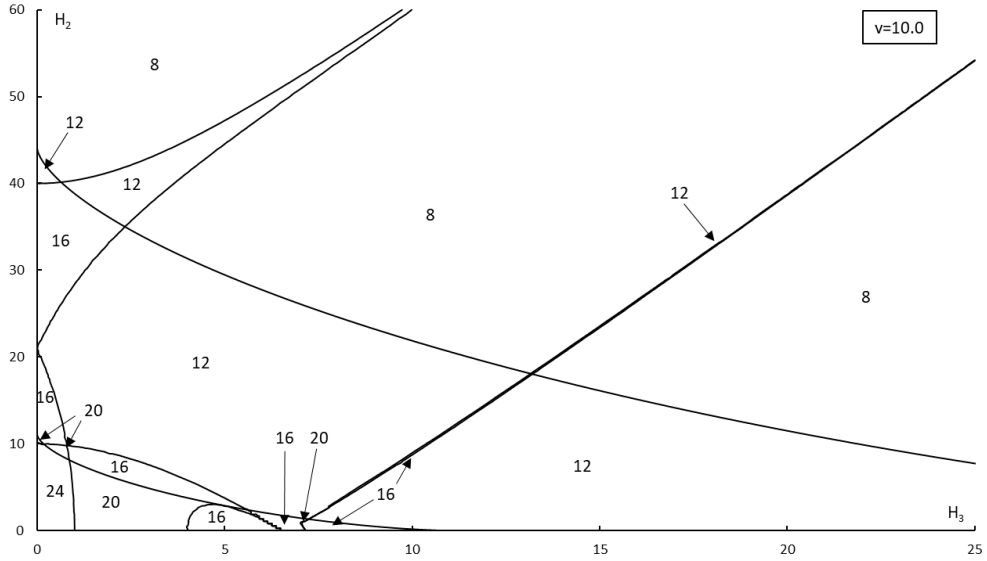

Figure 3.20 - Gyrostat's equilibria bifurcation at $v = 10.0$.

The results show that for every inertial configuration studied, there are no less than 8 equilibrium positions and no more than 24. In a general way, in regions with small values of H_3 and H_2, there are 24 equilibrium positions, with increase of H_3 and/or H_2, the 24 equilibrium positions region gives place to 20 equilibrium positions region, then to 16 equilibrium positions region, then to 12 equilibrium positions region and finally, to 8 equilibrium positions region.

There can be also found some peculiarities in this study: two small regions of 12 equilibrium positions, which tends to infinite, and two regions of 16 equilibrium positions inside one of 12 equilibria positions, that exists outside of the main regions. For the upper region of 16 equilibrium positions and 12 equilibria positions, they approach to an oblique asymptote, at which its slope is low for lower values of v $(v = 0.1)$, but increases with higher v. The difference between their borders increases with the value of v. On other hand, the lower region of 16 equilibria positions and 12 equilibria positions approach to an oblique asymptote too, almost in parallel way to the previous case, at which its slope is low for lower values of v and high for higher values of v. The difference between the boundaries of these regions is the reverse of the previous case, reduces with higher values of v.

A different case happens with a small region of 16 equilibria positions inside one of 20 equilibria positions, similar to the ones found in [8], derived from a_{31}^2 expression, that exists near $H_3 = 0$ and near $H_2 = 0.5$ for $v < 0.3$ and appears for $v \geq 4$ near $H_3 = 4$ and near $H_2 = 0$. These regions increase in size with lower values of v $(v < 0.3)$ and higher values of v $(v \geq 4)$.

3.1.3 Validation of small regions of 12 and 16 equilibrium positions

Santos in [14] and [20], as mentioned in Chapter 2, studied the dynamics of a gyrostat-satellite in a circular orbit, namely the general case of equilibria and stability. The author found small regions of 16 and 12 equilibria positions outside their main regions near $H_1 = 0$ and for high values of H_2.

In this chapter, a study about the validation of these small regions in [14] and [20], is conducted, focusing in six cases: (a) $v_L = 0.1$ and $H_3 = 0.4$; (b) $v_L = 0.1$ and $H_3 = 3.61$; (c) $v_L = 0.2$ and $H_3 = 0.4$; (d) $v_L = 0.2$ and $H_3 = 3.264$; (e) $v_L = 0.6$ and $H_3 = 0.4$ and (f) $v_L = 0.6$ and $H_3 = 3.08$. Taking note that in [14] and [20], inertial parameter $v_L = (B - A)/(B - C)$, it is necessary to convert it to the parameter used in this work, $v = (A - B)/(C - A)$, which takes on form:

$$v = v_L = \frac{B - A}{B - C} \Leftrightarrow$$

$$\Leftrightarrow (A - B) = -v_L(B - C) \tag{3.7}$$

$$v = \frac{A - B}{C - A} = \frac{-v_L(B - C)}{C - A} \Leftrightarrow$$

$$\Leftrightarrow v = v_L(1 + v) \Leftrightarrow$$

$$\Leftrightarrow v_L = \frac{v}{1 + v} \tag{3.8}$$

Converting the inertial parameters $v_L = 0.1$, $v_L = 0.2$ and $v_L = 0.6$ using equation (3.8), the studied inertial parameters v are $v = 0.11$, $v = 0.25$ and $v = 1.5$, respectively. The results are shown side by side with figures from [14], the case (a) and (b) along Figures 3.21 to 3.23.; the case (c) and (d) along Figures 3.24 and 3.26; and case (e) and (f) along Figures 3.27 to 3.29.

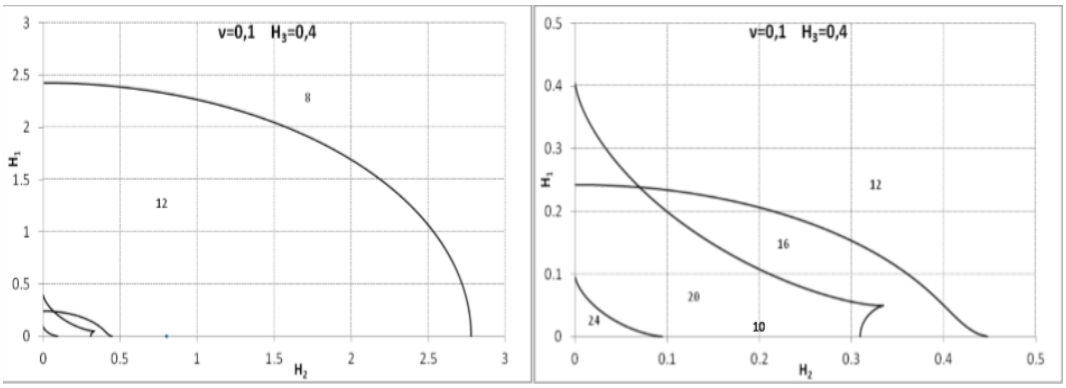

Figure 3.21 – Equilibria Picture for $v_L = 0.1$ and $H_3 = 0.4$ [14].

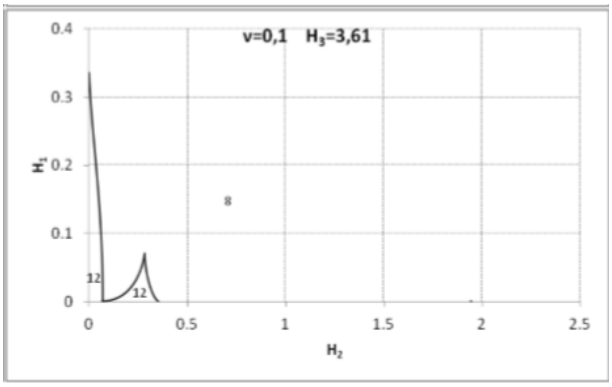

Figure 3.22 – Equilibria Picture for $v_L = 0.1$ and $H_3 = 3.61$ [14].

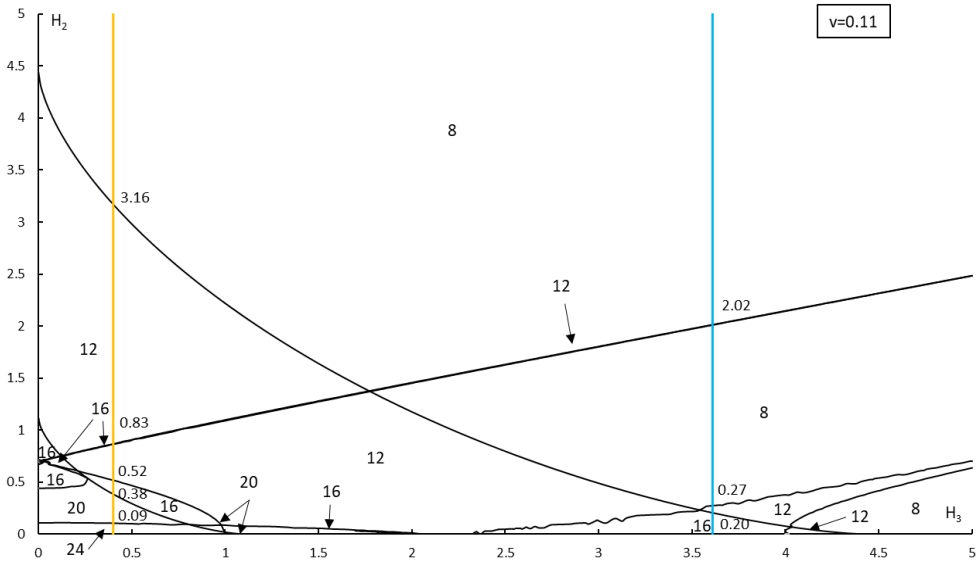

Figure 3.23 – Gyrostat's equilibria bifurcation at $v = 0.11$ with straight lines $H_3 = 0.4$ and $H_3 = 3.61$.

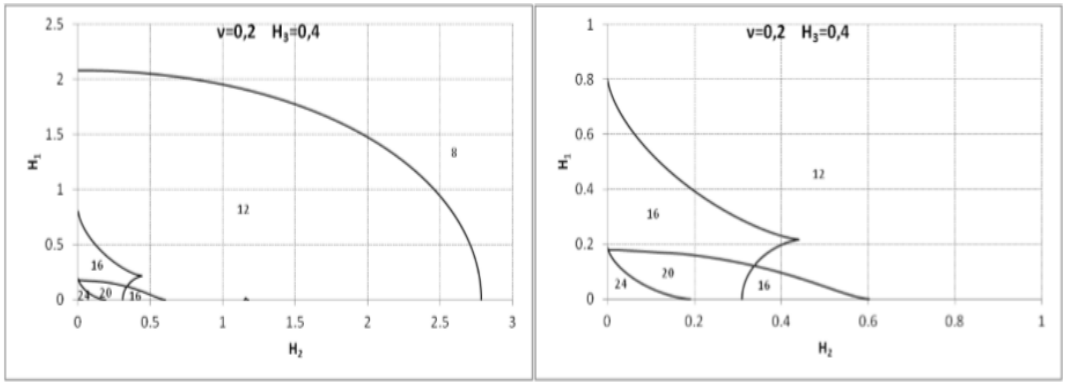

Figure 3.24 – Equilibria Picture for $v_L = 0.25$ and $H_3 = 0.4$ [14].

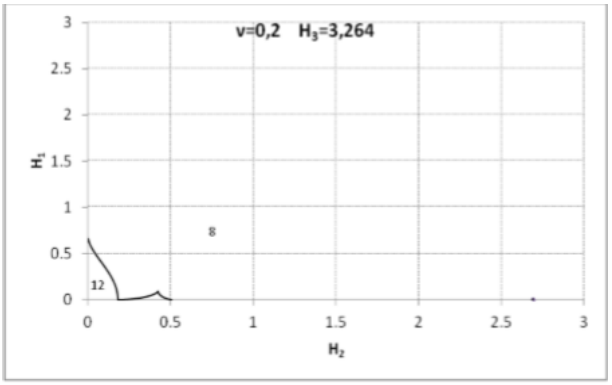

Figure 3.25 – Equilibria Picture for $v_L = 0.25$ and $H_3 = 3.264$ [14].

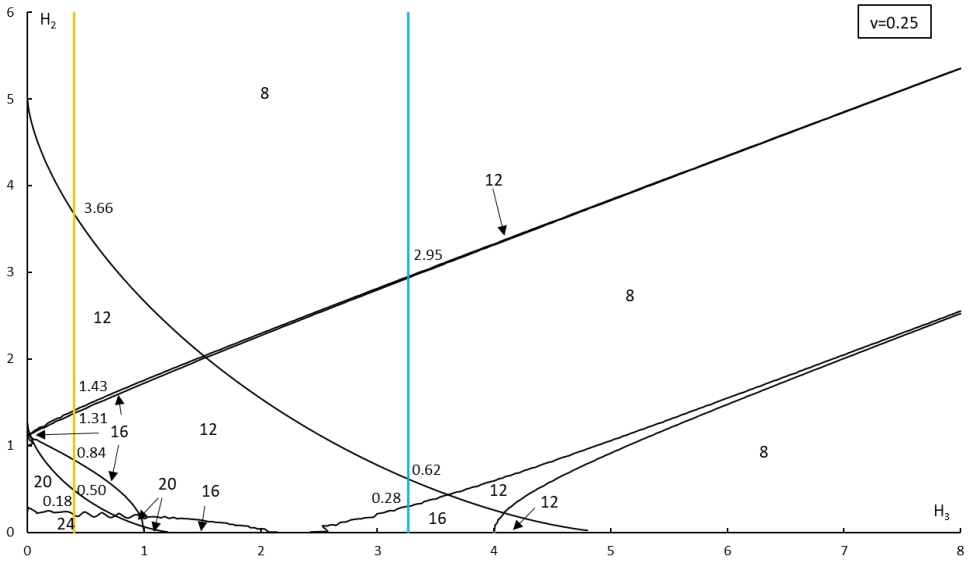

Figure 3.26 – Gyrostat's equilibria bifurcation at $v = 0.25$ with straight lines $H_3 = 0.4$ and $H_3 = 3.264$.

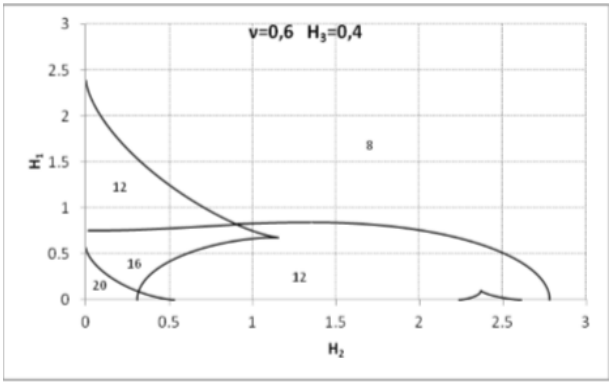

Figure 3.27 – Equilibria Picture for $v_L = 0.6$ and $H_3 = 0.4$ [14].

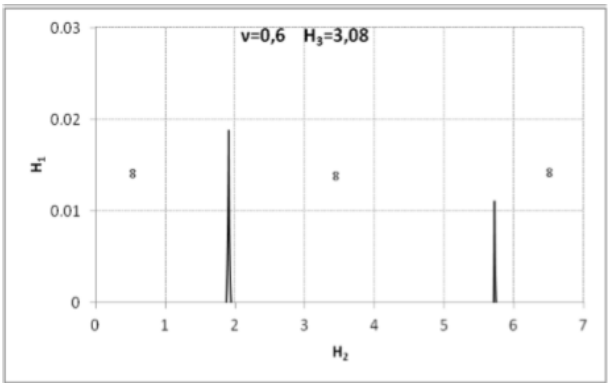

Figure 3.28 – Equilibria Picture for $v_L = 0.6$ and $H_3 = 3.08$ [14].

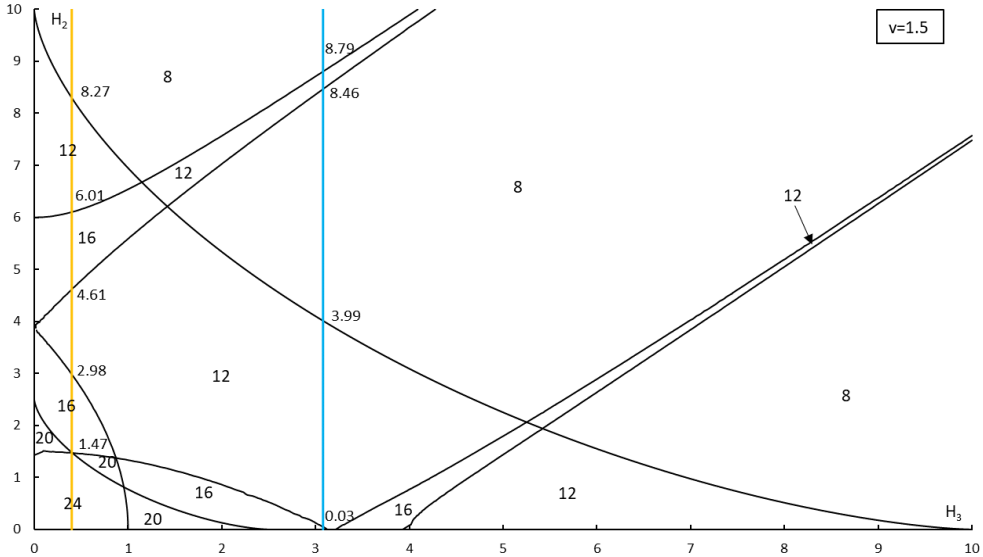

Figure 3.29 – Gyrostat's equilibria bifurcation at $v = 0.6$ with straight lines $H_3 = 0.4$ and $H_3 = 3.08$.

For each case, the intersection points between the vertical H_3 lines and the curves in the chart are shown.

One can see from Figure 3.23, for case (a) the bifurcation points for regions 24, 20, 16 and 12 correspond to the same bifurcation points of the same regions in [14] with a small displacement.

For case (b), the first bifurcation point in [14] is for a 12 equilibrium positions region but, in this study, is a 16 equilibrium positions region, on other hand, the bifurcation point of the other 12 equilibrium positions region corresponds with a small displacement to the one here.

For cases (c) and (d), in Figure 3.26, the scenario is similar, but the difference between the values of bifurcation points of the study [14] and this work, increases, so the displacement is higher.

On other hand, the cases (e) and (f), in Figure 3.29, are very different from previous ones, the values of bifurcations points of equilibrium regions are very different from this work, only the region of 16 equilibrium positions is near ($H_3 = 0.4$ and $H_2 = 2.3 - 2.6$).

The results confirm the existence of the small regions referenced in [14], but for some conditions, the results do not coincide, in terms of accuracy, with the ones found in the general case. The displacement may be due to the fact that $H_1 = 0$ is not considered in the general case, since in this case, the results are much higher than zero.

3.2 Gyrostat's stability

In this chapter, it will be analyzed the problem of stability of a gyrostat satellite, namely when the gyrostat has a component of the gyrostatic moment vector equal to zero ($H_1 = 0$). There is made a study in function of a fixed v, a fixed H_3 and variable H_2. The method is similar to the one used in chapter 3.1.1, at which it is calculated the equilibrium positions for the three groups (Group I, II and III), then, remembering expressions (2.63) and system (2.65) from Chapter 2.3, the sufficient conditions of stability of the equilibrium solutions are calculated and it is determined if the equilibrium solutions are stable or unstable.

In the present case, and following the results from Chapter 3.1.1 and 3.1.2, the computations were made for the inertial parameters: $v = 0.1$, $v = 0.5$, $v = 1.0$, $v = 1.5$, $v = 5$, $v = 10$ and for three different values of H_3, one in the beginning of the chart ($H_3 = 0.1$), one in the middle of the chart ($H_3 = 2$) and finally, one near the end of the chart ($H_3 = 3.5 - 10$), depending on the v selected. The cases studied, although they are not part of exhaustive analysis, show an overall image of the behavior of the equilibrium positions stability along the plane (H_3, H_2).

The results are shown in Figures 3.30-3.47 in function of spacecraft angle γ and H_2. The colored dashed lines represent when a specific equilibrium position is unstable and the colored full lines represent when a specific equilibrium position is stable (sufficient conditions of stability (2.65) are valid). The colors blue, orange and dark yellow represent equilibrium solutions of group I, II and III, respectively. The black vertical dashed lines (R_i) in the stability chart correspond to intersection points ($i = 1,2, \ldots$) between the green line and equilibria regions, in the equilibria chart. Finally, the black horizontal dashed line corresponds to notable points ($\pi/2$ and π) in the axis $\gamma[rad]$.

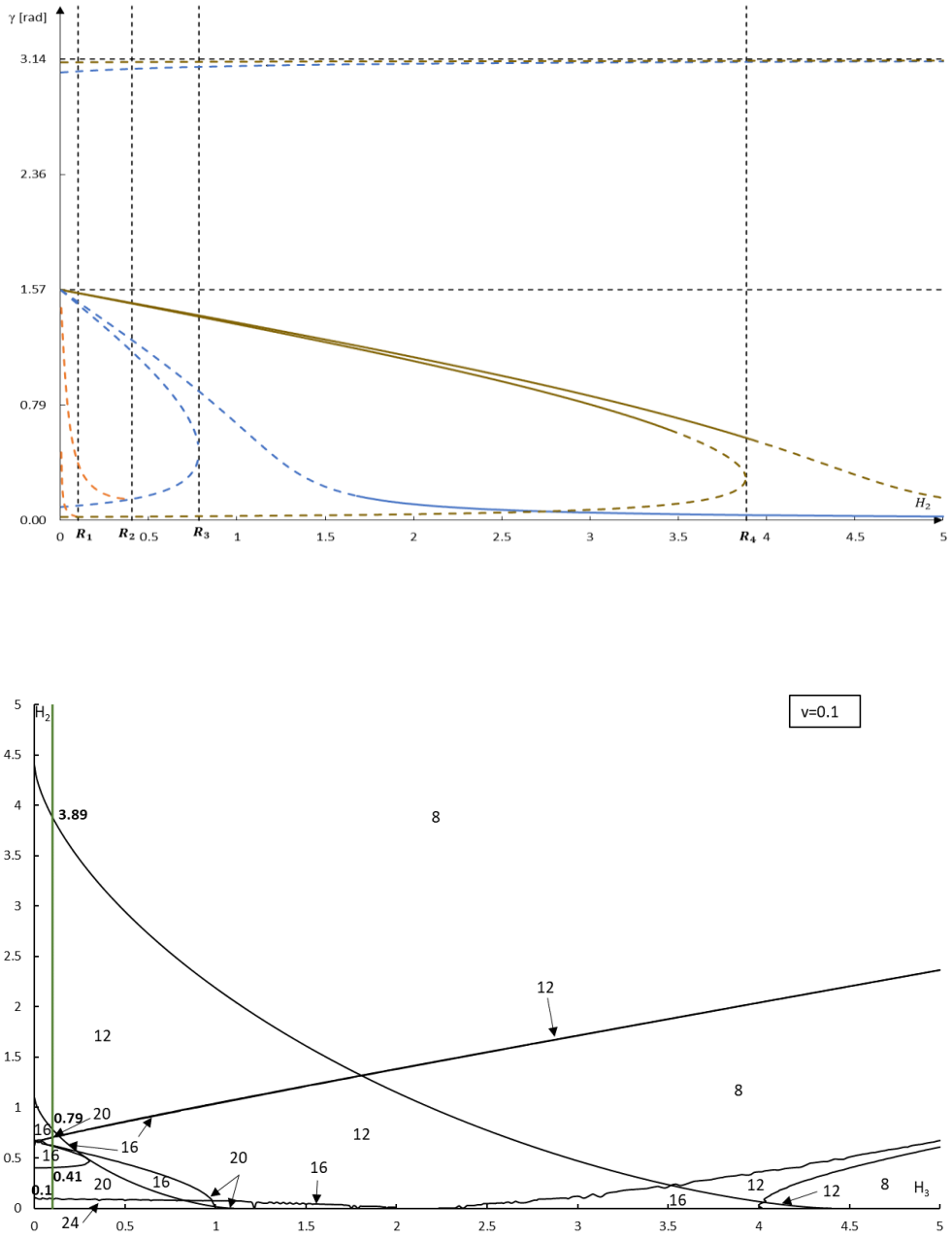

Figure 3.30 – Stability in function of angle γ and H_2 and respective equilibria chart for $v = 0.1$ and $H_3 = 0.1$.

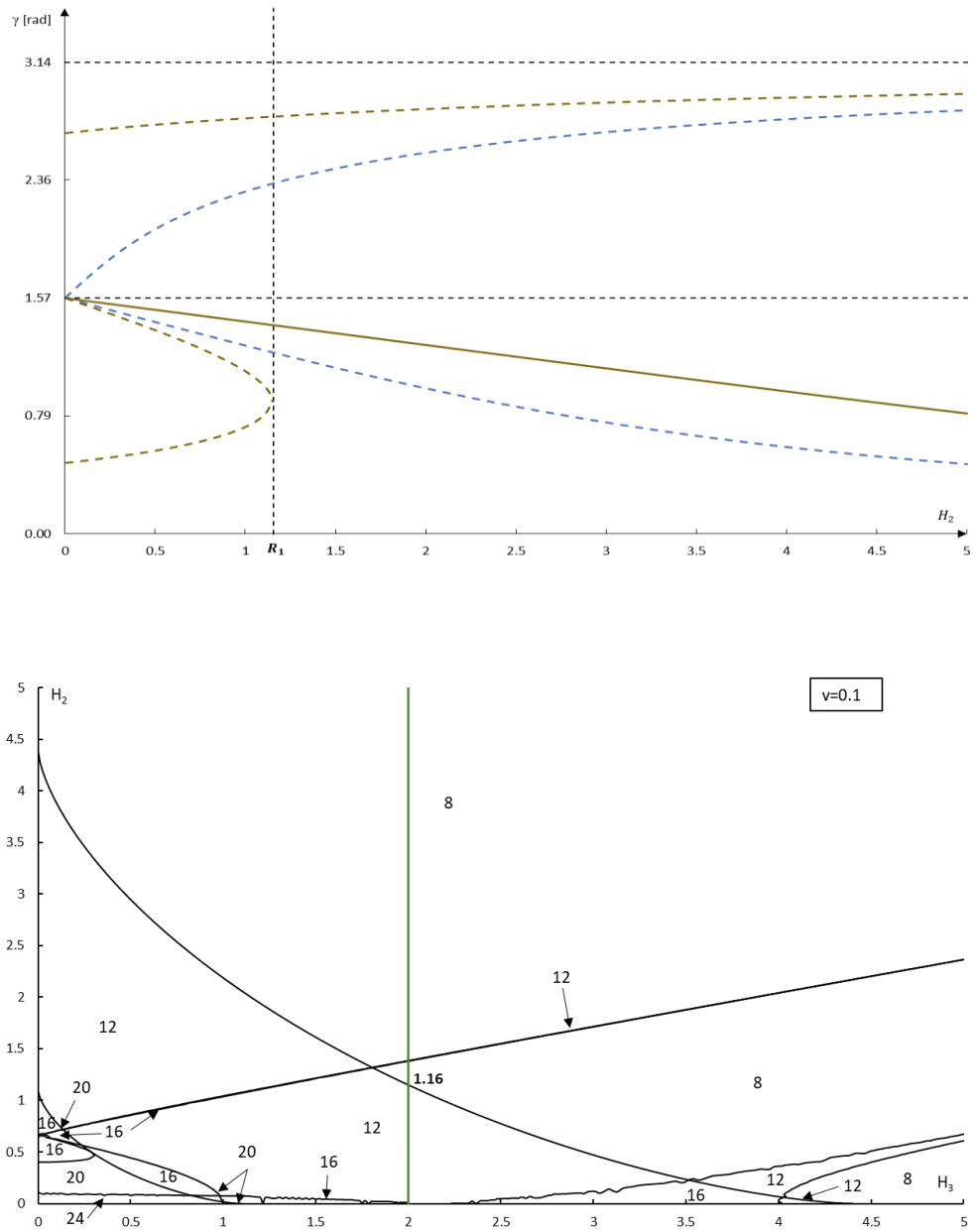

Figure 3.31 – Stability in function of angle γ and H_2 and respective equilibria chart for $v = 0.1$ and $H_3 = 2$.

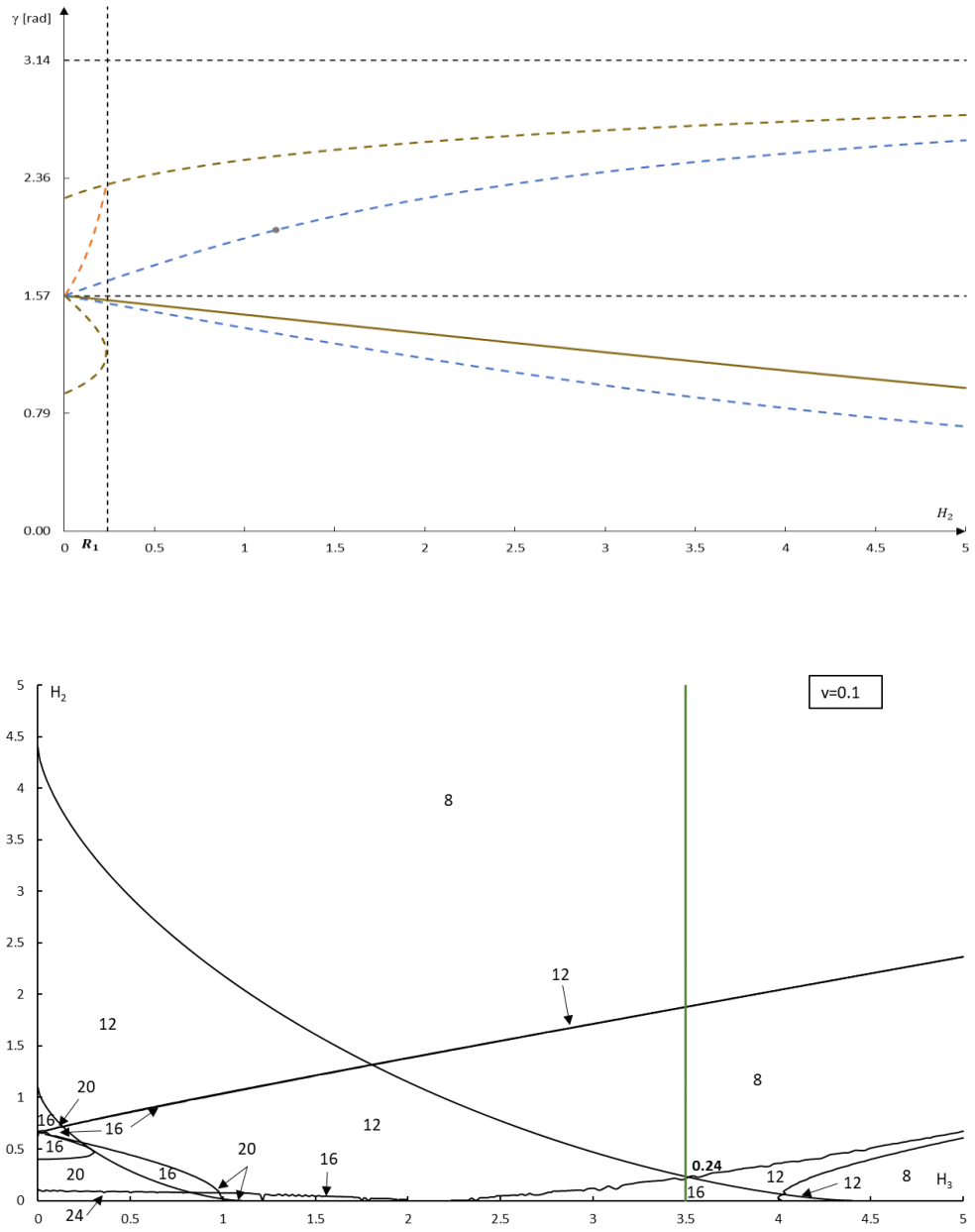

Figure 3.32 – Stability in function of angle γ and H_2 and respective equilibria chart for $v = 0.1$ and $H_3 = 3.5$.

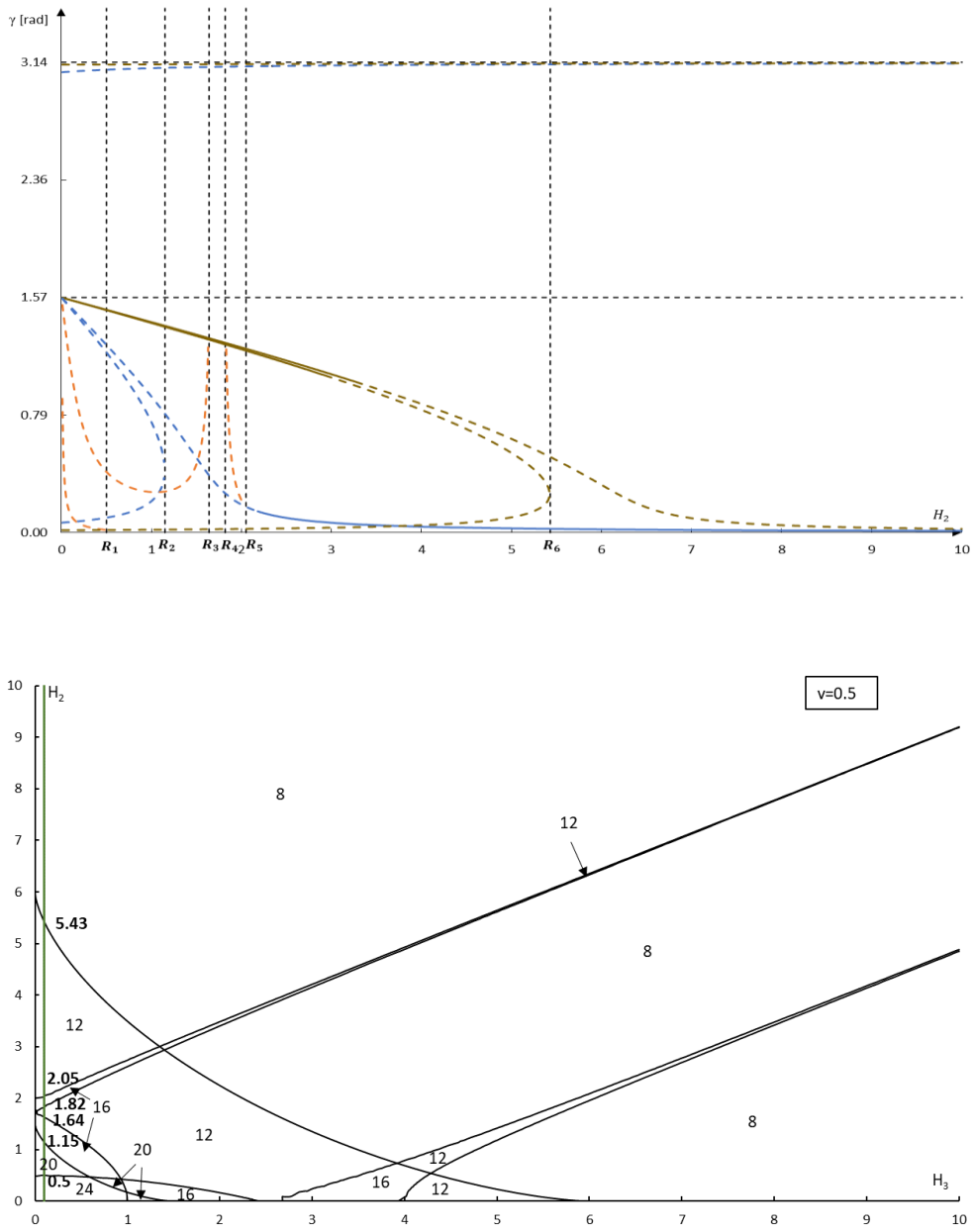

Figure 3.33 – Stability in function of angle γ and H_2 and respective equilibria chart for $v = 0.5$ and $H_3 = 0.1$.

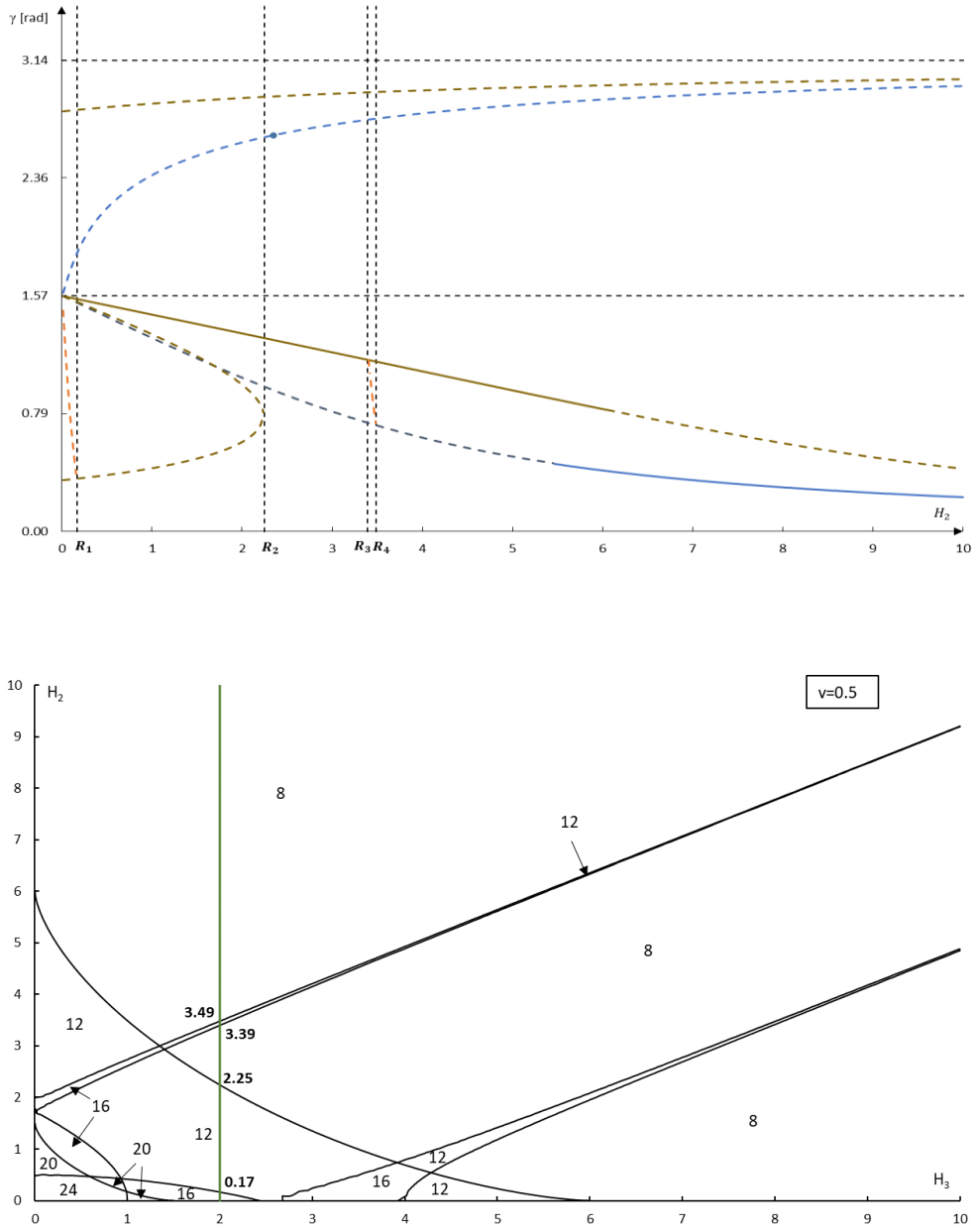

Figure 3.34 – Stability in function of angle γ and H_2 and respective equilibria chart for $v = 0.5$ and $H_3 = 2$.

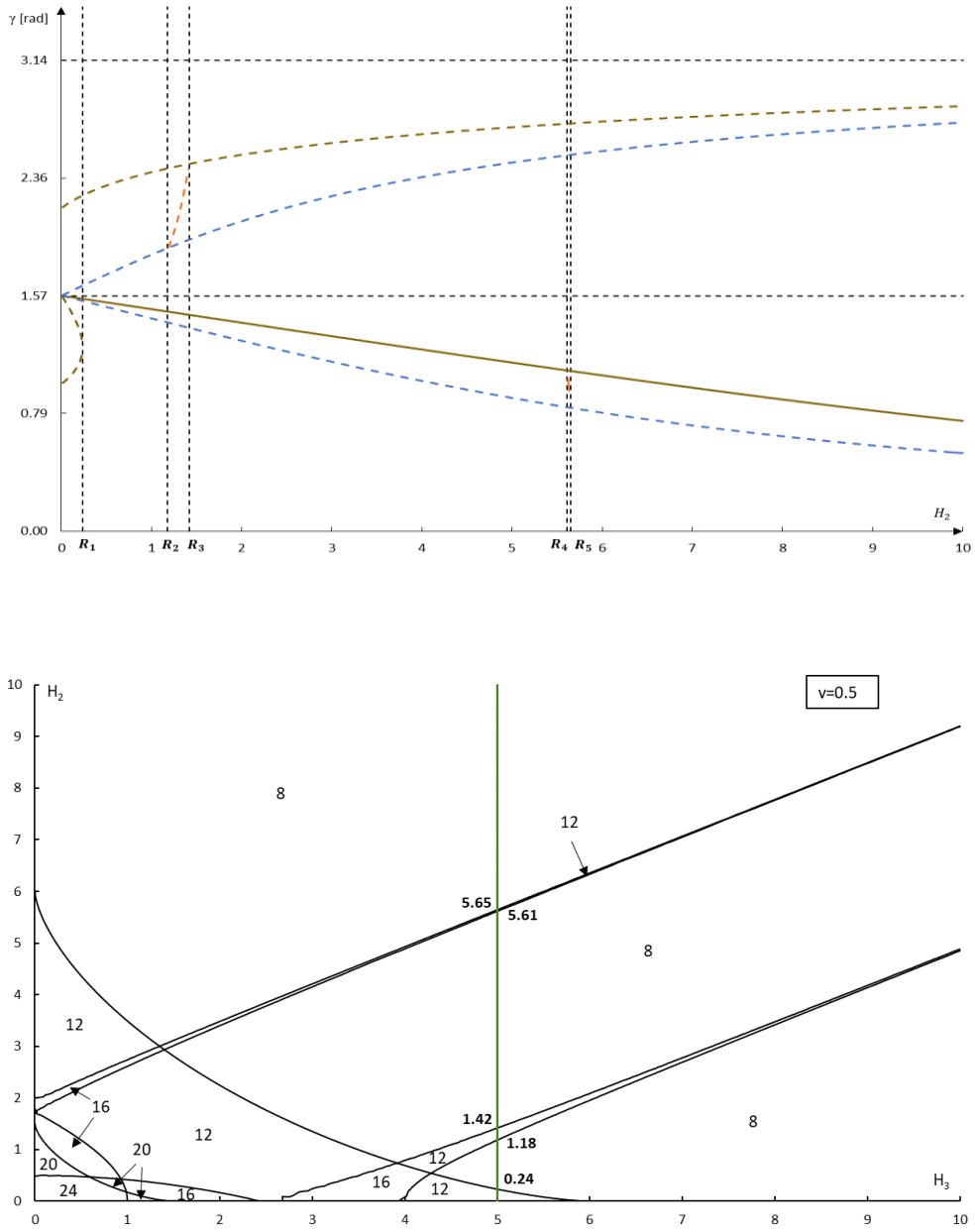

Figure 3.35 – Stability in function of angle γ and H_2 and respective equilibria chart for $v = 0.5$ and $H_3 = 5$.

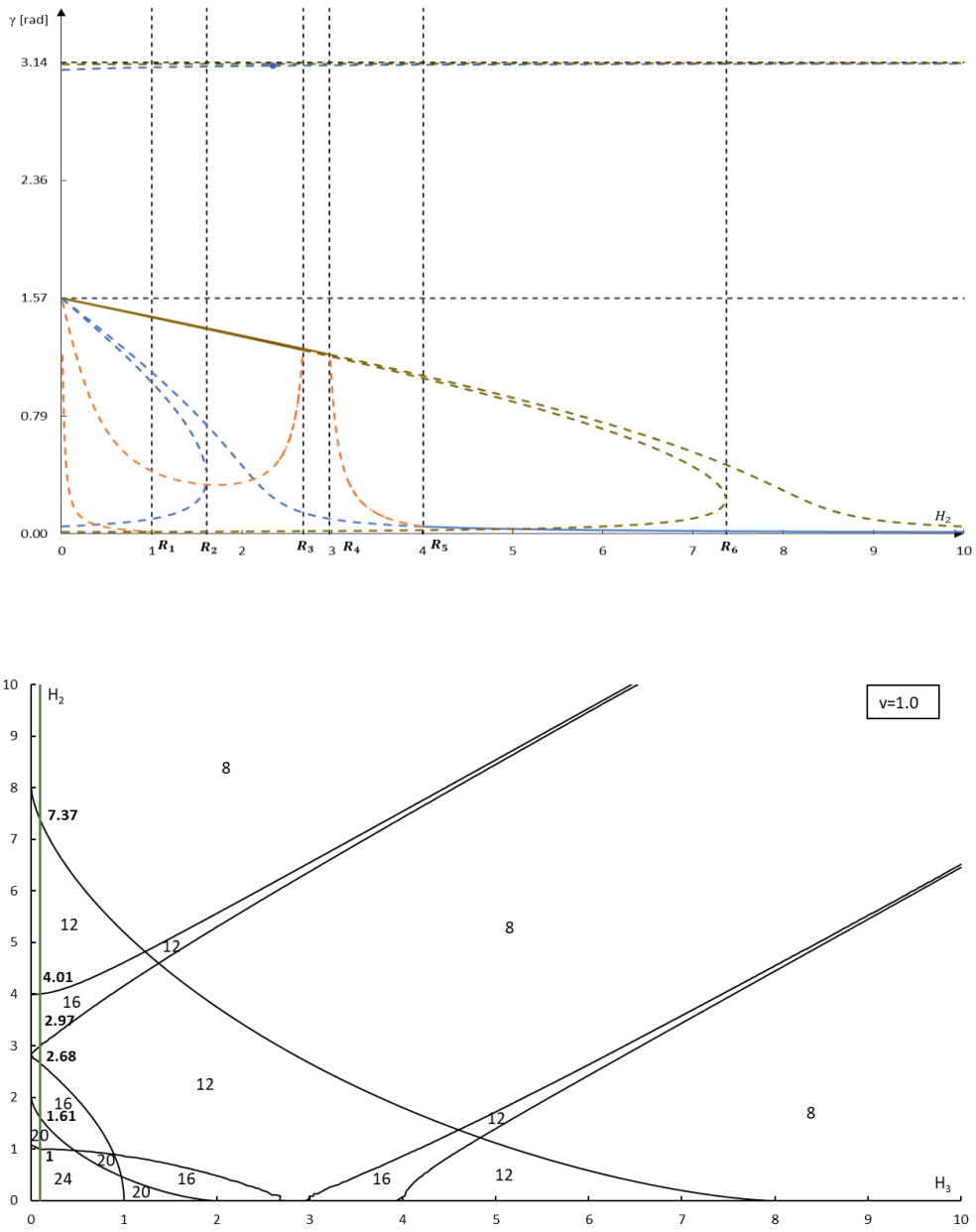

Figure 3.36 – Stability in function of angle γ and H_2 and respective equilibria chart for $v = 1.0$ and $H_3 = 0.1$.

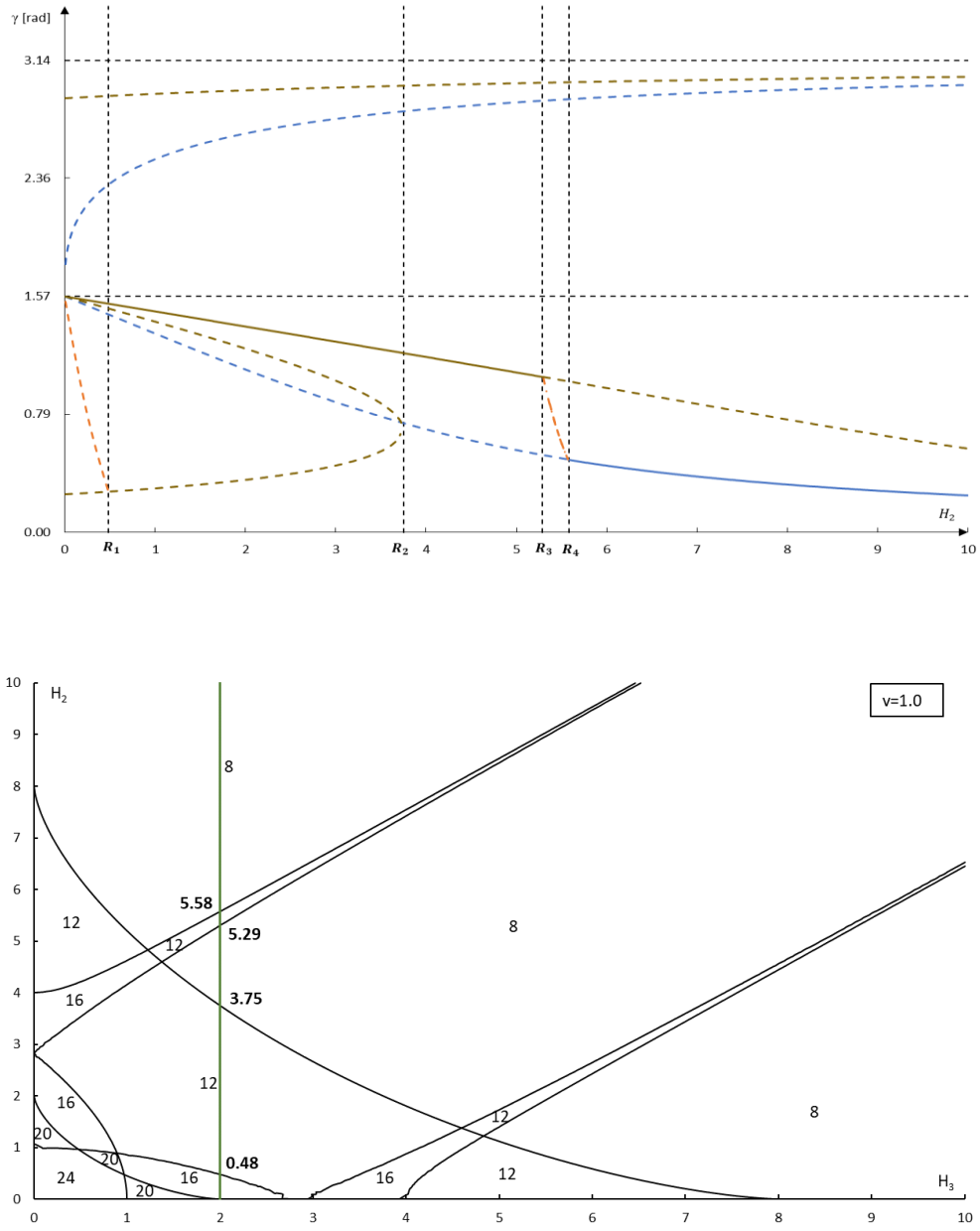

Figure 3.37 – Stability in function of angle γ and H_2 and respective equilibria chart for $v = 1.0$ and $H_3 = 2$.

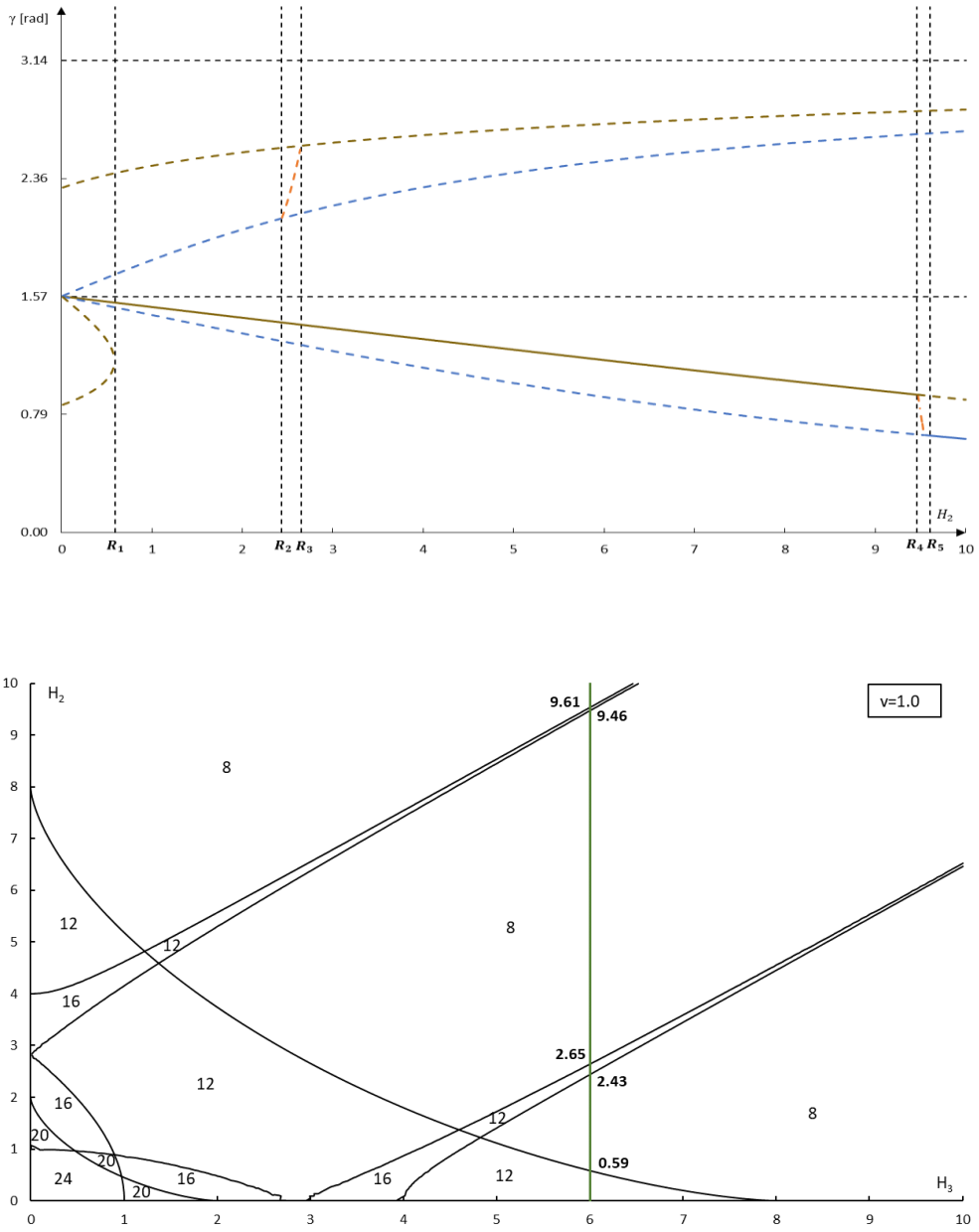

Figure 3.38 – Stability in function of angle γ and H_2 and respective equilibria chart for $v = 1.0$ and $H_3 = 6$.

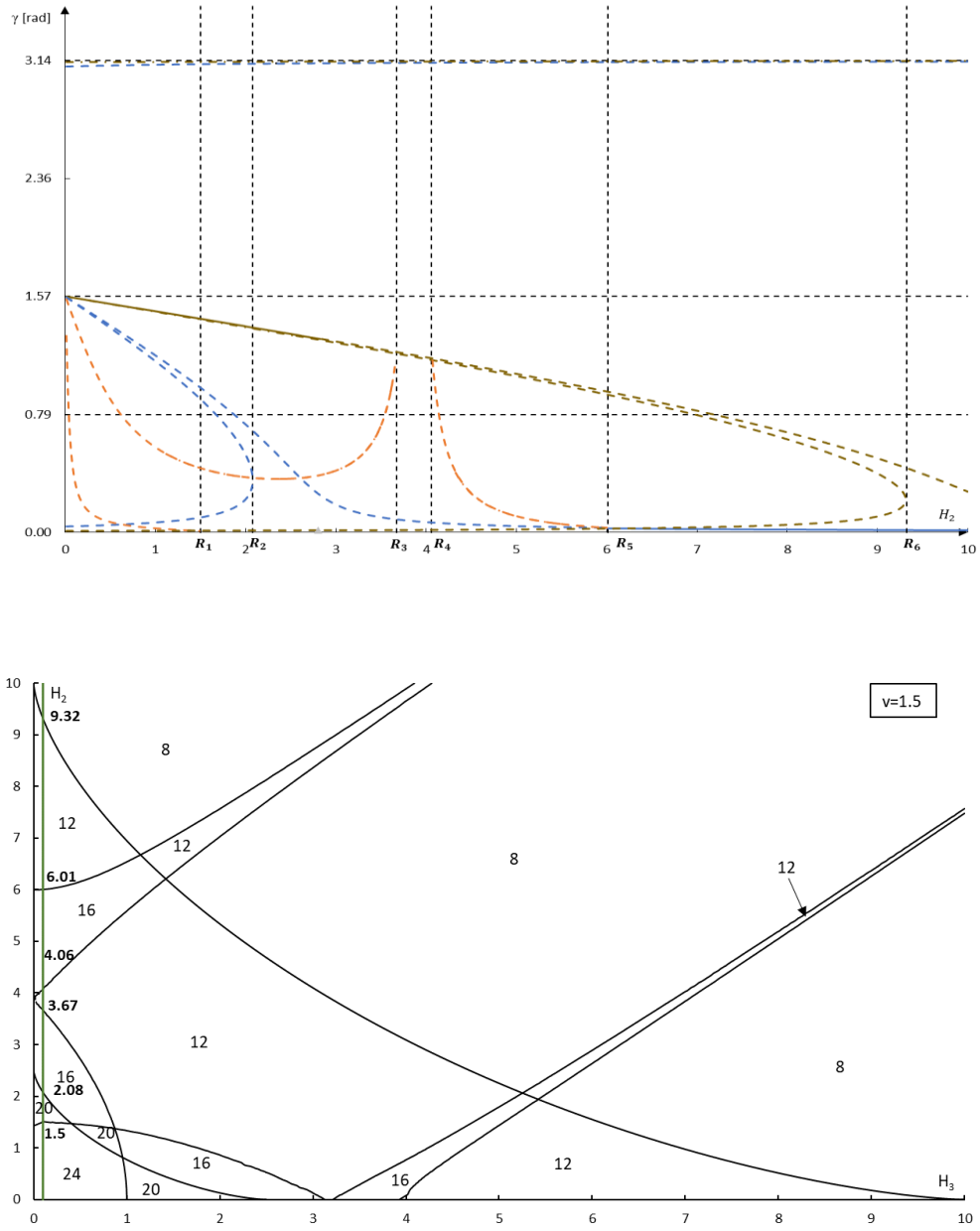

Figure 3.39 – Stability in function of angle γ and H_2 and respective equilibria chart for $v = 1.5$ and $H_3 = 0.1$.

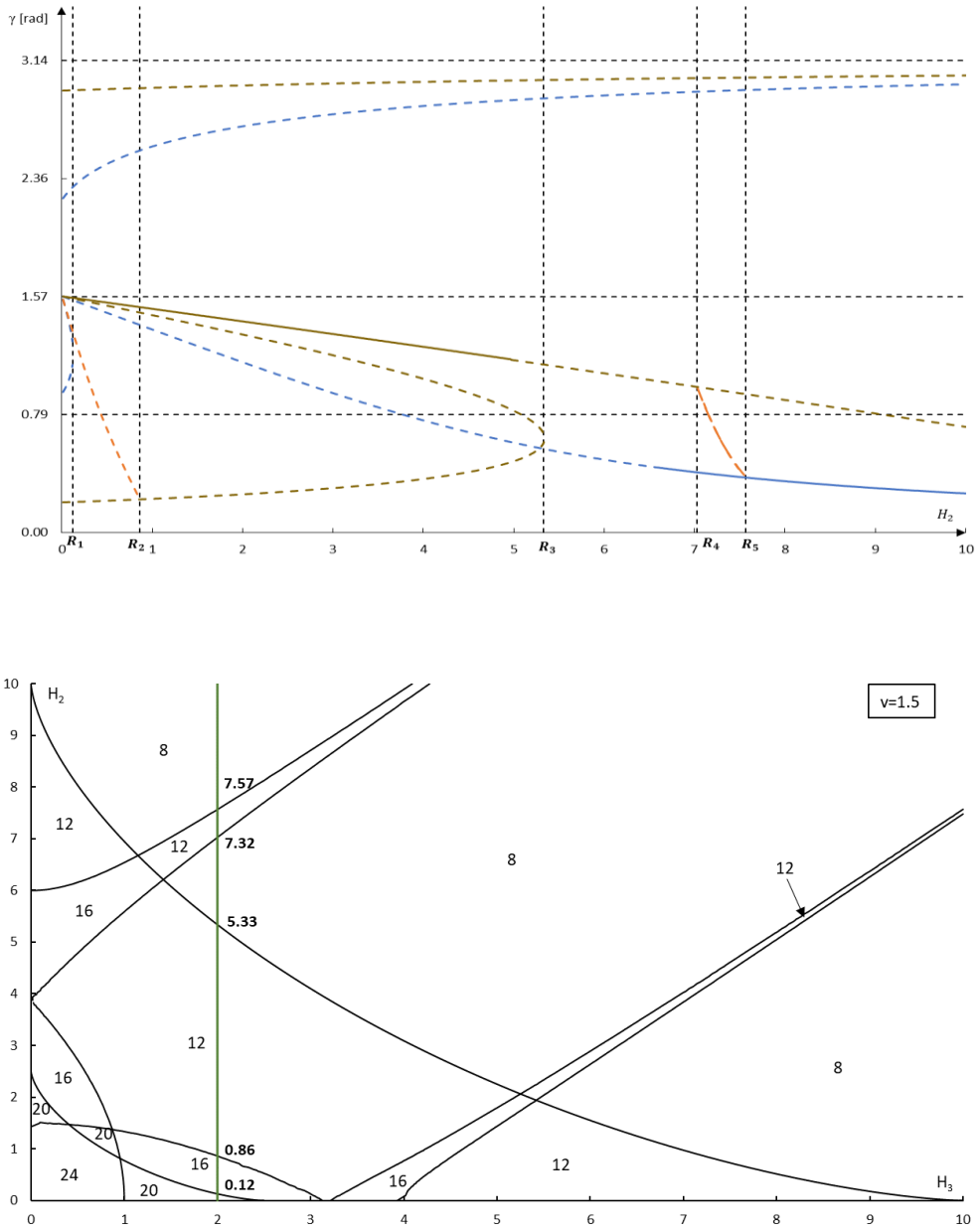

Figure 3.40 – Stability in function of angle γ and H_2 and respective equilibria chart for $v = 1.5$ and $H_3 = 2$.

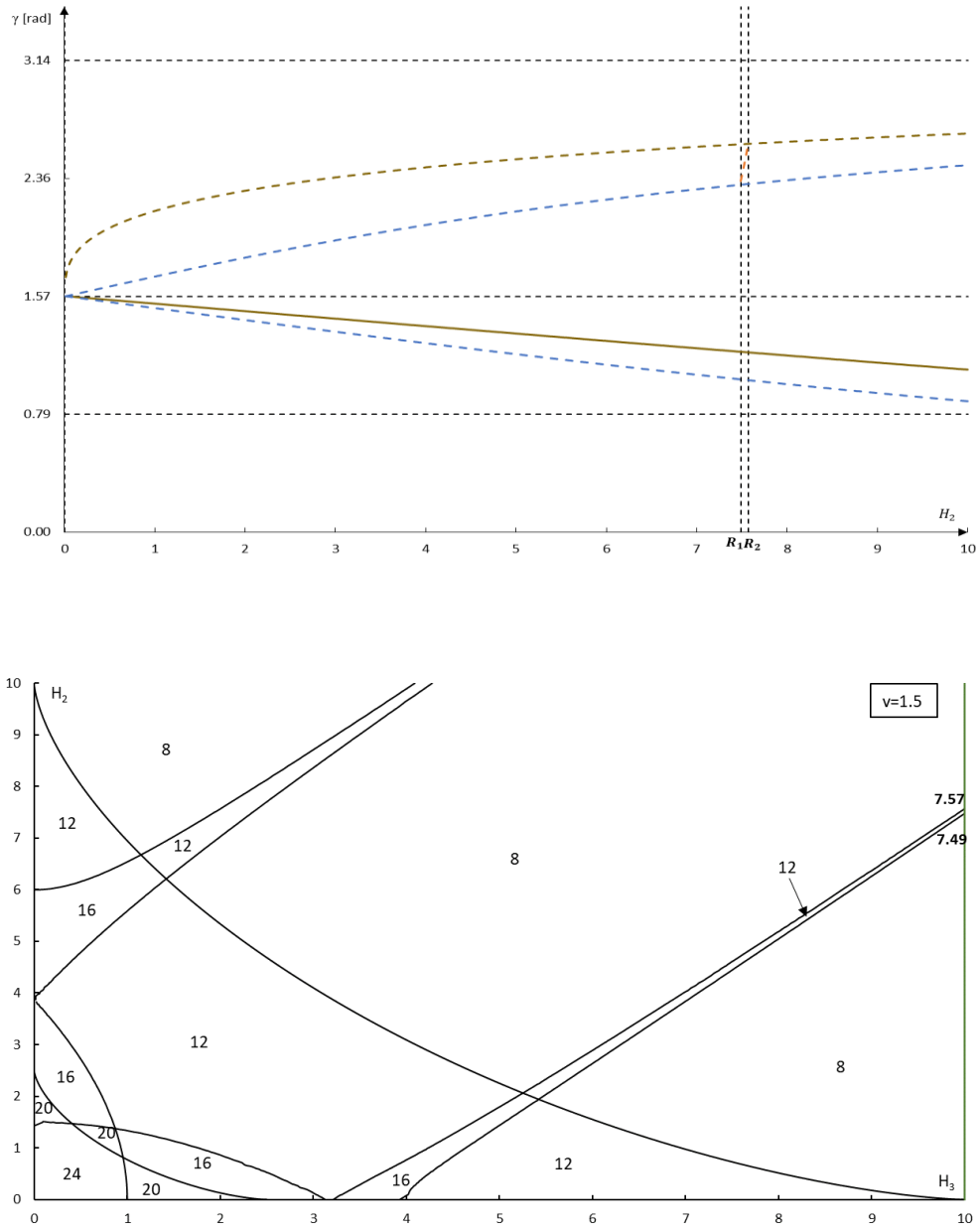

Figure 3.41 – Stability in function of angle γ and H_2 and respective equilibria chart for $v = 1.5$ and $H_3 = 10$.

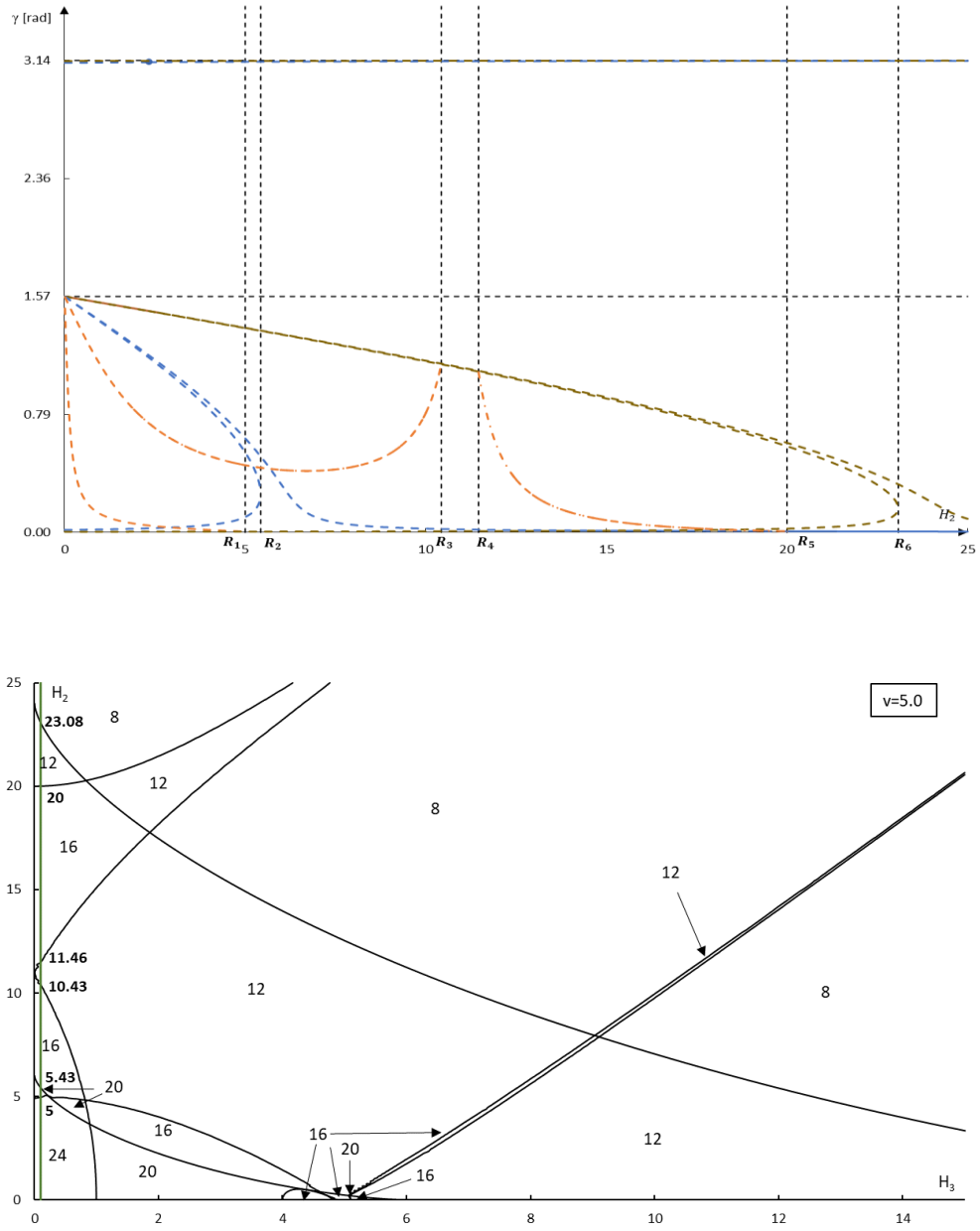

Figure 3.42 – Stability in function of angle γ and H_2 and respective equilibria chart for $v = 5$ and $H_3 = 0.1$.

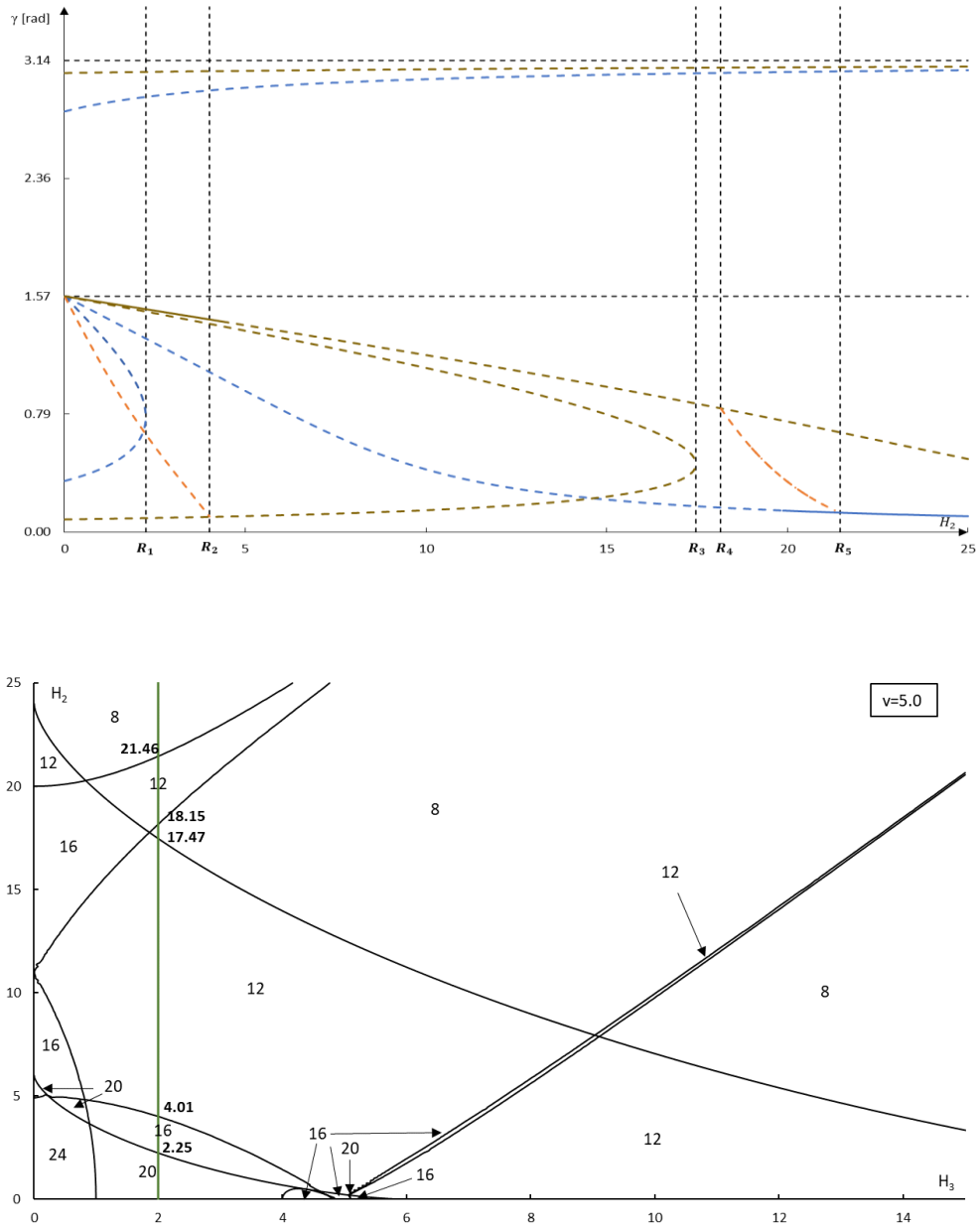

Figure 3.43 – Stability in function of angle γ and H_2 and respective equilibria chart for $v = 5$ and $H_3 = 2$.

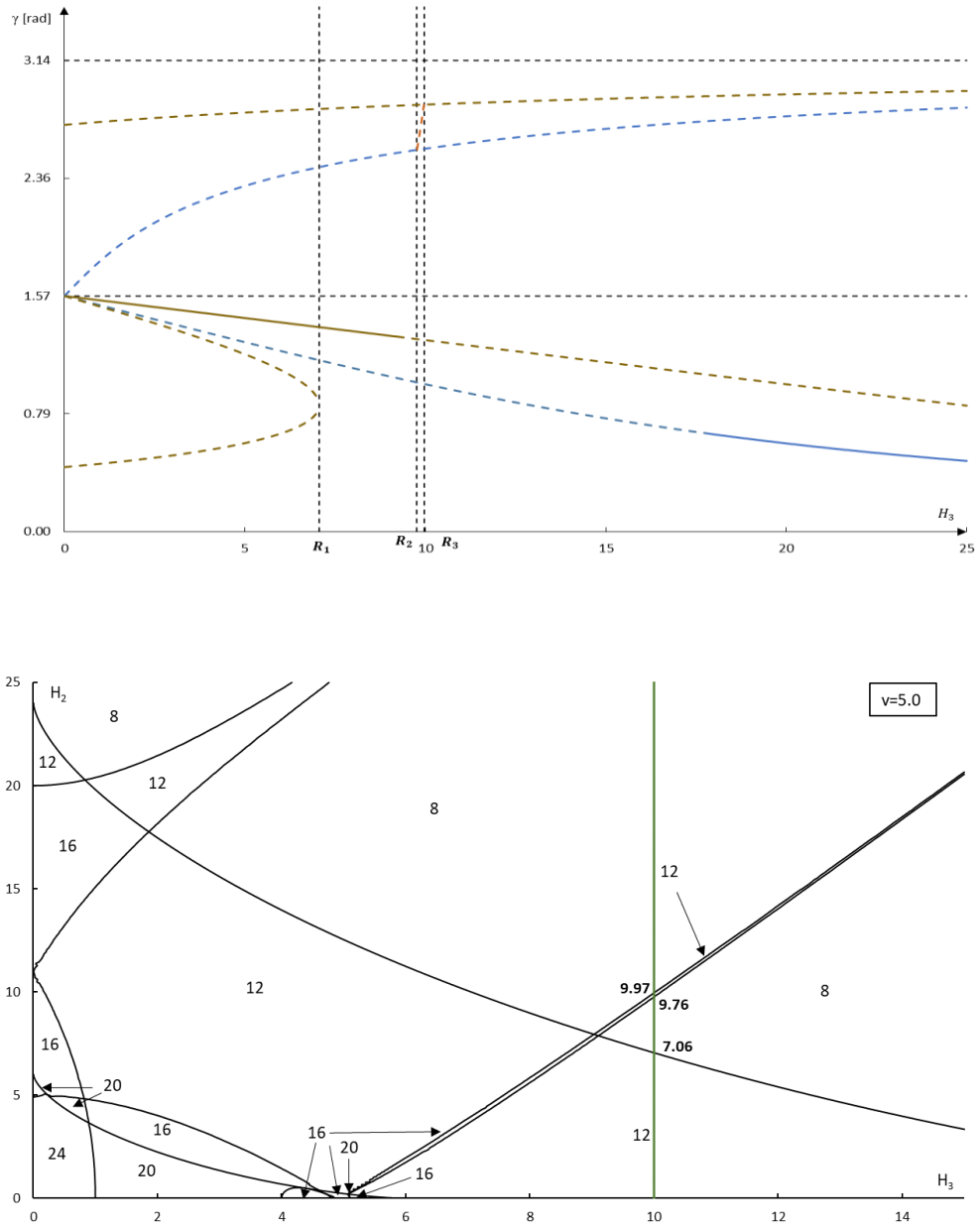

Figure 3.44 – Stability in function of angle γ and H_2 and respective equilibria chart for $v = 5$ and $H_3 = 10$.

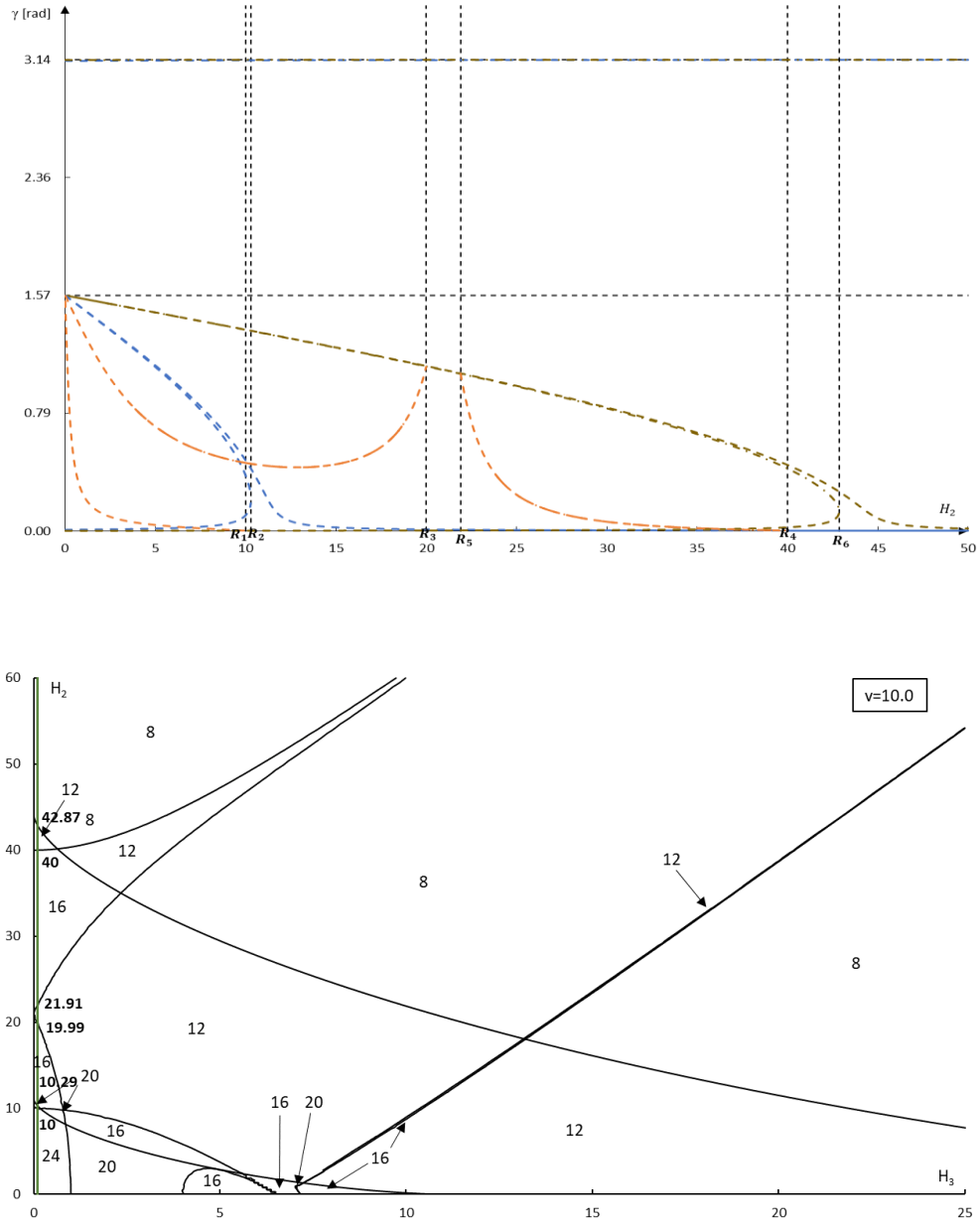

Figure 3.45 – Stability in function of angle γ and H_2 and respective equilibria chart for $v = 10$ and $H_3 = 0.1$.

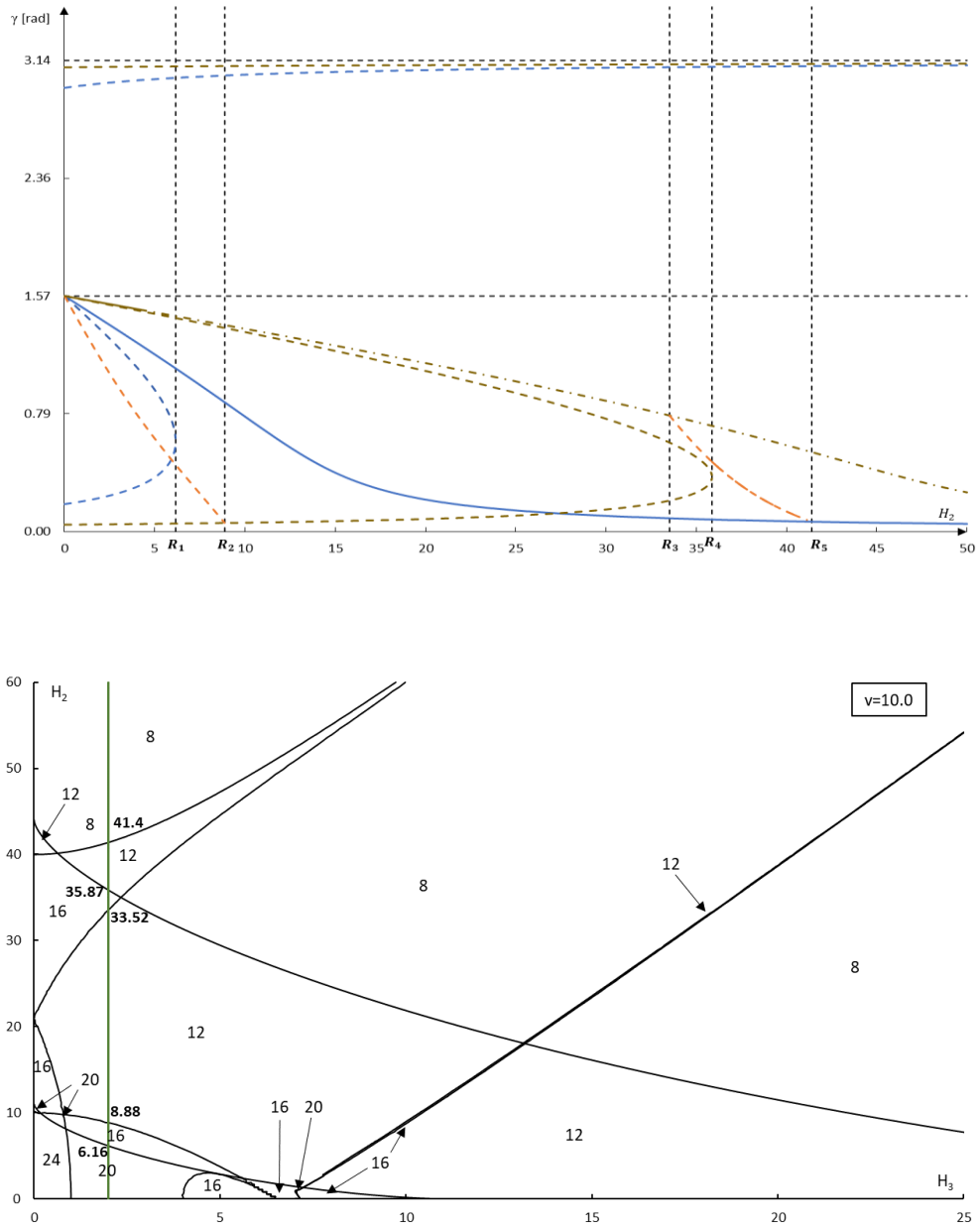

Figure 3.46 – Stability in function of angle γ and H_2 and respective equilibria chart for $v = 10$ and $H_3 = 2$.

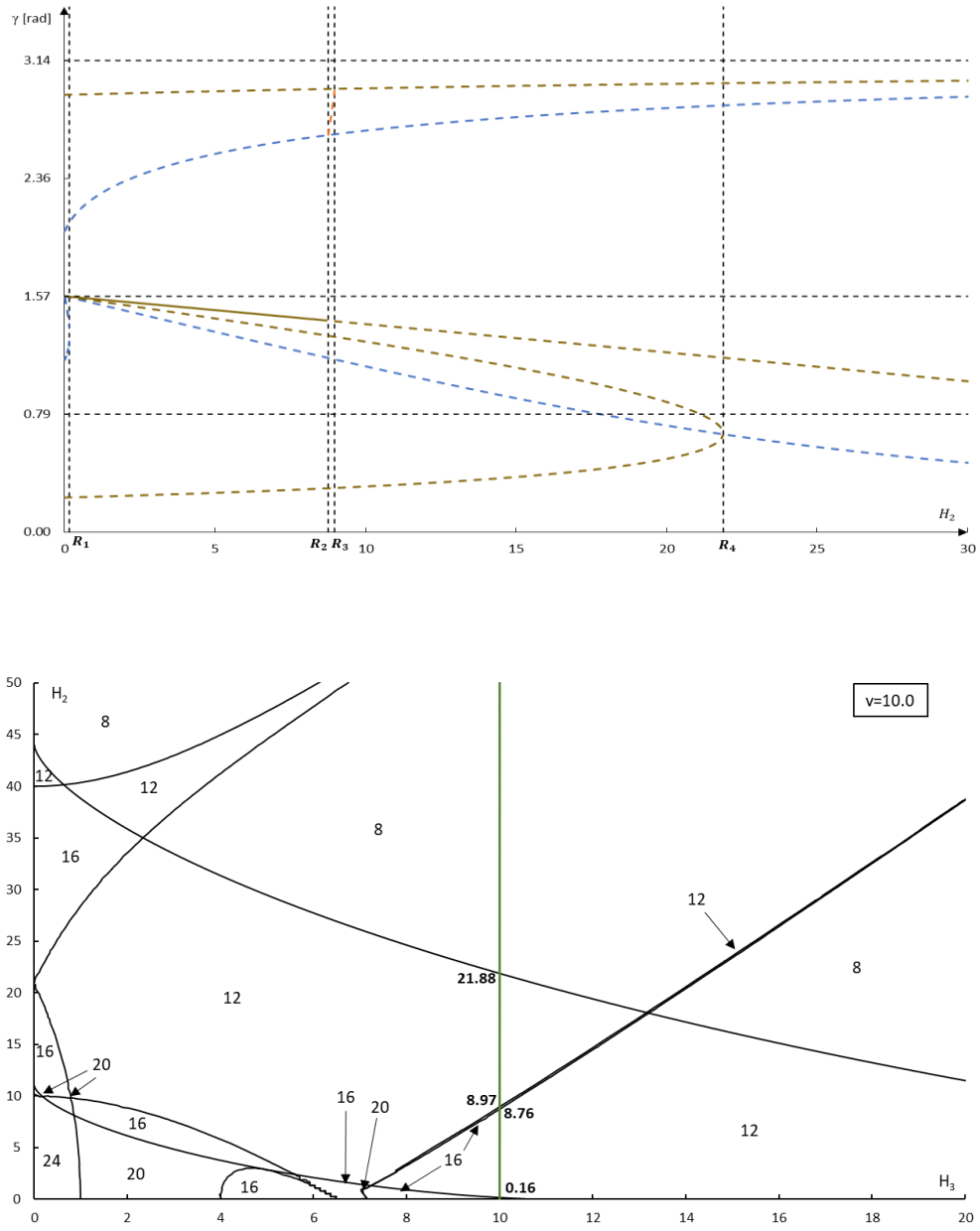

Figure 3.47 – Stability in function of angle γ and H_2 and respective equilibria chart for $v = 10$ and $H_3 = 10$.

The results obtained for all cases, in first place, show that the angle γ can vary between 0 and π; second, there is a minimum of two stable equilibrium solutions and a maximum of six stable equilibrium positions for each case analyzed, e.g., Figures 3.30 and 3.33.

Remembering the chapter 3.1.1, each group of two consecutive equilibrium positions from group I and III have the same value of angle γ. This means that each equilibrium curve in each chart represents two equilibrium positions.

In the case of group II, it has also been proven that the eight equilibrium positions can be reduced to two equilibrium curves in each chart. Analyzing the stability of these solutions of group II, for the same value of angle γ, a group of four solutions can have two solutions stable and two solutions unstable at the same time. An example can be seen in Figure 3.43 between R_4 and R_5, a full line matches a dashed line. This discovery is entirely new in the study of the stability of the gyrostat satellite and should be further analyzed in future work.

For lower values of v ($v = 0.1$ and $v = 0.5$), the regions defined by the upper oblique asymptote became very narrow, which also makes the equilibrium curves very narrow or even disappear, for instance Figures 3.30 and 3.34. For higher values of v ($v = 5$ and $v = 10$), in a similar way, the regions defined by the lower oblique asymptote became very narrow, which makes the equilibrium curves have small intervals or vanish, this can be seen in Figures 3.47 and 3.44. For high values of H_3 ($H_3 \geq 10$), both regions mentioned before became very narrow, which has the same consequence of previous cases.

The increase of parameter H_2, in the case of group I and III, makes the equilibrium curves converge to a certain angle γ, and in the case of group II, can make the equilibrium curves vanish; this corresponds to the points of intersection (R_i) of the vertical line $H_3 = const$ with the borders of the regions with fixed number of equilibria. An example is shown in Figure 3.46.

Finally, analyzing the case when v varies and H_3 is constant (e.g. $H_3 = 0.1$), the size of the stable lines of group of solutions I and III decreases, on other hand, the size of stable lines of group of solutions II increases. Other case is when v is constant (e.g. $v = 1.5$) and H_3 varies, the size of stable lines of group of solutions I and III increases, on other hand, the two stable lines of group of solutions II became one from $H_3 = 0.1$ to $H_3 = 2$ and vanish at $H_3 = 10$.

Chapter 4

Conclusions and Future Work

The present dissertation investigated the dynamics of gyrostat-satellite subjected to gravitational torque and when the gyrostatic moment vector is along the satellite's principal planes of inertia, namely the particular case when $h_1 = 0$, $h_2 \neq 0$ and $h_3 \neq 0$, along a circular orbit.

A detailed and chronological literature review identified some topics which had not been analyzed in the published work yet. Most of the published work focus in the general case of the gyrostat satellite and some special cases: (a) ($h_1 \neq 0$, $h_2 = 0$ and $h_3 \neq 0$) and (b) ($h_1 = 0$, $h_2 \neq 0$ and $h_3 = 0$). Santos in [14] and [20], discovered small regions of 16 and 12 equilibrium positions that needed a more detailed analysis and properly substantiated, which are studied and given in the present work.

The focus of this dissertation was the innovative study of equilibria and stability of a gyrostat satellite when $h_1 = 0$, $h_2 \neq 0$ and $h_3 \neq 0$ and, on other hand, investigate the possibility of existence of the small regions found in [14] and [20] by Santos.

A mathematical analytical-numerical method was used to determine all equilibrium positions, the conditions of their existence and the sufficient conditions of stability. It was found three groups of equilibrium solutions: I, II and III, each one describing up to eight equilibrium positions, totalizing the maximum value of 24 equilibrium positions. The expressions of direction cosines are presented in the explicit form as function of system dimensionless parameters v, H_2 and H_3. The bifurcation curves of group of solutions I and III were determined analytically and the conditions of existence of equilibrium solutions of group II were obtained as function of parameters v, H_2 and H_3.

A detailed study of the evolution of the equilibria bifurcation of the gyrostat satellite and a study of the evolution of the validity of the sufficient conditions of stability for each equilibrium were conducted by a numerical-analytical method as function of system parameters v, H_2 and H_3. It was shown that there is no less than 8 and no more than 24 equilibrium positions for every studied case, specifically no less than 4 and more than 8 equilibrium positions for each group of solutions I, II and III. The same conclusions were given in [6], [8], [14] and [20].

It was confirmed two regions of 12 equilibria positions defined by oblique asymptote that tends to infinite and never vanish, they were not identified up to now by any author; other case was the small regions of 16 positions of equilibria inside one region of 20 for $v < 0.3$ and $v \geq 4$, similar to the ones in [8]. These regions exist near $H_3 = 0$ and near $H_2 = 0.5$ for $v < 0.3$ and, for $v \geq 4$, near $H_3 = 4$ and near $H_2 = 0$. These regions seem to increase in size for lower values of v ($v < 0.3$) and for higher values of v ($v \geq 4$), but they need further analysis.

The evolution of equilibrium positions for a specific v ($v = 1.5$) as function of angles α, β and γ were analyzed by the same numerical-analytical method. It was verified, in the case of group of solutions II, that the angle γ has always the same value for each root of equation (2.32), which means that each group of four solutions of group II has the same angle γ.

The existence of small regions of 16 and 12 equilibria discovered by Santos in [14] and [20] were confirmed; the regions of 12 equilibrium positions defined by oblique asymptotes suggest being related to the small regions referred by Santos (the position of the small regions, in the general case, match the ones present in this work). For some conditions, the results do not coincide, in terms of accuracy, with the ones found in the general case, this can be explained by the fact that $H_1 = 0$ is not considered in the general case

About the stability of the gyrostat, it can be said that the angle γ varies between 0 and π. There is a minimum of two stable equilibrium positions and maximum of six stable equilibrium positions, for each studied case.

In the case of group II, for the same angle γ, a group of four equilibrium solutions can have two stable equilibria positions and two unstable equilibria positions at the same time.

Analyzing the stability results, the case when parameters v varies and H_3 is constant (e.g. $H_3 = 0.1$), the size of the stable lines of group of solutions I and III decreases, on other hand, the size of stable lines of group of solutions II increases. Other case is when v is constant (e.g. $v = 1.5$) and H_3 varies, the size of stable lines of group of solutions I and III increases, on other hand, the two stable lines of group of solutions II became one from $H_3 = 0.1$ to $H_3 = 2$ and vanish at $H_3 = 10$.

In the end, future investigations in other particular cases would expand the knowledge about the problem of a gyrostat satellite. First, it would be interesting to study the particular case of equilibria and stability, when $h_1 \neq 0$, $h_2 \neq 0$ and $h_3 = 0$. Second, and as an extension of the present work, it would be interesting solving the stability problem using the same approach as Sarychev [8] and analyze the stability problem of group of solutions II. For a more extensive work, it would be also interesting to study the dynamics of a gyrostat-satellite in elliptic orbits.

Bibliography

[1] K. H. Shirazi and M. H. Ghaffari-Saadat. “Chaotic motion in a class of asymmetrical Kelvin type gyrostat satellite.” International Journal of Non-Linear Mechanics, vol. 39, no. 5, pp. 785-793, July, 2004.

[2] A. El-Gohary. “On the Stability of Relative Programmed Motion of Satellite-Gyrostat.” Mechanical Research Communications, vol. 25, no. 4, pp. 371-379, 1998.

[3] A. El-Gohary and S. Z. Hassan. “On the Exponential Stability of the Permanent Rotational Motion of a Gyrostat.” Mechanics Research Communications, vol. 26, no. 1, pp. 479-488, 1999.

[4] A. El-Gohary. “Optimal Control of a Rotational Motion of a Gyrostat on Circular Orbit.” Mechanics Research Communications, vol. 27, no. 1, pp. 59-67, 2000.

[5] A. El-Gohary. “On the orientation of a gyrostat using internal rotors.” International Journal of Mechanical Sciences, 43, pp. 225-235, 2001.

[6] V. A. Sarychev and S. A. Mirer. “Relative equilibria of a gyrostat satellite with internal angular momentum along a principal axis.” Acta Astronautica, vol. 49, no. 11, pp. 641-644, 2001.

[7] V. A. Sarychev, S. A. Mirer and A. A. Degtyarev. “The Dynamics of a Satellite-Gyrostat with a Single Nonzero Component of the Vector of Gyrostatic Moment.” Cosmic Research, vol. 43, no. 4, pp. 268-279, 2005.

[8] V. A. Sarychev, S. A. Mirer and A. A. Degtyarev. “Dynamics of a Gyrostat Satellite with the Vector of Gyrostatic Moment in the Principal Plane of Inertia.” Cosmic Research, vol. 46, no. 1, pp. 60-73, 2008.

[9] R. Molina and F. Mondéjar. “Equilibria and stability for a gyrostat satellite in circular orbit.” Acta Astronautica, 54, pp. 77-82, 2003.

[10] V. A. Sarychev, S. A. Gutnik, A. Silva and L. Santos. “Dynamics of gyrostat satellite subject to gravitational torque. Investigation of equilibria.” Keldysh Institute of Applied Mathematics, Russian Academy of Sciences, Moscow, Russia, 2012.

[11] V. A. Sarychev, S. A. Gutnik, A. Silva and L. Santos. “Dynamics of gyrostat satellite subject to gravitational torque. Stability Analysis.” Keldysh Institute of Applied Mathematics, Russian Academy of Sciences, Moscow, Russia, 2013.

[12] S. A. Gutnik and V. A. Sarychev. “Symbolic-Numerical Methods of Studying Equilibrium Positions of a Gyrostat Satellite.” Programming and Computer Software, vol. 40, no. 3, pp. 143-150, 2014.

[13] S. A. Gutnik and V. A. Sarychev, “Symbolic-Numerical Investigation of Gyrostat Satellite Dynamics”

[14] L. Santos. “Gyrostat dynamics on a circular orbit.” PhD thesis, Universidade da Beira Interior, Covilhã, Portugal, April, 2015.

[15] L. Santos, A. Silva, V. A. Sarychev and S. A. Gutnik. “Gyrostat dynamics on a circular orbit.” 3 EJIL – LAETA Young Researchers Meeting, ADAI, Coimbra, 7-8 May, 2015.

[16] S. A. Gutnik, L. Santos, V. A. Sarychev and A. Silva. “Dynamics of a Satellite-Gyrostat Subjected to the Action of Gravity Moment: Equilibrium Attitudes and Their Stability.” Journal of Computer and Systems Sciences International, vol. 54, no. 3, pp. 469-482, 2015.

[17] L. Santos, A. Silva, V. Sarychev and S. Gutnik. “Gyrostat satellite – General case of bifurcation of equilibria and analytical expressions.” CEM 2016 – Mechanical Engineering Conference, Porto, Portugal, 1-3 June, 2016.

[18] S. A. Gutnik and V. A. Sarychev. “Application of Computer Algebra Methods for Investigation of Stationary Motions of a Gyrostat Satellite.” Programming and Computer Software, vol. 43, no. 2, pp. 90-97, 2017.

[19] L. Santos, P. Dias and A. Silva. “Equilibria of a Gyrostat Satellite when the gyrostatic moment vector is parallel to the satellite principal central planes of inertia.” 4 EJIL – LAETA Young Researchers Meeting, Covilhã, Portugal, 9-10 Nov., 2017.

[20] L. Santos, R. Melício and A. Silva. "Gyrostat dynamics on a circular orbit: general case of equilibria bifurcation and analytical expressions" Proceedings of the International Symposium on Power Electronics, Electrical Drives and Motion — SPEEDAM 2018, pp. 1084–1088, Amalfi, Italy, 20–22 June 2018.

[21] R. M. Murray, Z. Li and S. S. Sastry. “A Mathematical Introduction to Robotic Manipulation” CRC Press, 1993.

Attachment A – Paper published at 4 EJIL - LAETA Young Researchers Meeting

Equilibria of a Gyrostat Satellite when the gyrostatic moment vector is parallel to the satellite principal central plains of inertia

Luis Filipe Santos[a,b*], Pedro Dias[a], André Silva[a]

a) AeroG - LAETA, Calçada Fonte do Lameiro, 6201-001 Covilhã
b) ISEC Lisboa, Alameda das Linhas de Torres 179, 1750-142 Lisboa
* e-mail: perigeu@gmail.com

Key words: Gyrostat, Satellite, Circular, Orbit, Equilibria

Abstract. *The attitude control of a modern satellite is a crucial condition for its operation. In this work, is study the general case of equilibria of an asymmetrical inertial distribution gyrostat satellite, subjected to gravitational torque, moving along a circular orbit in a central Newtonian gravitational field. To solve this problem, other authors proposed a symbolic-numerical method, for determining all equilibrium orientations of an asymmetrical gyrostat satellite in the orbital coordinate system with given gyrostatic torque and given principal central moments of inertia. The conditions of equilibria were obtained depending on four dimensionless system parameters. The evolution of the domains in the study of equilibria was carried out in great detail, and all bifurcation values of parameters at which there was a change of numbers of equilibrium orientations were determined with great accuracy. In the present study is developed the complete set of analytical equations describing the evolution of the different bifurcation of equilibria, and is also achieved an accurate analytical expressions for the evolution of small equilibria regions near an axisymmetric configuration.*

In the present paper is obtained in great detail, near the axisymmetric configuration, where $H_1=0$, and H_2 and H_3 different from zero, the evolution which confirm the existence on the general case of equilibria of the small equilibria regions near the axisymmetric configuration.

The knowledge and understanding of this new case study will permit a deeper understanding which will permit to optimize the design and operation of future spacecraft's.

1 EQUILIBRIA ANALYSIS

Consider the attitude motion of a gyrostat satellite, which can be defined as a rigid body with statically and dynamically balanced rotors inside its structure. The angular velocities of rotors relative to the satellite body are constant. The center of mass O of the gyrostat satellite is located in a circular orbit around a central orbiting mass. We introduce now a two right-hand Cartesian coordinate system with origin in the center of mass O of the gyrostat satellite.

$OX_1X_2X_3$ is the orbital coordinate system whose OX_3 axis is directed along the radius vector connecting the centers of mass of the central orbiting body and of the gyrostat

satellite; the OX_1 axis is directed along the vector of linear velocity of the center of mass O.

$Ox_1x_2x_3$ is the gyrostat-fixed coordinate system; $Ox_i\,(i=1,\,2,\,3)$ are the principal central axes of inertia of the gyrostat satellite.

The orientation of the $Ox_1x_2x_3$ coordinate system with respect to the orbital coordinate system is determined by Euler angles ψ, ϑ and φ and the direction cosines of the axes Ox_i in the orbital coordinate system $a_{ij}=\cos(X_i,x_j)$ can be written as:

$$\begin{aligned}
a_{11}&=\cos\psi\cos\varphi-\sin\psi\cos\vartheta\sin\varphi, & a_{23}&=-\cos\psi\sin\vartheta,\\
a_{12}&=-\cos\psi\sin\varphi-\sin\psi\cos\vartheta\cos\varphi, & a_{31}&=\sin\vartheta\sin\varphi,\\
a_{13}&=\sin\psi\sin\vartheta, & a_{32}&=\sin\vartheta\cos\varphi,\\
a_{21}&=\sin\psi\cos\varphi+\cos\psi\cos\vartheta\sin\varphi, & a_{33}&=\cos\vartheta.\\
a_{22}&=-\sin\psi\sin\varphi+\cos\psi\cos\vartheta\cos\varphi,
\end{aligned} \tag{1}$$

Then equations of motion of the gyrostat satellite relative to its center of mass take the form:

$$\begin{aligned}
A\dot{p}&+(C-B)qr-3\omega_0^2(C-B)a_{32}a_{33}-\bar{H}_2r+\bar{H}_3q=0,\\
B\dot{q}&+(A-C)rp-3\omega_0^2(A-C)a_{33}a_{31}-\bar{H}_3p+\bar{H}_1r=0,\\
C\dot{r}&+(B-A)pq-3\omega_0^2(B-A)a_{31}a_{32}-\bar{H}_1q+\bar{H}_2p=0;
\end{aligned} \tag{2}$$

$$\begin{aligned}
p&=\dot{\psi}a_{31}+\dot{\vartheta}\cos\varphi+\omega_0a_{21}=\bar{p}+\omega_0a_{21},\\
q&=\dot{\psi}a_{32}-\dot{\vartheta}\sin\varphi+\omega_0a_{22}=\bar{q}+\omega_0a_{22},\\
r&=\dot{\psi}a_{33}+\dot{\varphi}+\omega_0a_{23}=\bar{r}+\omega_0a_{23}.
\end{aligned} \tag{3}$$

In equations (2), (3) $\bar{H}_1=\sum_{k=1}^{n}J_k\alpha_k\dot{\varphi}_k$, $\bar{H}_2=\sum_{k=1}^{n}J_k\beta_k\dot{\varphi}_k$, $\bar{H}_3=\sum_{k=1}^{n}J_k\gamma_k\dot{\varphi}_k$; J_k is the axial moment of inertia of k-th rotor; α_k, β_k, γ_k are the constant direction cosines of the symmetry axis of the k-th rotor in the coordinate system $Ox_1x_2x_3$; $\dot{\varphi}_k$ is the constant angular velocity of the k-th rotor relative to the gyrostat; A, B, C are the principal central moments of inertia of the gyrostat; p, q, r are the projections of the absolute angular velocity of the gyrostat satellite in the axes Ox_i; ω_0 is the angular velocity of motion of the center of mass of the gyrostat satellite along a circular orbit. Dots designate differentiation with respect to time t.

Further it will be more convenient to use parameters $H_i=\bar{H}_i/\omega_0\ (i=1,\,2,\,3)$.

For the systems of Eq. 2 and Eq. 3 the generalized energy integral exists in the form:

$$\begin{aligned}
&\frac{1}{2}(A\bar{p}^2+B\bar{q}^2+C\bar{r}^2)+\frac{3}{2}\omega_0^2[(A-C)a_{31}^2+(B-C)a_{32}^2]+\\
&+\frac{1}{2}\omega_0^2[(B-A)a_{21}^2+(B-C)a_{23}^2]-\omega_0^2(H_1a_{21}+H_2a_{22}+H_3a_{23})=const.
\end{aligned} \tag{4}$$

1.1 Equilibrium Orientations

Setting in (2) and (3) $\psi = \psi_0 = const,\ \vartheta = \vartheta_0 = const,\ \varphi = \varphi_0 = const$, we obtain at $A \neq B \neq C$ the equations:

$$\begin{aligned}
&(C-B)(a_{22}a_{23} - 3a_{32}a_{33}) - H_2a_{23} + H_3a_{22} = 0,\\
&(A-C)(a_{23}a_{21} - 3a_{33}a_{31}) - H_3a_{21} + H_1a_{23} = 0,\\
&(B-A)(a_{21}a_{22} - 3a_{31}a_{32}) - H_1a_{22} + H_2a_{21} = 0,
\end{aligned} \tag{5}$$

Allowing us to determine the gyrostat satellite equilibria in the orbital coordinate system. System (5) depends on four dimensionless parameters:

$$h_1 = \frac{H_1}{B-C},\ h_2 = \frac{H_2}{B-C},\ h_3 = \frac{H_3}{B-C},\ \nu = \frac{B-A}{B-C}. \tag{6}$$

Eq. 5 can be rewritten in the equivalent form

$$\begin{aligned}
&4(Aa_{21}a_{31} + Ba_{22}a_{32} + Ca_{23}a_{33}) + (H_1a_{31} + H_2a_{32} + H_3a_{33}) = 0,\\
&Aa_{11}a_{31} + Ba_{12}a_{32} + Ca_{13}a_{33} = 0,\\
&(Aa_{11}a_{21} + Ba_{12}a_{22} + Ca_{13}a_{23}) + (H_1a_{11} + H_2a_{12} + H_3a_{13}) = 0
\end{aligned} \tag{7}$$

or using dimensionless parameters (6) in the form

$$\begin{aligned}
&-4(\nu a_{21}a_{31} + a_{23}a_{33}) + (h_1a_{31} + h_2a_{32} + h_3a_{33}) = 0,\\
&\nu a_{11}a_{31} + a_{13}a_{33} = 0,\\
&\nu a_{11}a_{21} + a_{13}a_{23} - (h_1a_{11} + h_2a_{12} + h_3a_{13}) = 0.
\end{aligned}$$

(8)

Taking into account expressions (1), system (5) or system (8) can be considered as a system of three equations with unknowns $\psi_0, \vartheta_0, \varphi_0$. The second more convenient method to close Eq. 8 consists in adding six conditions of orthogonality for the direction cosines (1)

$$\begin{aligned}
&a_{11}^2 + a_{12}^2 + a_{13}^2 = 1, \qquad a_{11}a_{21} + a_{12}a_{22} + a_{13}a_{23} = 0,\\
&a_{21}^2 + a_{22}^2 + a_{23}^2 = 1, \qquad a_{11}a_{31} + a_{12}a_{32} + a_{13}a_{33} = 0,\\
&a_{31}^2 + a_{32}^2 + a_{33}^2 = 1, \qquad a_{21}a_{31} + a_{22}a_{32} + a_{23}a_{33} = 0.
\end{aligned} \tag{9}$$

Further, we will study the equilibrium orientations of the gyrostat satellite using systems (8) and (9).

As it was shown in Sarychev and Gutnik (1984), the system of second equation in (8) and first, second, fourth, fifth and sixth equations in (9) can be solved for $a_{11}, a_{12}, a_{13}, a_{21}, a_{22}, a_{23}$ if $A \neq B \neq C$, using dimensionless parameters (6) in the form:

$$\begin{aligned} a_{11} &= -4a_{32}a_{33}/F, & a_{21} &= 4[\nu a_{32}^2 - (1-\nu)a_{33}^2]a_{31}/F, \\ a_{12} &= 4(1-\nu)a_{33}a_{31}/F, & a_{22} &= -4(\nu a_{31}^2 + a_{33}^2)a_{32}/F, \\ a_{13} &= 4\nu a_{31}a_{32}/F, & a_{23} &= 4[(1-\nu)a_{31}^2 + a_{32}^2]a_{33}/F, \end{aligned} \tag{10}$$

where $F = h_1a_{31} + h_2a_{32} + h_3a_{33}.$

Substituting Eq. 10 in the first and third Eq. 8 and adding the third Eq. 9 we get three equations:

$$\begin{aligned} &16[a_{32}^2a_{33}^2 + (1-\nu)^2a_{33}^2a_{31}^2 + \nu^2a_{31}^2a_{32}^2] = (h_1a_{31} + h_2a_{32} + h_3a_{33})^2(a_{31}^2 + a_{32}^2 + a_{33}^2), \\ &4\nu(1-\nu)a_{31}a_{32}a_{33} + [h_1a_{32}a_{33} - h_2(1-\nu)a_{33}a_{31} - h_3\nu a_{31}a_{32}](h_1a_{31} + h_2a_{32} + h_3a_{33}) = 0, \\ &a_{31}^2 + a_{32}^2 + a_{33}^2 = 1 \end{aligned} \tag{11}$$

For the determination of direction cosines a_{31}, a_{32}, a_{33}, if system (11) will be solved then relations (10) allow us to find the other six direction cosines. In (11) the right part of first equation was multiplied by $a_{31}^2 + a_{32}^2 + a_{33}^2 = 1.$ Note that solutions (10) exist only in the case when any two direction cosines of a_{31}, a_{32}, a_{33} set do not vanish simultaneously. Specific cases $a_{31} = a_{32} = 0, \ a_{32} = a_{33} = 0, \quad a_{33} = a_{31} = 0,$ must be examined by the direct investigation of systems (8) and (9).

The problem has been solved for some particular cases when the vector of gyrostatic moment is located along the satellite's principal central axis of inertia Ox_2, when $h_1 = 0, \ h_2 \neq 0, \ h_3 = 0$ in Sarychev and Mirer (2001) and Sarychev et al. (2005), Longman et al. (1981), and when the vector of gyrostatic moment locates in the satellite's principal central plane of inertia Ox_1x_3 of the frame $Ox_1x_2x_3$ and $h_1 \neq 0, \ h_2 = 0, \ h_3 \neq 0$, Sarychev et al. (2008), Longman (1971). Also, the General Case has been deeply investigated by Santos. L. in [10] to [13] were $H_1 \neq H_2 \neq H_3$. The study of the General Case has brought very new and exciting innovative results in the study of gyrostat satellites.

Let us introduce the values $x = a_{31}/a_{33}, \ y = a_{32}/a_{33}$ and divide all terms of first equation in (11) by a_{33}^4 and second equation by a_{33}^3. Then we will have the system of two equations with unknown values x, y:

$$\begin{aligned} &16[y^2 + (1-\nu)^2x^2 + \nu^2x^2y^2] = (h_1x + h_2y + h_3)^2(1 + x^2 + y^2), \\ &4\nu(1-\nu)xy + [h_1y - h_2(1-\nu)x - h_3\nu xy](h_1x + h_2y + h_3) = 0. \end{aligned} \tag{12}$$

Now substituting expressions $a_{31} = xa_{33}, \ a_{32} = ya_{33}$ in the last equation of the system (11), we receive:

$$a_{33}^2 = \frac{1}{1 + x^2 + y^2}. \tag{13}$$

The Eq. 12 can be presented in such form:

$$\begin{aligned} &a_0 y^2 + a_1 y + a_2 = 0, \\ &b_0 y^4 + b_1 y^3 + b_2 y^2 + b_3 y + b_4 = 0. \end{aligned} \tag{14}$$

Where after introducing $H_1 = 0$, the following coefficients can be found:

$$\begin{aligned} a_0 &= -h_2 h_3 \nu x \\ a_1 &= h_3 \left[4\nu(1-\nu) - (1-\nu)h_2^2 - \nu h_3^2\right] x \\ a_2 &= -(1-\nu) h_2 h_3 x \\ b_0 &= h_2^2 \\ b_1 &= 2 h_2 h_3 \\ b_2 &= \left(h_2^2 + h_3^2 - 16\right) + \left(h_2^2 - 16\nu^2\right) x^2 \\ b_3 &= 2 h_2 h_3 (1 + x^2) \\ b_4 &= h_3^3 (1 + x^2) - 16(1-\nu)^2 x^2 \end{aligned} \tag{15}$$

Using the resultant concept, we eliminate variable y from the Eq. 14. Resultant $R(x)$ of Eq. 14 has the form

$$R(x) = \begin{bmatrix} a_0 & a_1 & a_2 & 0 & 0 & 0 \\ 0 & a_0 & a_1 & a_2 & 0 & 0 \\ 0 & 0 & a_0 & a_1 & a_2 & 0 \\ 0 & 0 & 0 & a_0 & a_1 & a_2 \\ b_0 & b_1 & b_2 & b_3 & b_4 & 0 \\ 0 & b_0 & b_1 & b_2 & b_3 & b_4 \end{bmatrix}$$

Let us consider equation $R(x) = 0,$ which can be presented with the help of Mathematica symbolic matrix function in the form:

$$p_0 x^8 + p_1 x^6 + p_2 x^4 = 0 \tag{16}$$

where:

$$\begin{aligned} p_0 = -16 h_2^2 h_3^2 v^2 \Big[& h_2^6 (-1+v)^4 + (h_3^2 - 16(-1+v)^2) v^4 (-4 + h_3^2 + 4v)^2 \\ & + h_2^4 (-1+v)^2 v \left(-8(-1+v)^2(1+2v) + h_3^2(-2+3v)\right) \\ & + h_2^2 (-1+v) v^2 \left(h_3^4(-1+3v) + 16(-1+v)^3(1+8v)\right. \\ & \left. + h_3^2(17 - 49v + 64v^2 - 32v^3)\right)\Big] \end{aligned}$$

$$
\begin{aligned}
p_1 = -16\mathrm{h}_2^2 \Big[& h_2^8(-1+v)^6 - 2h_2^6(h_3^2(1-2v) + 8(-1+v)^2)(-1+v)^4 v \\
& - 2h_2^2(-1+v)v^3 \Big(-84h_3^2(-1+v)^3 + 128(-1+v)^5 \\
& + 17h_3^4(-1+v)v + h_3^6(-1+v-2v^2)\Big) \\
& + v^4(-4+h_3^2+4v)^2 \Big(-17h_3^2(-1+v)^2 + 16(1-v)^4 \\
& + h_3^4(1+v^2)\Big) \\
& + h_2^4(-1+v)^2 v^2 \Big(96(1-v)^4 - 3h_3^2(-1+v)^2(3+8v) \\
& + h_3^4(2-6v+6v^2)\Big)\Big]
\end{aligned}
$$

$$
\begin{aligned}
p_2 = -16h_2^2h_3^2 \Big[& h_2^6(-1+v)^4 + (h_3^2 - (-1+v)^2)v^4(-4+h_3^2+4v)^2 \\
& - h_2^4(-1+v)^2 v \Big(h_3^2(2-3v) + (-1+v)^2(8+v)\Big) \\
& + h_2^2(-1+v)v^2 \Big(8(-1+v)^3(2+v) + h_3^4(-1+3v) \\
& + h_3^2(17-19v+4v^2-2v^3)\Big)\Big]
\end{aligned}
$$

Substituting the value of a real root of Eq. 16 into the Eq. 14, we can find roots of these equations.

In [14], Santos L. et all verified that the General Case near $H_1 = 0$ contained very small off-setted equilibria regions. The study of these regions cannot be properly made without studying the case where $H_1 = 0$, which match to the gyrostatic moment parallel to the satellite principal central plain of inertia. In the General Case, the regions with 12 equilibria become smaller with the increase of h_3 values. These regions are vanishing in the center of system of coordinates for $h_3 = 4$. For $h_3 \geq 4$ there are small regions of 12 equilibria near h_2 axis with the size along h_1 and h_2 axes less than 10^{-1}. And as bigger the h_3 value, the further from the center of coordinate system these small regions take position along the h_2 axis.

2 Equilibrium Orientations

Santos L. et all demonstrate that with the use of (16), it is possible to determine numerically all equilibrium orientations of the gyrostat satellite in the orbital coordinate system and analyze their stability for the General Case. Dependence of the number of real solutions of (16) on the parameters analyzed numerically, using Mathematica factorization method. It was also have been proved that is possible to provide the numerical calculations, without breaking a generality for the case when $B > A > C$. From these inequalities it follows that $0 < \nu < 1$. The parameters h_1, h_2, h_3 can take on any nonzero values.

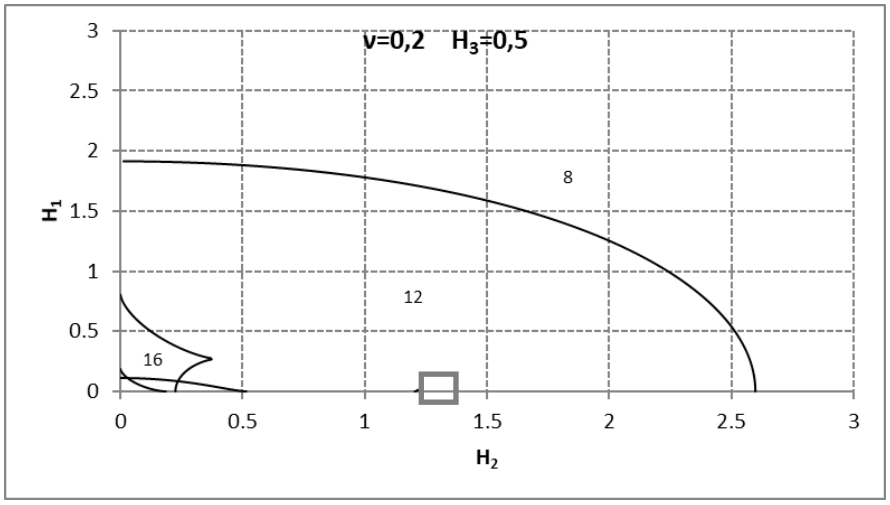

Figure 1 – General Case $\nu = 0.2\ and\ H_3 = 0.5$

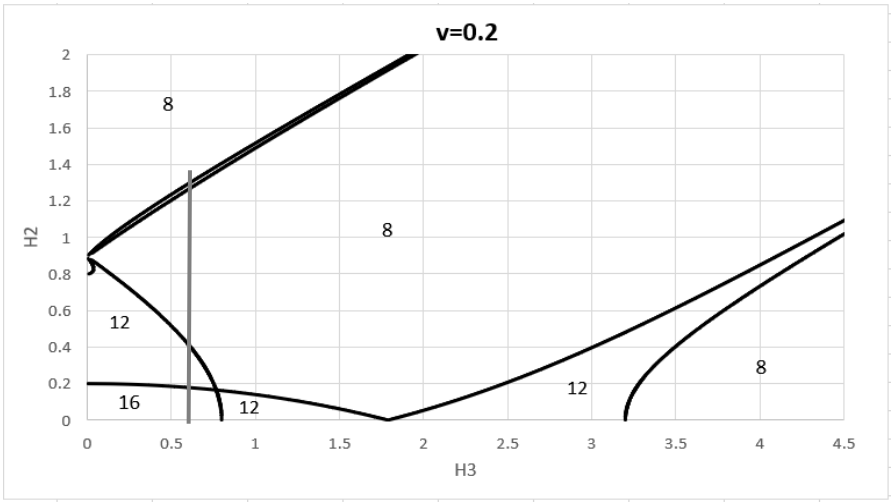

Figure 2 – Case $\nu = 0.2\ and\ H_1 = 0$

Taking Figure 1 and Figure 2 as our first example, in the study of the small regions near $H_1 = 0$ found during the study and analysis of the General Case [10][12][13][14], it can be clearly seen that for $H_3 = 0.5$ a small region appears near $H_2 = 1.2$. Regarding the main regions, it can also be noticed some clear resemblances between these regions.

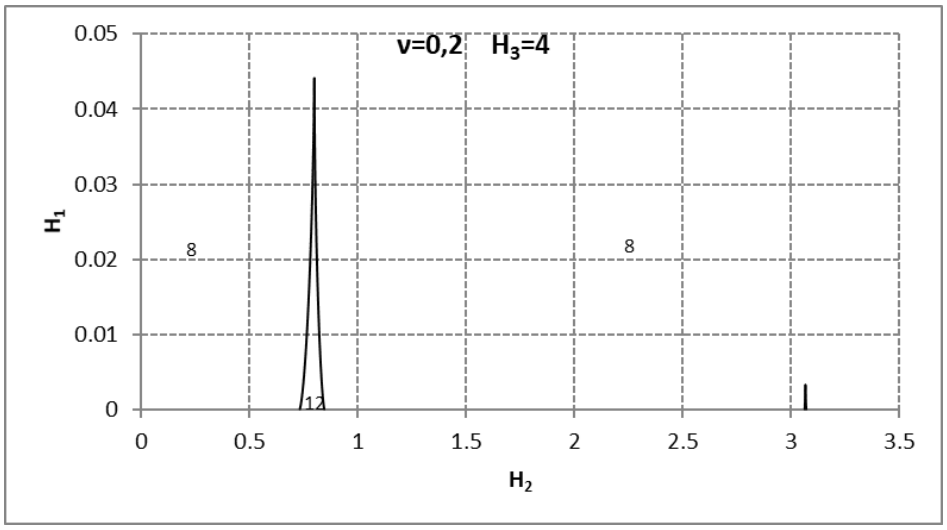

Figure 3 – General Case $\nu = 0.2$ *and* $H_3 = 4$

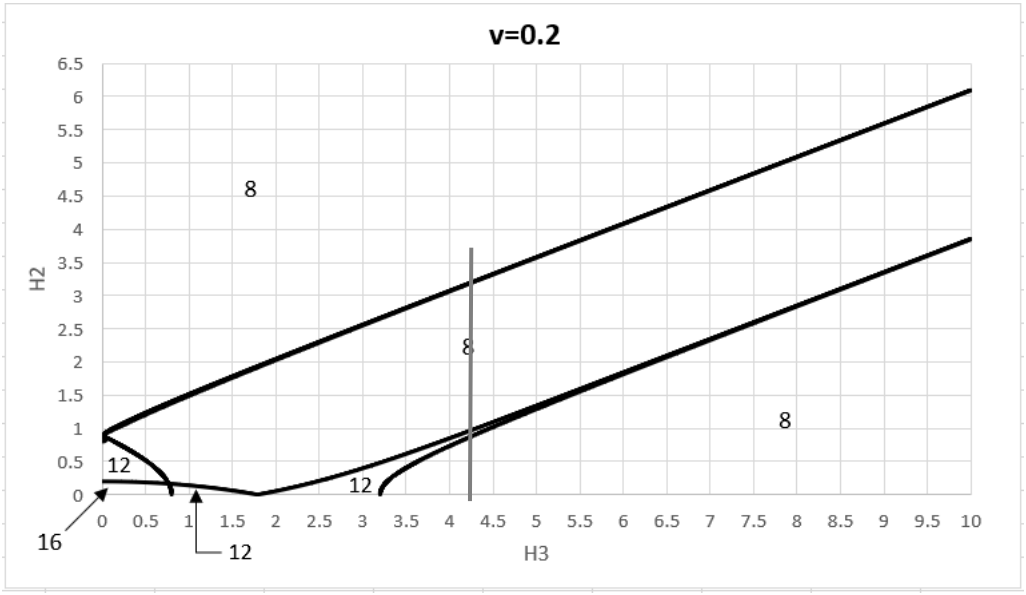

Figure 4 – Case $\nu = 0.2$ *and* $H_1 = 0$

Checking Figure 3 taken from the General Case and Figure 4 from $H_1 = 0$, it can be verified that the small regions start around $H_2 = 0.7$ and $H_2 = 3.1$. For the case where $\nu = 0.2$ and $H_1 = 0$ and making $H_3 = 4$, can be verified that exists two small regions located in the proximity of coordinates as also verified in the General Case.

3 CONCLUSIONS

After analyzing the situation were $H_1 = 0$, it is possible to ensure that the small regions found on the General Case exists, and can bring very new and excitement new satellites design configurations. These new regions need now to be more deeply analyzed and studied, particularly in the study of the Stability.

Also, the equilibria properties can be now more accurately understand and studied, which will also bring new results into the real applications.

4 REFERENCES

1. Likins, P.W., Roberson, R.E.: Uniqueness of equilibrium attitudes for Earth-pointing satellites. J. Astronaut Sci. **13** (2), 87–88 (1966)
2. Longman, R.W.: Gravity-gradient stabilization of gyrostat satellites with rotor axes in principal planes. Celestial Mechanics **3**, 169-188 (1971)
3. Longman, R.W., Hagedorn, P., Beck, A.: Stabilization due to gyroscopic coupling in dual-spin satellites subject to gravitational torques. Celestial Mechanics **25**, 353-373 (1981)
4. Sarychev, V.A.: Asymptotically stable stationary rotational motions of a satellite. In: Proceedings of 1st IFAC Symposium on Automatic Control in Space, pp. 277–286, Plenum Press, New York, (1965)
5. Sarychev, V.A.: Problems of Orientation of Satellites, Itogi Nauki i Tekhniki. Ser. “Space Research”, vol. 11, 224 pp. VINITI, Moscow (1978)
6. Sarychev V.A., Gutnik S.A.: Relative equilibria of a gyrostat satellite. Cosmic Research. **22**, 257-260 (1984)
7. Sarychev, V.A., Mirer, S.A.: Relative equilibria of a gyrostat satellite with internal angular momentum along a principal axis. Acta Astronautica 49, 641-644 (2001)
8. Sarychev, V.A., Mirer, S.A., Degtyarev, A.A.: The dynamics of a satellite gyrostat with a single nonzero component of the vector of gyrostatic moment. Cosmic Research 43, 268-279 (2005)
9. Sarychev, V.A., Mirer, S.A., Degtyarev, A.A.: Dynamics of a gyrostat satellite with the vector of gyrostatic moment in the principal plane of inertia. Cosmic Research 46, 61-74 (2008)
10. S. A. Gutnik, L. Santos, V. A. Sarychev, A. Silva. Dynamics of gyrostat satellite subject to gravitational torque. Investigation of stability equilibria. Journal of Computer and Systems Sciences International. 2015, No.3.
11. S. A. Gutnik, L. F. Santos, V. A. Sarychev, A. Silva. Equilibria of gyrostat satellite in a circular orbit. Paper in XII th International Conference “Stability and Oscillations of Nonlinear Control Systems". June 2012, Moscow, Russia.
12. V. A. Sarychev, S. A. Gutnik, A. Silva, L. Santos. Dynamics of gyrostat satellite subject to gravitational torque. Investigation of equilibria. Keldysh Institute of Applied Mathematics, Russian Academy of Sciences. 2012, Preprint No.63, 35 Pages.
13. V. A. Sarychev, S. A. Gutnik, A. Silva, L. Santos. Dynamics of gyrostat satellite subject to gravitational torque. Stability analysis. Keldysh Institute of Applied Mathematics, Russian Academy of Sciences. 2013, Preprint No.25, 36 Pages.
14. L.Santos, A. Silva, V.A.Sarychev, S.A. Gutnik. Gyrostat Dynamics on a Circular Orbit, paper on 3 EJIL – LAETA Young Researchers Meeting.